# NBS SPECIAL PUBLICATION 641



**U.S. DEPARTMENT OF COMMERCE** / National Bureau of Standards

# Technical Digest - Symposium on Optical Fiber Measurements, 1982

Sponsored by the National Bureau of Standards
in cooperation with the IEEE Transmission Systems
Subcommittee on Fiber Optics (COMMSOC)
and the Optical Society of America.

# NATIONAL BUREAU OF STANDARDS

The National Bureau of Standards[1] was established by an act of Congress on March 3, 1901. The Bureau's overall goal is to strengthen and advance the Nation's science and technology and facilitate their effective application for public benefit. To this end, the Bureau conducts research and provides: (1) a basis for the Nation's physical measurement system, (2) scientific and technological services for industry and government, (3) a technical basis for equity in trade, and (4) technical services to promote public safety. The Bureau's technical work is performed by the National Measurement Laboratory, the National Engineering Laboratory, and the Institute for Computer Sciences and Technology.

**THE NATIONAL MEASUREMENT LABORATORY** provides the national system of physical and chemical and materials measurement; coordinates the system with measurement systems of other nations and furnishes essential services leading to accurate and uniform physical and chemical measurement throughout the Nation's scientific community, industry, and commerce; conducts materials research leading to improved methods of measurement, standards, and data on the properties of materials needed by industry, commerce, educational institutions, and Government; provides advisory and research services to other Government agencies; develops, produces, and distributes Standard Reference Materials; and provides calibration services. The Laboratory consists of the following centers:

Absolute Physical Quantities[2] — Radiation Research — Chemical Physics — Analytical Chemistry — Materials Science

**THE NATIONAL ENGINEERING LABORATORY** provides technology and technical services to the public and private sectors to address national needs and to solve national problems; conducts research in engineering and applied science in support of these efforts; builds and maintains competence in the necessary disciplines required to carry out this research and technical service; develops engineering data and measurement capabilities; provides engineering measurement traceability services; develops test methods and proposes engineering standards and code changes; develops and proposes new engineering practices; and develops and improves mechanisms to transfer results of its research to the ultimate user. The Laboratory consists of the following centers:

Applied Mathematics — Electronics and Electrical Engineering[2] — Manufacturing Engineering — Building Technology — Fire Research — Chemical Engineering[2]

**THE INSTITUTE FOR COMPUTER SCIENCES AND TECHNOLOGY** conducts research and provides scientific and technical services to aid Federal agencies in the selection, acquisition, application, and use of computer technology to improve effectiveness and economy in Government operations in accordance with Public Law 89-306 (40 U.S.C. 759), relevant Executive Orders, and other directives; carries out this mission by managing the Federal Information Processing Standards Program, developing Federal ADP standards guidelines, and managing Federal participation in ADP voluntary standardization activities; provides scientific and technological advisory services and assistance to Federal agencies; and provides the technical foundation for computer-related policies of the Federal Government. The Institute consists of the following centers:

Programming Science and Technology — Computer Systems Engineering.

[1]Headquarters and Laboratories at Gaithersburg, MD, unless otherwise noted;
mailing address Washington, DC 20234.
[2]Some divisions within the center are located at Boulder, CO 80303.

# Technical Digest - Symposium on Optical Fiber Measurements, 1982



Digest of a Symposium sponsored by the
National Bureau of Standards
in cooperation with the
IEEE Transmission Systems Subcommittee
on Fiber Optics (COMMSOC)
and the Optical Society of America

October 13-14, 1982
National Bureau of Standards
Boulder, Colorado 80303

Edited by
D. L. Franzen
G. W. Day
R. L. Gallawa

Electromagnetic Technology Division
National Engineering Laboratory
National Bureau of Standards
Boulder, Colorado 80303

DEPARTMENT OF COMMERCE · UNITED STATES OF AMERICA

U.S. DEPARTMENT OF COMMERCE, Malcolm Baldrige, Secretary

NATIONAL BUREAU OF STANDARDS, Ernest Ambler, Director
Issued October 1982

Library of Congress Catalog Card Number: 82–600594

National Bureau of Standards Special Publication 641
Nat. Bur. Stand. (U.S.), Spec. Publ. 641, 156 pages (Oct. 1982)
CODEN: XNBSAV

U.S. GOVERNMENT PRINTING OFFICE
WASHINGTON: 1982

For sale by the Superintendent of Documents, U.S. Government Printing Office, Washington D.C. 20402
Price $6.50
(Add 25 percent for other than U.S. Mailing.)

## PREFACE

This digest contains summaries of papers presented at the 1982 Symposium on Optical Fiber Measurements, Boulder, Colorado. The program consists of invited papers (7), contributed papers (25), and workshops (2). Approximately 60 percent of the papers submitted to the Symposium as contributed papers were accepted for presentation.

A breakdown of the contributed papers by country and subject matter reveals the international interest in optical fiber measurements and indicates the areas of most intense interest. According to country, the 25 contributed papers have the following distribution:

U.S.A. - 9
U.K. - 6
Japan - 3
Australia - 1
Canada - 1
France - 1
Germany - 1
Italy - 1
Netherlands - 1
Norway - 1

According to subject matter, the 25 contributed papers were grouped into the following measurement areas which also formed symposium sessions:

Multimode Bandwidth - 7
Single Mode - 6
Attenuation - 4
Joint/Defect - 3
Applied/Field - 3
Index Profile/Geometry - 2

It is interesting to contrast this distribution with that of the 1980 Symposium. In 1982, the dominant subject areas are multimode bandwidth and single mode measurements; whereas, in 1980, the emphasis was on attenuation and joint/defect. Apparently laboratories are beginning to understand the problems of multimode fiber attenuation, and emphasis is shifting to bandwidth and, in particular, the prediction of concatenated lengths. Increased interest in single mode measurements naturally occurs as these fibers move out of the laboratory and into installed systems.

The National Bureau of Standards is indebted to the IEEE Transmission Systems Subcommittee on Fiber Optics (COMMSOC), the Optical Society of America, and members of the conference committee for their assistance in organizing this symposium.

D. L. Franzen
G. W. Day
R. L. Gallawa
Boulder, Colorado
October 1982

## CONFERENCE COMMITTEE

R. L. Gallawa, NBS, General Chairman
D. L. Franzen, NBS, Program Co-Chairman
G. W. Day, NBS, Program Co-Chairman
W. B. Gardner, Bell Laboratories
E. H. Hara, CRC, Ottawa
P. Kaiser, Bell Laboratories
F. P. Kapron, ITT
D. B. Keck, Corning Glass Works
M. Koyama, NTT, Tokyo
D. A. Pinnow, Times Fiber
C. J. Todd, British Telecom

CONTENTS

## Attenuation Measurements



## Measurements on Single Mode Fibers

## Standards



## Joint/Defect Measurements



## Index Profile and Geometric Measurements

PREDICTION OF LENGTH PERFORMANCE OF MULTIMODE GRADED-INDEX FIBER

P. R. Reitz
Corning Glass Works
Waveguide Product Engineering Laboratory
Canada Road Facility
Corning, New York 14831

## INTRODUCTION

The accurate prediction of the performance of concatenated lengths of graded-index multimode optical fibers is a basic requirement to meet the industry's need for reliable installations while simultaneously avoiding the over-design for which early fiber systems were noted. At present, the technical community is actively exploring the limits of this technology, trying to determine where multimode fibers best fit into the existing and expected communications system hierarchy. In general, these limits are determined by available fiber performance and by the ability of designers to make full use of this performance. While there is still room for fiber improvement, it is clear that much more work remains to be done to improve predictions of link performance, especially with regard to information transmission capacity. This paper provides a review of the progress toward this goal over the last several years, and highlights present directions.

### Prediction of Link Attenuation

Perhaps the most dramatic change that has taken place in recent years is the ability to predict link attenuation performance from individual fiber measurements, which leads to the more practical ability to select individual fiber to meet a specific link budget requirement. This situation is, in part, a result of improved fiber transmission characteristics. The tendency for fibers to create a restricted "equilibrium" mode distribution (EMD), as measured by differential mode attenuation, has been considerably reduced. Table 1 compares the attenuation difference between the fully-moded launch condition and an approximate "equilibrium" distribution for typical past and present fibers. The use of restricted launching conditions has become rather universally accepted as the best means of obtaining suitably accurate length-additive attenuation values.

Two particular methods of restricting the launched power distribution are widely used. The Limited Phase Space (LPS) method creates a launch beam spot size and numerical aperture somewhat smaller than fiber core diameter and NA, usually about 70% of the fiber parameters. That launch distribution has been shown to be capable of providing length scaling to an accuracy of about 0.05 to 0.10 dB/km.[3-6] A second method, the mandrel-wrap mode filter has also been shown to provide acceptable length scaling.[7] Both methods have been accepted by the U.S. Electronic Industries Association, and are included by the IEC's proposed definition of an equilibrium mode volume.

Although both methods launch an "equilibrium" or "quasi-equilibrium" distribution, their distributions are not identical. The mandrel wrap mode filter has the primary advantage of simplicity in use, and has become particularly widespread in field measurements. While the mandrel wrap allows precise measurements, there are concerns that the distribution may not be truly representative of an EMD,[8,9] mainly because of the sharp cutoff the distribution assumes at some high relative mode group number, $\left(\frac{m}{M}\right)$. The LPS launch, on the other hand, couples progressively less relative power as $\left(\frac{m}{M}\right)$ increases from 0.5 to 1.0, thereby creating a distribution similar to what one would expect for an equilibrium process created by power diffusion from the core. However, the launched distribution is sensitive to fiber end preparation and requires precision optical equipment to achieve best results. On typical fibers, measurement differences between the techniques are usually less than 0.10 dB/km, which is small enough that either can be used for link prediction. At 0.10 dB/km, residual differences between predicted and actual link performance are difficult to separate from splice loss measurement inaccuracy.

Optical Time Domain Reflectometry (OTDR) is widely used in fiber cable installation for splice optimization. Improvements in cabling technology have reduced excess cabling loss to a point where the OTDR is an acceptable technique for locating occasional defects, although some claim the ability to obtain accurate results.[6] However, the OTDR is not generally used by those attempting link performance prediction, as it sometimes produces "misleading results."[2]

Prediction of Link Bandwidth

A subject noted for its complexity, the prediction of link bandwidth performance from individual fiber measurement has not yet been attained with any regularity. Most papers on the subject can be divided into two general categories: those which cite average behavior of quantities of fiber, usually from a practical viewpoint, and those which attempt a theoretical approach.

In the first category, an assortment of results have been obtained. Kitayama et al[10] showed a bandwidth length dependence of ∿.73 on 48km of fiber, and found those measured results agreed with a theoretical calculation assuming 60% mode conversion. Others[1,5,11,12] have found bandwidth length dependence to be from ∿.54 to ∿1.0; some do not speculate on the cause for the observed behavior. Those who do generally cite index profile error compensation. Others relate the length dependence of bandwidth to the average relationship between systematic and random profile errors. An interesting observation is contained in (2) that shows high performance fibers tending toward the less favorable unity exponent, linear dependence.

Virtually all in-depth studies contain a common thread: that to predict link bandwidth one must know how to predict the law of addition of group delay. Several studies have dealt with direct measurement of differential mode delays (DMD).[11,13] Others, such as Love,[14] have shown that the mode delay characteristics of moderately high bandwidth fibers can be considered in terms of an optimum wavelength $\lambda_p$, and the bandwidth at that wavelength, $BW_p$. Matsumoto[15] has recently expanded this concept by showing agreement between calculations and measurements on 20 concatenated fibers by knowing optimum wavelength, peak bandwidth, a spectral bandwidth shape factor k, but he also uses factors said to represent average values of internal mode coupling and other parameters.

## Conclusion

Although practical experience has shown good agreement between predicted and actual link attenuation, a large amount of work remains. In particular, the adoption of test methods for individual fibers and the mathematical models that will, together, allow successful prediction of link bandwidth performance for a wide variety of fibers are still a challenge.

## References

1) R. Bouillie et al, "Tuileries-Phillipe August: The First Operation Junction Line in France," 7th European Conference on Optical Communications (ECOC) 1981, Copenhagen, Denmark Paper 15.3.

2) C. J. Lilly and D. R. Bissell, "Some Initial Results and Experience of Operational Optical Fibre Systems in the UK," 7th ECOC, 1981, Copenhagen, Paper 15.4.

3) G. T. Holmes, 6th European Conference on Optical Communications, York, U.K., 1980.

4) R. M. Hawk, "Multimode Waveguide Attenuation Measurements," Technical Digest, Symposium of Optical Fiber Measurements, 1980.

5) P. R. Reitz, "Characterization of Concatenated Multimode Optical Fibers with Time Domain Measurement Techniques," p. L-14, Digest, Conference on Precision Electromagnetic Measurements, Boulder, Co., 1982.

6) F. Cairglia et al, "Field Measurement, Testing, and Maintenance of Installed Optical Cable and Systems," p. 15.6, 7th European Conference on Optical Communications, Copenhagen, Denmark, 1981.

7) A. H. Cherin and E. D. Head, "A Fiber Concatenation Experiment Using A Standardized Loss Measurement Method," Symposium on Optical Fiber Measurements, 1980, Boulder, Co., Technical Digest, p. 19.

8) P. Kaiser, "Loss Measurements of Graded-Index Fibers: Accuracy Versus Convenience," Symposium on Optical Fiber Measurements, 1980, Boulder, Co., Technical Digest, p. 11.

9) P. Kaiser, "Loss Characterization of Biconic Single-Fiber Connectors," Symposium on Optical Fiber Measurements, 1980, Boulder, Co., Technical Digest, p. 73

10) K. Kitayama et al, "Transmission Characteristics of Long Spliced Graded-Index Optical Fibers at 1.27μm," IEE Journal of Quantum Electronics, Vol. QE 15, No. 7, July 1979.

11) J. V. Wright and B. P. Nelson, "Bandwidth Studies of Jointed Multimode Fibres," Paper 4.2, 7th European Conference of Optical Communications, Copenhagen, Denmark, 1981.

12) M. C. Hudson and L. C. Kenyon, "Installation and Measurement of an 18.7 and 23.5km Unrepeatered Fiber-Optic Interoffice Trunk," Technical Digest, Topical Meeting on Optical Fiber Communication, Phoenix, Az., 1982, (Optical Society of America, Washington, D.C.)

13) M. J. Buckler, "Optimization of Concatenated Fiber Bandwidth Via Differential Mode Delay," Technical Digest, Symposium on Optical Fiber Measurements, Boulder, Co., 1980. NBS Special

Publication 597.

14) W. F. Love, "Bandwidth Spectral Characterization of Modal Compensation in Multimode Optical Fibers," Paper 4.4, 7th European Conference of Optical Communications, Copenhagen, Denmark, 1981

15) T. Matsumoto, "Bandwidth Estimation of Multispliced GRIN Fibers," Applied Optics, Vol. 21, No. 11, p. 1956, June, 1982.

## TABLE 1

Relative Improvement in Fiber Differential Mode Attenuation

| | 850nm, dB/km | 1300nm, dB/km |
|---|---|---|
| 2-3 Years Ago | 0.5 - 2.0 | 0.75 - 2.0 |
| Present Fibers | 0.1 - 0.4 | 0.2 - 0.6 |

NOTE: The values in the table are the difference, in dB/km, of attenuation measurements using uniformly excited and restricted launching conditions.

# BANDWIDTH STUDIES OF CONCATENATED MULTIMODE FIBRE LINKS

J.V.WRIGHT and B.P.NELSON

BRITISH TELECOM RESEARCH LABORATORIES, MARTLESHAM HEATH, IPSWICH, UK

Introduction: A difficult problem facing the designer of high bit-rate multimode systems is that of fibre bandwidth specification. For economic reasons, he must reject only those fibres from a jointed link which would otherwise prevent the necessary system bandwidth being achieved. The factors which are important in determining the resultant bandwidth include mode coupling, differential mode attenuation and the equalisation of modal delays between adjacent fibres. The first two effects may operate throughout the length of the fibre (due to micro-bending for instance) or be localised at the joints. Further complications arise because the bandwidth of a fibre is sensitive to the exact launch conditions and also to its enviroment, if this introduces significant micro-bending. These problems have been studied at BTRL over a number of years using a variety of dispersion and differential mode delay measurements (DMD) [1] on a number of different fibre links. The results of our most recent studies will be compared to our earlier work.

Experimental: The source for both dispersion and DMD measurements was a mode-locked, Q-switched Nd:YAG laser which generated narrow pulses (130ps FWHM) at 1.06μm. After a single pass through a Raman generating monomode fibre [2,3], pulses tunable over the wavelength range 1.06 to 1.6μm were selected by a monochromator. To maintain standard launch conditions, the output of the monochromator was coupled into each fibre via a step-graded-step mode scrambler using a V-groove joint.

All dispersion measurements were made in the time-domain with results collected using a combination of analogue and digital averaging. Bandwidths were provided by discrete Fourier transform techniques. The selective excitation for the DMD measurements was achieved using the output of a monomode fibre imaged onto the core of the multimode fibre. Again these measurements were made in the time-domain because experience showed that too much information was lost in the frequency-domain measurement.

Results: Our latest measurements have been made on a link of high bandwidth germanium doped fibres (NA = 0.20), made by Corning using the OVPO process. The link contained 15 fibres in loose tube packaging (which alleviated drum effects) and fusion spliced to give a total length of 16.2km. Initially the bandwidth of each fibre was measured as a function of wavelength over the range 1.06 to 1.6μm. Bandwidth spectra for 10 of the fibres are shown in Fig 1 where they have been arranged into two sub-groups of 5 fibres each. The first sub-group was chosen, as far as possible, to contain fibres whose bandwidth spectra peaked around 1.3μm. The other sub-group was chosen to contain fibres whose spectra peaked alternately on either side of 1.3μm. The first arrangement of fibres would be appropriate to links made from the fibres of a manufacturer who was achieving a uniform product optimised for 1.3μm operation. Whereas the second arrangement gives the greatest opportunity for the equalisation of modal delay between adjacent fibres [4].

The resultant bandwidth spectrum of each sub-group is shown in Fig 2. A peak bandwidth of 480MHz is achieved with the first sub-group whereas the "alternated" sub-group achieves a peak greater than 600MHz (the average fibre bandwidths at 1.3μm were 1380 and 1000MHz respectively). More detail is given in Table 1, which is expressed in terms of the concatenation exponent q [5], defined by

$$(B_{total})^{-1/q} = \Sigma (B_{individual})^{-1/q}$$

where B is the 3dB optical bandwidth.

A number of general features are apparent. The smallest values of q are observed in the sub-group of alternated fibres. Indeed, zero values of q are recorded which indicate that the resultant bandwidth is greater than the smallest individual bandwidth. This is a result of modal equalisation which is most marked at 1.33μm where the adjacent fibres have bandwidths of similar magnitude but spectral bandwidth curves of opposite slope. The value of q tends to increase with the number of sections, rising to 0.3 after 4 or 5 sections. This arises because perfect equalisation is not maintained throughout the link. Degradation occurs when the mode delays become scrambled (in the sense that the delay is no longer a monotonic function of mode-number). This scrambling may be introduced by "profile errors" in the fibres or by mode coupling at the joints [6,7].

Now although the scrambling is detrimental to an alternated or equalised link, it is beneficial to a link of similar fibres. Without any scrambling effects, a perfect link of identical fibres would have an exponent q=1. In a practical situation, mode coupling at the joints and profile differences reduce the value of q towards a lower limit of 0.5 (square-root broadening). This reduction will be most marked at the wavelengths where the fibres introduce the maximum amount of scrambling. We may expect this where the bandwidth peaks. In this region, the delay vs. mode-number curve changes slope and folds back on itself. Slight profile differences will then introduce significant scrambling which is evident in sub-group 1 where q reduces to a value of 0.64 after 5 sections.

Table 1, Concatenation exponents q

| | Sub-group 1 | | | | Sub-group 2 | | | |
|---|---|---|---|---|---|---|---|---|
| | λ = 1.06 | 1.20 | 1.33 | 1.60μm | λ = 1.06 | 1.20 | 1.33 | 1.60μm |
| section = 2 | 1.04 | .68 | .80 | .70 | .77 | 0 | 0 | 0 |
| 3 | 1.01 | .75 | .58 | .71 | .76 | 0 | 0 | .93 |
| 4 | .97 | .80 | .63 | .74 | .79 | .57 | .30 | .80 |
| 5 | .93 | .84 | .64 | .72 | .80 | .56 | .29 | .71 |

For a final series of measurements, sub-groups 1 and 2 were jointed to give an 11km link, and this was further extended to 16.2km using a mixed sub-group of 5 fibres which did not fall into either category 1 or 2. At 1.33μm, bandwidths of 353MHz and 192MHz were measured after 10 and 15 sections, corresponding to q-values of 0.49 and 0.64 respectively.

Discussion: Previous measurements on high bandwidth multimode links at 1.3μm had revealed an almost linear extrapolation law [7] and this behaviour was dominated largely by the presence of pre-pulses in the impulse response function (IRF), caused by a dip in the refractive index profile. The present measurements were made on fibres which had no refractive index dips or pre-pulses and very good extrapolation laws were obtained. This indicates the importance of rejecting fibres containing spurious structure in the IRF from high bandwidth systems.

Acknowledgements: We gratefully acknowledge BICC and Plessey Ltd. for helpful discussions and the loan of Corning fibre used in our measurement programme.

References: [1] L.Jeunhomme and J.P.Pocholle; Applied Optics 17, 463, 1978
[2] R.K.Jain et al; Appl. Phys. Lett. 30, 162, 1977
[3] K.I.White et al; Radio and Electronic Eng. 51, 385, 1981
[4] M.Eve; Opt. and Quant. Electron. 10, 41, 1978
[5] S.Suzuki et al; Fifth ECOC 12.6, Amsterdam, 1979
[6] J.V.Wright et al; Sixth ECOC 13.1, York, 1980
[7] J.V.Wright and B.P.Nelson; Seventh ECOC 4.2, Copenhagen, 1981

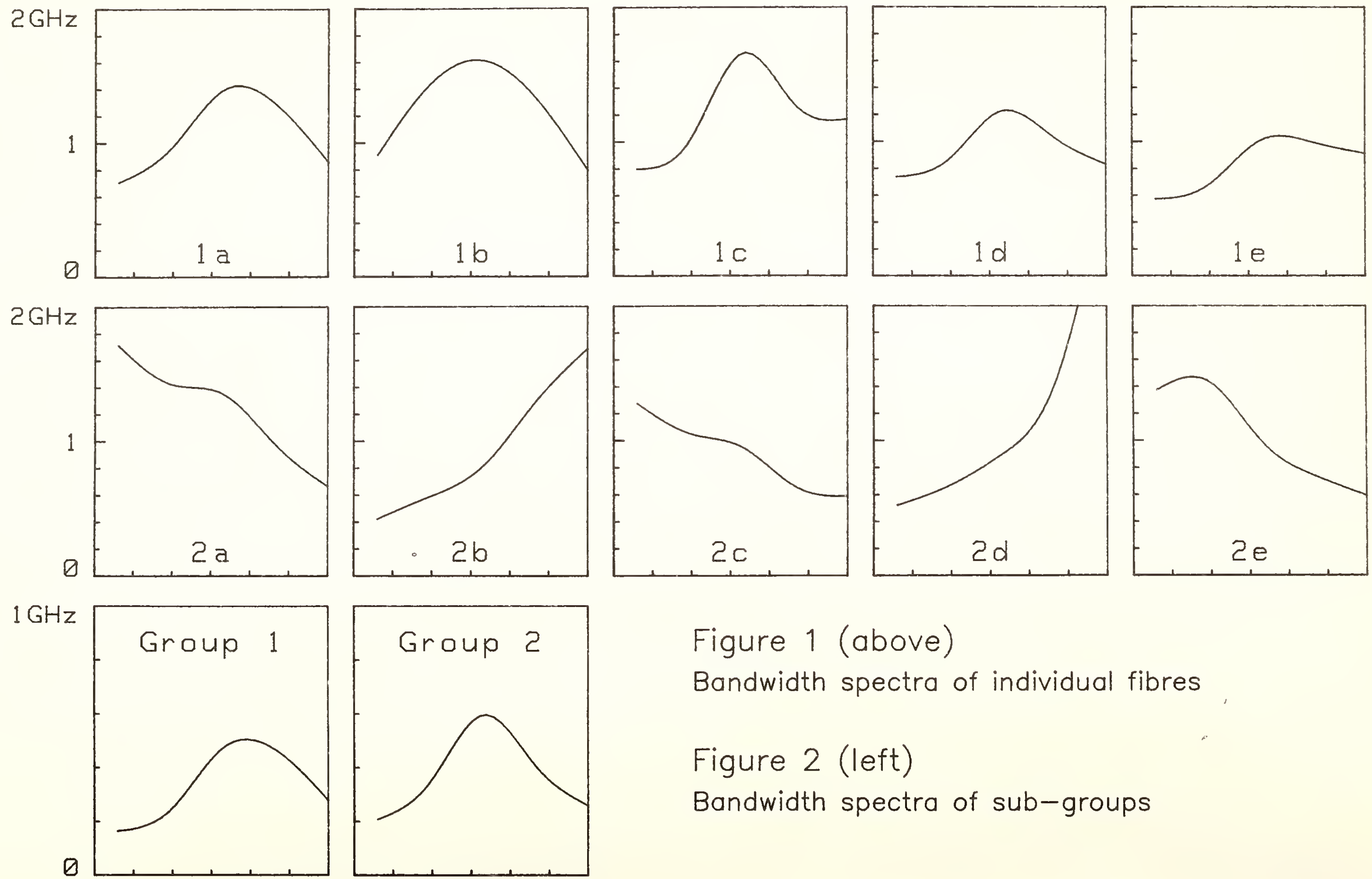


Figure 1 (above)
Bandwidth spectra of individual fibres

Figure 2 (left)
Bandwidth spectra of sub-groups

All horizontal scales are wavelengths, from 1.0 to 1.6 microns

# Determining the Concatenated Dispersion of Multimode Fibres

R.W BLACKMORE AND N.G. BATTY

PLESSEY TELECOMMUNICATIONS RESEARCH LTD., U.K.

Most multimode fibres have discrete defects in their profiles such as the central dip, and such a defect introduces a small shift in the mean group velocity of a small number of modes from the mean velocity of the main group. This results in the modes travelling as two separate groups, so that a small pulse is produced in the impulse response of a single length of fibre. Experience has shown that when lengths of such fibres are spliced together the overall impulse is of the form of figure 1, in which there is a series of side pulses of decending order. J. Wright et al (1) suggested that this could be explained by assuming 50% of mode mixing at each splice, so that there is a continual interchange of energy between the two modal groups. As it is not possible to accumulate enough fibres to explore experimentally the effect of variations in the magnitude and displacement of the minor group on the concatenated bandwidth, a computer simulation based on this relatively simple concept, was established to determine the variation.

To demonstrate that the simulation produces satisfactory results, comparison is made in figure 2 of measured and simulated accumulations of bandwidth with fibre length. Their shapes are very similar, starting with a slope around unity that falls to a value of 0.65 for the measured group and 0.7 for the simulation after ten lengths. Having shown that the model produces a sensible output, it is used to determine the effect on the overall bandwidth of ten lengths of fibre whose impulse responses have minor pulses of 5, 10 and 15% of the main energy separated up to 1.5ns from the main pulse. The data produced by the simulation is presented in figure 3 and that shows that there can be a variation of two to one bandwidth. Each of the fibres used in the model would have had a bandwidth of 1GHz, and thus it is demonstrated that bandwidth is not a suitable parameter for determining the dispersion of individual length of fibre.

The cause of variation in the concatenated bandwidth can be identified in the impulse response, so that it would seem preferable to use a time domain function for the evaluation of the performance of an individual length. The impulse response itself is not a suitable function, because its often irregular shape makes it difficult for making comparisons. A better function to use is the autocorrelation function of the impulse response, because it is normalised to its value at zero, and thus produces a clear datum line from whcih to make evaluations. It has the further advantage that:

1) It smooths out many of the irregularities, making it easier for making comparisons.
2) Its Fourier transform is the power spectral density function.

Thus it can be readily derived from the deconvolved frequency response of a measured impulse response or from a directly measured frequency response.

The autocorrelation furnction of the concatenated impulse response smooths the series of side pulses into functions with 'tails', and these 'tails' have marked influences on the corresponding frequency response. In order to establish a relationship between the 'tail' length and the frequency response, functions of the type $(mt)^m \exp(-mt)$ were used to simulate time functions with 'tails'. Three such autocorrelation functions are produced in figure 4, and are compared with the autocorrelation of the Gaussian functions that have the same electrical bandwidth i.e. the 3dB point on the electrical response produced in the measurement. In each instance the two functions intersect at approximately the 10% value. Thus there is a strong relationship between the interval to the 10% height of the 'tail' and the electrical bandwidth. As the 'tail' is produced by the spurious pulses, it follows that these pulses have a marked influence on the overall bandwidth. Figure 5 shows the relationship between the tail length and the fibre length for a measured result, and it too has a slope of 0.65. Providing the spurious pulses is greater than 10%, the line intersects with the 10% value for the first length, showing this close relationship between the spurious pulse and bandwidth. However spurious pulses of less than 10% have significant influence on the performance, therefore a lower limit of 5% is suggested. The broken line of figure 3 gives the bandwidth derived from the autocorrelation functions for 10% spurious pulses. Compared with the directly derived results, the indirect method produces pessimistic values, but a suitable correction can be applied that produces EFFECTIVE BANDWIDTH = $0.3dBm + .454T^{-1}$, where Bm is the measured bandwidth of the fibre and T is the interval to the 5% height of the autocorrelation function. Using the appropriate law of concatenation it is then possible to derive the EFFECTIVE BANDWIDTH of concatenated lengths. This together with measured results will be discussed.

ACKNOWLEDGEMENT

The authors wish to thank the directors of the Plessey Company for permission to publish.

(1) Bandwidth studies of Joined Multimode Fibres - J.V. Wright and B.P. Nelson E.C.O.C. 1981 (COPENHAGEN).

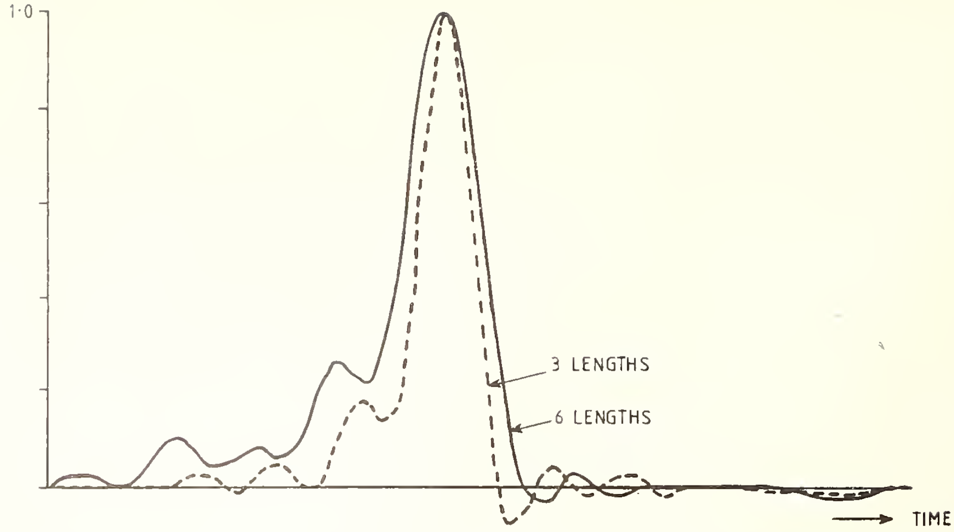


FIG.1 MEASURED IMPULSE RESPONSE OF CONCATENATED FIBRES

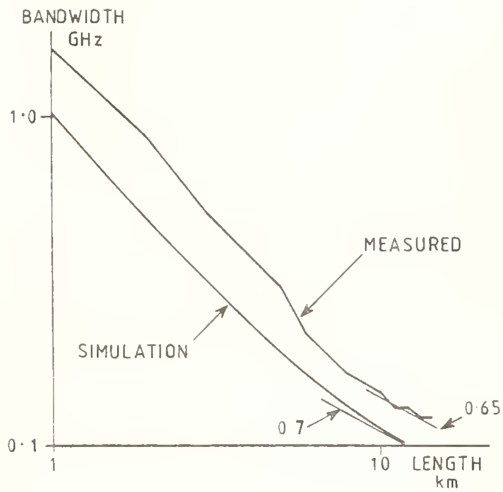


FIG. 2 ACCUMULATED BANDWIDTHS

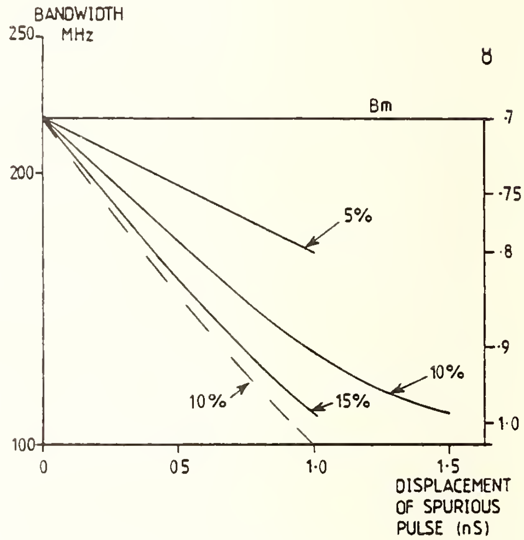


FIG. 3 EFFECT OF SPURIOUS PULSE ON CONCATENATED BANDWIDTH

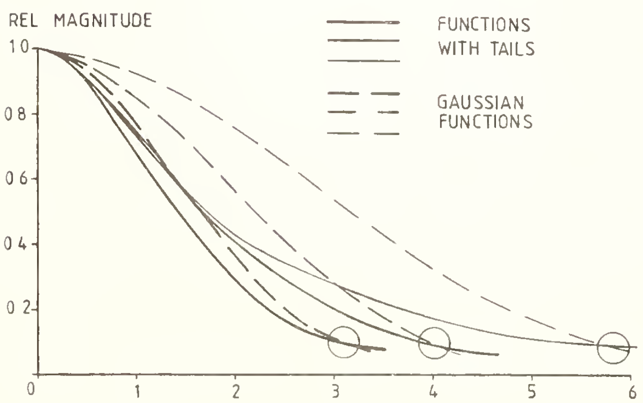


FIG. 4 COMPARISON OF AUTOCORRELATION

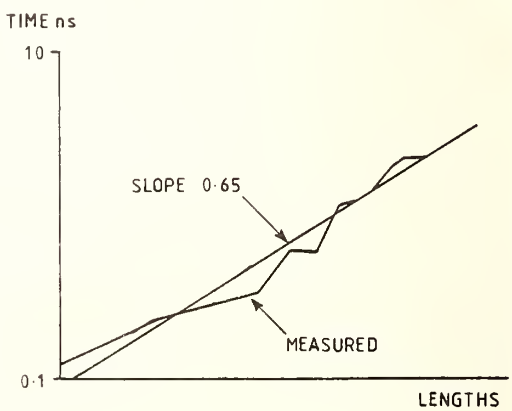


FIG. 5 ACCUMULATED AUTOCORRELATION LENGTHS

# IS THE -6 DB BANDWIDTH FIBER SELECTION CRITERION STILL VALID?

R. Bouillie
J. C. Bizeul
Division R.O.C., 22301 Lannion, France

## INTRODUCTION

The commercial availiability of graded index multimode fibers with a very low attenuation (0,7 dB/km) at 1,3 µm, allows for a near feature the installation of high speed systems ( ⩾ 140 Mb/s on long repeater sections (25 km, for the French experimental line LE MANS-ANGERS).

The optical power budget indicate that the limitative factor, for these systems, is the baseband response of the concatenated link. The precise knowledge of the attenuation/frequency characteristic for each fiber is therefore, of paramount importance.

We proposed in this paper a new criterion for the selection of fibers to be used for long repeater section systems, which is independant from the classical -6 dB cut-off frequency.

## Measurements on individual fiber lengths

The reported results in this paper have been obtained using indifferently time-domain or frequency-domain measurements. These two techniques give reliable and comparable results (± 10 MHz) when using the same source, launching conditions and detection.

From a batch of 30, 2,2 km, fibers produced by two manufacturers and optimised for 1,3 µm, we have recorded the baseband frequency response for each fiber length. From the results, the fibers can be classified in two categories :

a) - Those with a perfectly smooth curve all over the frequency range (fig. 1)

b) - Those with a "bumpy" frequency characteristic as shown on fig. 2, which corresponds, in time-domain to the appearance, at the fiber output, of precursors. This classification is not directly comparable with one done on the - 6dB cut-off frequency. Figure 3 presents a smooth and a "bumpy" curve for 2 fibers which have the same - 6 dB value.

On our batch of fibers 40 % belongs to the smooth category.

## Measurements on concatenated links

From the previous results we have selected 11 fibers in each categorie (a) and (b) and we have spliced them to obtain two links of 24,2 km. The - 6 dB cut-off frequency for each fiber lenght is on the order of 700 MHz. The overall attenuation of the concatenated links is 27 dB.

Figure 4 presents the frequency response for the two links. The one with the "smooth" fibers has a - 6 dB cut-off frequency of 140 MHz. The one with "bumpy" fibers has 60 MHz. Obviously the use of fibers with a regular characteristic give a much wider bandwith than with "bumpy" fibers, even though the individual fibers have the same cut-off frequency.

The absence of "bumpy" region in the fiber characteristic is a parameter of great importance to obtain large bandwith on concatenated links.

## Theorical model

We tried to apply the linear four poles theory to the optical fibers, making the summation (in dB) of all the fibers characteristics belonging to the concatenated links.

The cable below shows for the "smooth" fibers the comparison for different lengths between measurements and computed results.

| Length (km) | Measured (MHz) | Calculated (MHz) |
|---|---|---|
| 6,6 | 310 | 305 |
| 13,2 | 260 | 250 |
| 19,8 | 180 | 175 |
| 24,2 | 140 | 135 |

We found a very good agreement between model and measurements.

For the "bumpy" fibers the fitting was not good at all. We draw the conclusion that for fibers with a regular characteristic the linear four poles theory can be applied.

## A new criterion for the fiber selection

The previous results show that a simple classification of the fibers on their -6 dB value is absolutly insufficient to insure large bandwith on long lengths. A particular attention must be paid to the smoothness of the frequency characteristic. One must eleminate all the fibers with holes in their characteristics in the range of the system frequency.

The formula below gives the maximum acceptable holes amplitude (A) in the "bumpy" frequency characteristic for a given system frequency (F). If (B) is the attenuation provided at (F) by the system design :

$A = \frac{B}{N}$ where N is the number of the cable lengths which constituted the link.

## Conclusion

A new criterion for the selection of optical fibers is proposed. The -6 dB characteristic is not yet considered as being an important parameter, it is now replaced by the regularity of the frequency characteristic in the system frequency range where the fibers are to be used. A formula for the maximum acceptable holes amplitude for each fiber length is established. A theorical model based on the linear four poles theory gives in the case of regular fibers, a solution to the cancatenated link problem.

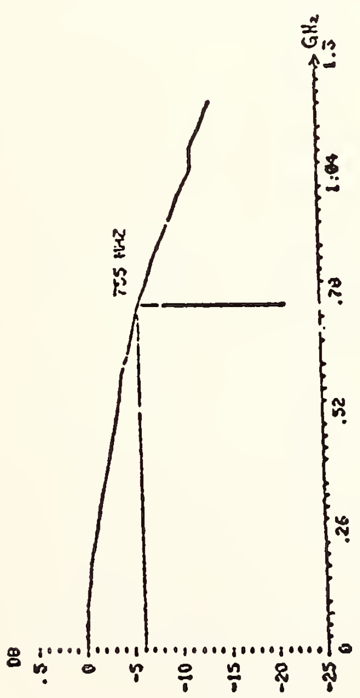

Figure 1

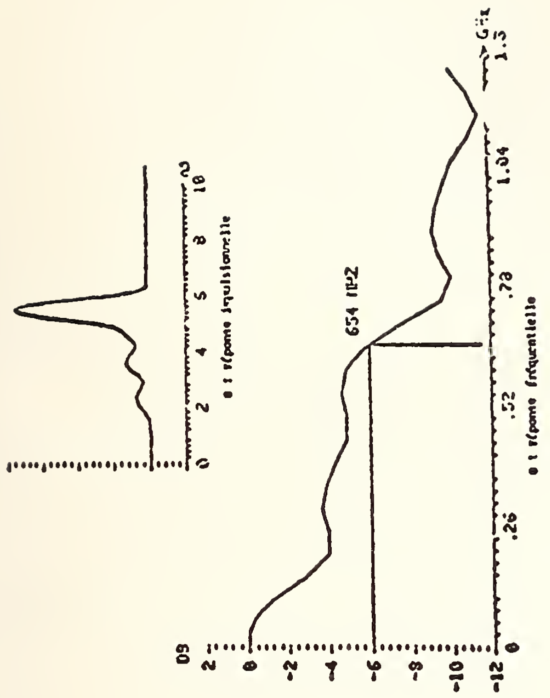

Figure 2

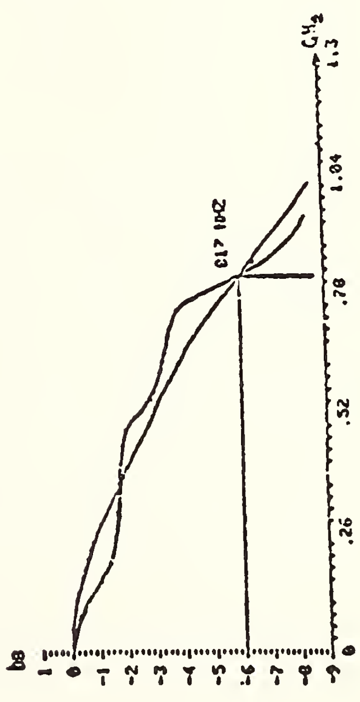

Figure 3

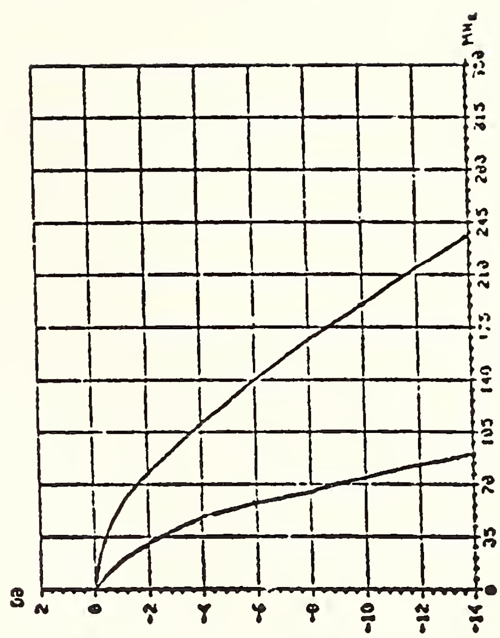

Figure 4

# INVESTIGATION ON LAUNCHING CONDITIONS IN THE BANDWIDTH MEASUREMENT OF GRADED-INDEX FIBERS

M. Nishimura and S. Suzuki

Sumitomo Electric Industries, Ltd.

1, Taya-cho, Totsuka-ku, Yokohama, Japan

## Introduction

Accurate measurements of the baseband frequency response of graded-index fibers are required both for quality assurance of fiber cables and for design of fiber transmission systems. As is well-known, the measured bandwidth is strongly affected by the launching conditions, that is, how the launched optical power is distributed among the propagating modes. This paper describes the experiments showing the dependence of the bandwidth upon the launching spot size and numerical aperture (NA). It is also reported that theoretical analysis can explain the experimental results especially for MCVD fibers.

## Experiment

Two launching systems with different launching spot size and NA were prepared. They are illustrated in Fig. 1. The output of a mode scrambler is imaged by a couple of microscope objectives on the launch end of a test fiber. Those objectives and an aperture placed between them were chosen in each system so as to realize the launching conditions summarized in Table 1.

Ten graded-index fibers were measured with these two launching systems by the swept-frequency method. Five fibers among them were MCVD fibers and the others were VAD fibers. Figure 2 shows the values of the measured bandwidths. Examples of the frequency response waveforms are shown in Fig. 3. From Fig. 2 it is found that the bandwidths of some of MCVD fibers tend to decrease when the launching spot size is reduced to 25 μm and the launching NA is 0.1. On the contrary, in the case of VAD fibers the measured bandwidths are unchanged or slightly increased. The averaged relative difference of the bandwidths between the two launching conditions is -11% for MCVD fibers, and +4% for VAD fibers.

## Theoretical Analysis

Influence of the launching conditions upon the baseband frequency response of a graded-index fiber with a central dip was investigated by using the finite element method.[1] Such index distribution are well simulated by the function as

$$n(r)^2 - n_c^2 = 2\Delta n_c^2\{1 - (\frac{r}{a})^\alpha\}\{1 - \exp(-\frac{r^2}{w^2})\},$$

where $n_c$, $\Delta$ and a denote the refractive index of the cladding, the relative index difference and the core radius, respectively, $\alpha$ is the power-low parameter and w is the dip width.

The impulse response can be calculated by summing up all the propagating modes whose group delay time is computed by FEM. The baseband frequency response can be obtained from the impulse response using FFT techniques. In the calculation differential mode attenuation was taken into account. Besides modes with high principle mode number (PMN), modes with the lowest azimuthal mode number ($\nu = 0$) were assumed to suffer high loss, since irregularity of the dip tends to scatter these modes whose field amplitudes are maximized near the center.

Examples of the numerical results are shown in Figs. 4 and 5. Calculated mode group delays for a profile with $\alpha = 1.95$ and $(w/a) = 0.05$ are plotted as a function of PMN in Fig. 4. Solid curves in Fig. 5 show the impulse response and the baseband frequency response computed from Fig. 4 assuming that all propagating modes are equally excited at the launch end. Broken curves and dash-dotted curves represent the response waveforms when assumed that excited modes are restricted to only modes with normalized PMN less than 0.5 and 0.25 respectively.

By comparing these response waveforms, it is found that

(1) the relative amplitude of the fast-arriving pulse (mainly consisting of mode with $\nu = 1$) increases, and

(2) the 6-dB electrical bandwidth decreases,

as the excited modes are restricted to modes with low PMN. Further calculations have suggested that this tendency is almost always found independent of slight variation of $\alpha$ as far as a dip exists, unless the modes with $\nu = 1$ are assumed to be strongly attenuated by the dip.

## Conclusion

From the experiments it has been found that in some cases the bandwidths of graded-index fibers with a dip decrease when measured with small launching spot size and small NA. Theoretical analysis has revealed that this phenomenon is due to the existence of the fast-arriving pulse peculiar to such fibers.

## Reference

[1] K. Okamoto, "Comparison of Calculated and Measured Impulse Responses of Optical Fibers", Appl.Opt., Vol. 18, No. 13, P. 2199 (1979).

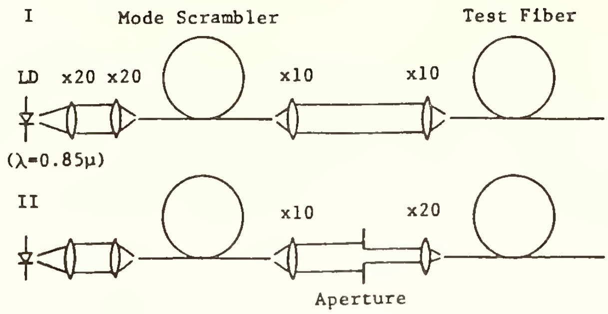


Fig.1. Launching systems used in the experiment.

| | Spot size | NA |
|---|---|---|
| I | 50um | 0.20 |
| II | 25um | 0.10 |

Table I Characteristics of launch spot in the launching systems shown in Fig.1.

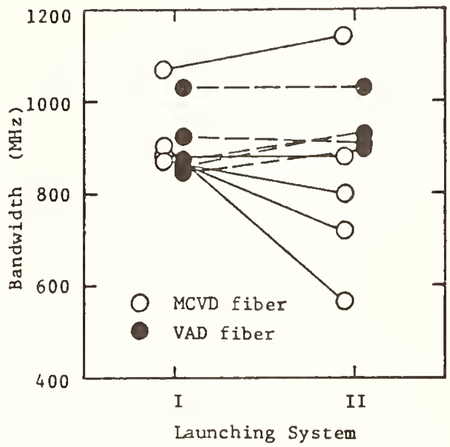


Fig.2. Bandwidths of 10 graded-index fibers measured using the launching systems shown in Fig.1.

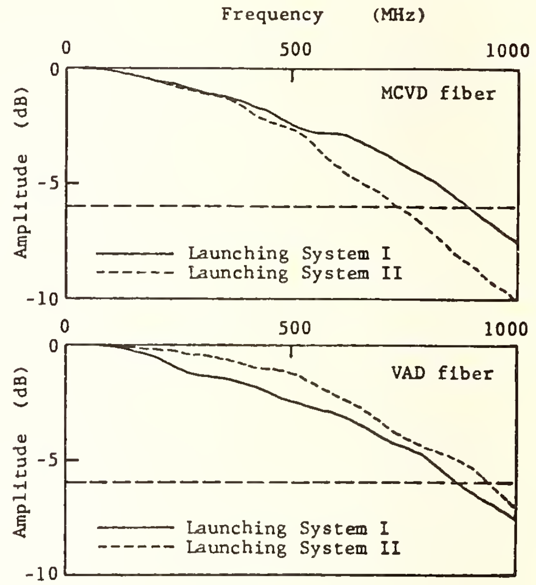


Fig.3. Examples of measured base-band frequency response.

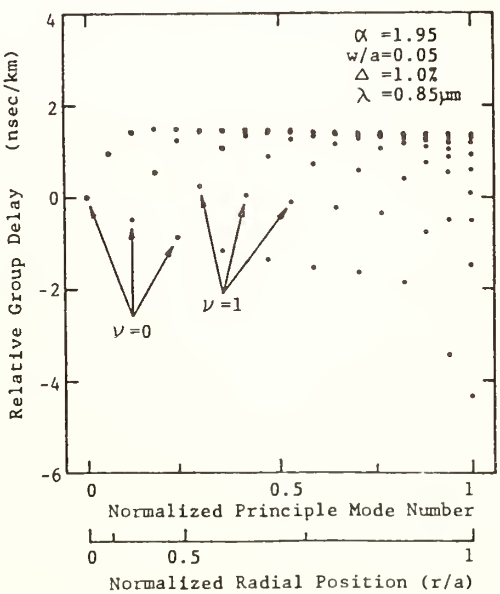


Fig.4. Mode group delays calculated for α=1.95 profile with a dip.

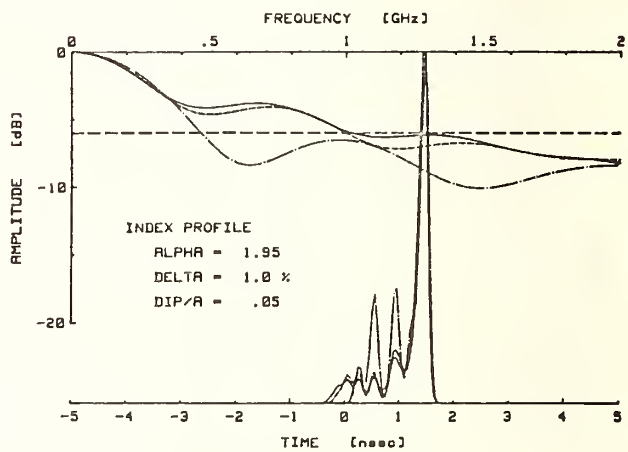


Fig.5. Impulse responses and baseband frequency responses calculated from Fig.4 assuming different exciting conditions

# RESULTS OF A BELL SYSTEM BANDWIDTH MEASUREMENT ROUND ROBIN

F. T. Stone
Bell Laboratories
Norcross, Georgia 30071

Recently a multimode-fiber bandwidth-measurement round robin was conducted among several locations of Bell Laboratories and Western Electric. Analysis of the results has clarified some of the problems in obtaining agreement between test sets. The five participants measured the seven fibers in the study three times each. Fibers 1-5 had low OH content and were measured at both short (825 nm) and long (1300 nm) wavelengths. Fibers 6 and 7 had high OH content and were only measured at the short wavelength. The instructions requested that the participants overfill the fiber, use a mandrel wrap (3 turns around a 20-mm-diameter mandrel) at the input end, and break off a piece of the input end containing the mandrel for the short length measurement (without disturbing the launch conditions). All test sets operated in the time domain.

Table I summarizes the results. The long wavelength measurements experienced a considerably lower $\sigma/\mu$ (5.6%) than the short wavelength measurements (17.9%). Overall, $\sigma/\mu$ was 12.7%. Participant 3 used the anti-Stokes radiation from a fiber-Raman laser to perform the short wavelength measurements. If those results are excluded, the overall $\sigma/\mu$ was 9.9% and the short wavelength $\sigma/\mu$ was 12.9%, which is comparable to the $\sigma/\mu$ achieved in an earlier NBS-coordinated round robin involving short wavelength diodes.[1]

TABLE I

Average($\mu_i$)/Standard Deviation($\sigma_i$) of Three 3-dB-Bandwidth Measurements (in MHz). Short Wavelength Measurements are on Top. The Last Column Gives the Average $\mu = \Sigma\mu_i/5$, the Interlocation $\sigma = [\Sigma(\mu_i-\mu)^2]^{1/2}/4$, and the Ratio $\sigma/\mu$ in Percent.

| Participant i = | 1 | 2 | 3 | 4 | 5 | Average |
|---|---|---|---|---|---|---|
| Fiber 1 | 906/39 | 852/28 | 1019/22 | 849/29 | 822/88 | 890/78/8.8% |
| | 1023/24 | 1037/56 | 1065/23 | 1068/30 | 1203/24 | 1079/72/6.6% |
| 2 | 675/12 | 627/22 | 710/24 | 602/18 | 740/43 | 671/57/8.5% |
| | 292/4 | 313/6 | 311/9 | 316/5 | 313/11 | 309/10/3.1% |
| 3 | 296/13 | 291/12 | 290/4 | 272/11 | 330/16 | 296/21/7.2% |
| | 505/6 | 563/9 | 614/5 | 661/17 | 582/11 | 585/58/9.9% |
| 4 | 274/1 | 279/5 | 234/10 | 247/2 | 266/4 | 260/19/7.3% |
| | 135/1 | 144/3 | 125/3 | 143/6 | 137/4 | 137/8/5.6% |
| 5 | 620/16 | 491/30 | 378/20 | 526/206 | 715/15 | 546/128/23.4% |
| | 462/8 | 480/4 | 473/3 | 454/15 | 466/10 | 467/10/2.1% |
| 6 | 398/16 | 375/14 | 200/5 | 363/21 | 390/11 | 345/82/23.8% |
| 7 | 526/11 | 257/6 | 236/20 | 293/14 | 633/63 | 389/179/46.0% |

One observation from this round robin is that fibers exhibiting bimodal behavior can be extremely sensitive to excitation conditions and, for short wavelength measurements, source spectral width. The three measurements of Table I with $\sigma/\mu > 10\%$ were on such fibers. Figure 1 illustrates the sensitivity of fiber 7 to launch conditions. The mode scrambler launched additional energy in the secondary peak, which significantly affected the 3-dB bandwidth. Participants 1 and 5, who did not use a mode scrambler, measured high bandwidth values (Table I). Participants 3 and 4 used a mode scrambler and measured lower values. Participant 2 measured low values but did not use a mode scrambler. Possibly, as discussed below, the larger spectral width of the source used by that participant produced the low measurement values. Figure 2 indicates that the higher short-wavelength bandwidths measured on fiber 5 by participants 1 and 5 persist even after a mode scrambler is inserted. In addition to being sensitive to excitation conditions, however, fibers with double-peaked pulse shapes such as in Figure 2 can have an extreme sensitivity to source spectral width: a small increase can lower the first dip in the transfer function below the 3 dB level and halve the measured 3-dB bandwidth. Participants 1 and 5 used sources with a narrow spectral width, participants 2 and 4 used sources with a wider spectral width, and participant 3 used a fiber-Raman laser with the widest spectral width. The short wavelength results in Table I are consistent with these relative widths. These results suggest that achieving better than 10% agreement among test sets will require more careful control over launch conditions and, for short-wavelength measurements, source spectra.

I gratefully acknowledge the efforts of Doug Head, Bill Reed, and Laura Short of Bell Labs and Mary Potasek and Ron Smith of Western Electric, who performed the measurements reported in Table I.

1. D. L. Franzen et al., Appl. Opt. 20, 2412 (1981).

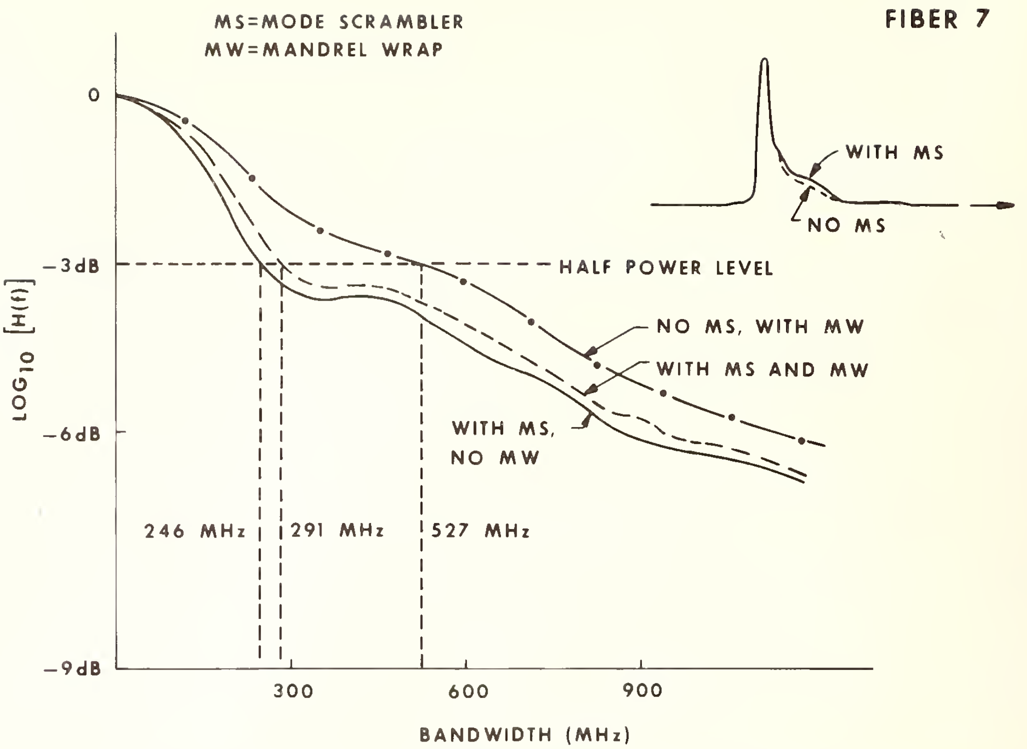


FIGURE 1. TRANSFER FUNCTION H(F) AND PULSE SHAPES OF FIBER 7 MEASURED AT 825nm UNDER A VARIETY OF LAUNCH CONDITIONS.

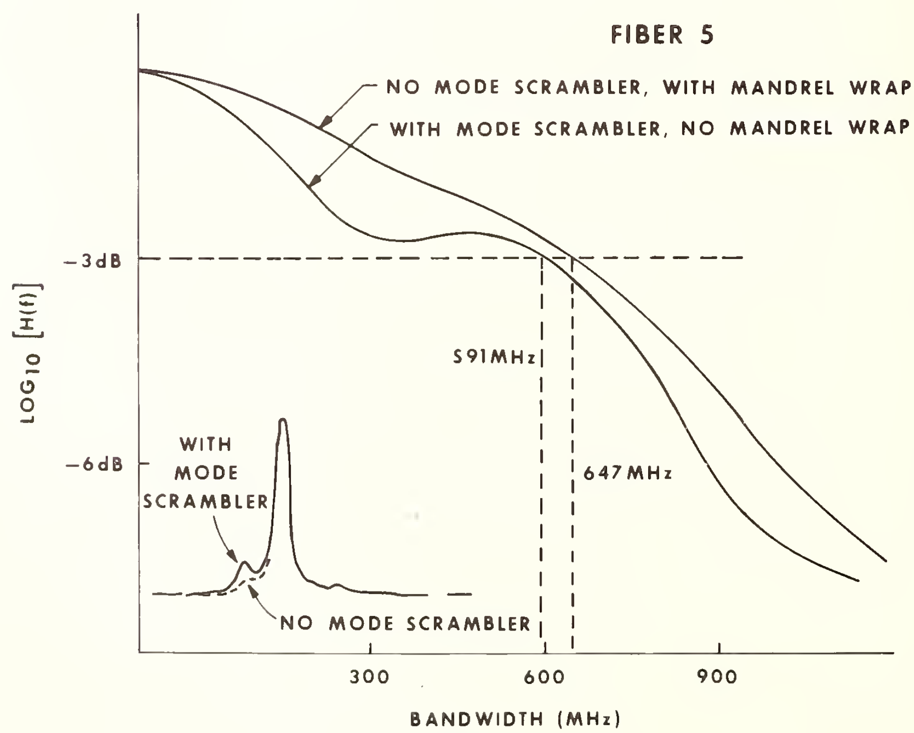


FIGURE 2. TRANSFER FUNCTION AND PULSE SHAPES OF FIBER 5 WITH AND WITHOUT A MODE SCRAMBLER.

# Wavelength Dispersion Measuring Equipment

J. Saito T. Oki H. Yamamoto

Ando Electric Co., Ltd.

19-7 Kamata-4chome Ota-ku Tokyo Japan

## 1. Introduction

Baseband frequency response of graded-index multimode fibers depends on several dispersion factors; intermodal, material and construction dispersion. Generally, in graded-index multimode fibers, intermodel dispersion > material dispersion > contruction dispersion. Therefore, baseband frequency response depends mainly on intermodal dispersion. However, recently, the characteristics of graded-index multimode fibers have been improved so that material and construction dispersion are not negligible.

In this paper, equipment designed to measure the wavelength dependent dispersion of multimode fibers is described. (Wavelength dependent dispersion of multimode fibers is related to material and construction dispersion.) Measurement method of this equipment is as follows. Intensity modulated optical signals from various wavelength LEDs are emitted into the fiber under test. The output end of the fiber is connected to a monochromator which uses a pair of fibers to select two close wavelength from the incoming wavelengths. These two optical signals from the fiber are demodulated by APDs and a Vector Voltmeter which measure the phase difference between the signals. The wavelength dependent dispersion is then obtained to calculate the phase difference of these two signals.

## 2. Principle

A block diagram of this equipment is shown in Fig. 1. Each LED light source is intensity modulated by a sine waveform and one of the optical signals is emitted into the fiber under test. The spectral width of the LED is rather broad, so while the optical signal propagates through the fiber, a propagation time difference occurs in every spectrum of the LED.

In the receiver, a monochromator is used to select two close wavelength ( $\lambda_1$, $\lambda_2$ ). Then it selects the spectrum of the LED which has propagated through the fiber.

These two optical signals are modulated by a sine waveform and the resultant propagation time difference is regarded as the phase difference ( $\psi$ ) of the modulated waveform. Therefore the wavelength dependent dispersion D of a fiber is described in equation (1).

$$D = \frac{\psi}{L \cdot 2\pi f \cdot |\lambda_1 - \lambda_2|} \quad (ps/km \cdot nm) \quad \cdots\cdots\cdot \ (1)$$

where L = Optical fiber length (km),
f = Modulation frequency (Hz) and
$\lambda_1$, $\lambda_2$ = Wavelengths (nm).

The wavelength dependent dispersion is obtained by measuring both phase difference ($\psi$) and wavelength difference ($\Delta\lambda = \lambda_1 - \lambda_2$).

## 3. Measuring Equipment

### 3.1 Transmitter

The transmitter of this equipment has eight LEDs in which the center wavelengths are 729, 798, 850, 889, 1060, 1145, 1255 and 1474 nm. Each LED is intensity modulated by a sine waveform of 50MHz and each optical signal is launched into a fiber to a 8x1 Optical Switch. The individual wavelengths are selected by the switch, and output through a connector.

### 3.2 Receiver

The receiver consists of a Monochromator, APDs, Frequency Converters and a Vector Voltmeter. The received optical signal goes through a pigtail fiber to the Monochromator, which has two pigtail fibers for output, enabling two slightly different wavelengths to be separated from the input LED's wide spectrum. Each electrical signal converted by the APD is then converted into an intermediate frequency by the Frequency Converter. The Vector Voltmeter measures the phase difference between the two intermediate frequencies.

### 3.3 Monochromator

The Monochromator configuration is shown in Fig. 2. The input optical fiber and the concave grating which move around the Rowland Circle are fixed on a plane which rotates on the base corresponding to the wavelength to be set.
Output optical fibers are fixed on the base and also on the Rowland Circle.
In the concave grating, the relationship between the incident angle $\alpha$ and the diffraction angle $\beta$ is expressed in equation (2).

$$\sin \beta - \sin \alpha = \frac{m\lambda}{d} \qquad \ldots\ldots\ldots\ldots\ldots \quad (2)$$

where m = The order (±1, ±2, .....) and

d = Groove spacing (mm).

When a pair of output fibers with a core center spacing of 300 μm are fixed, the wavelength difference (Δλ) between the two diffraction rays separated is expressed as,

$$\Delta\lambda = \frac{d\cos \beta}{m} \cdot \Delta\beta$$

where $\Delta\lambda = |\lambda_2 - \lambda_1|$,

Also, $\Delta\ell = r\cos \beta \cdot \Delta\beta$ where,

$\Delta\ell$ = Core spacing

$r$ = Curvature radius of the concave grating

giving
$$\Delta\lambda = \frac{d\Delta\ell}{mr} \qquad \ldots\ldots\ldots\ldots\ldots (3)$$

Every item on the right of equation (3) is constant. If an aberration has no influence on this diffraction, the wavelength difference should be constant. In this case, the concave grating has a groove spacing of 1/300 mm and a curvature radius of 50 mm. Therefore the wavelength difference Δλ becomes 20 nm by equation (3). Fig.3 shows the wavelength characteristics of the two output type monochromator.

## 4. Results

A wavelength dispersion data of 1 km graded-index multimode fiber of 50/125 μm is shown in Fig. 4. An outside view of this apparatus is shown in Fig.5.

## 5. Conclusions

A wavelength dispersion measurement method is proposed and effective wavelength dispersion measuring equipment has been manufactured.

## 6. Acknowledgements

The authors wish to thank Mr. M. Koyama and Mr. K. Okada of the Yokosuka Electrical Communication Laboratory, N.T.T., and Mr. E. Tanaka of Ando Electric for their great encouragement and useful suggestions.

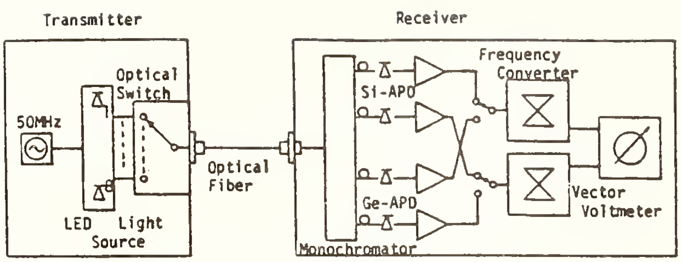


Fig.1 Block Diagram of Wavelength Dispersion Measuring Equipment

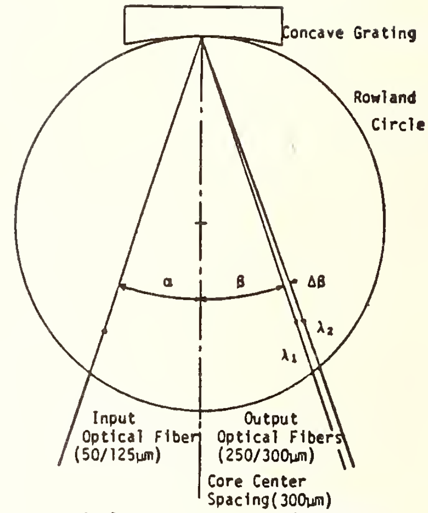


Fig.2 Monochromator Configuration

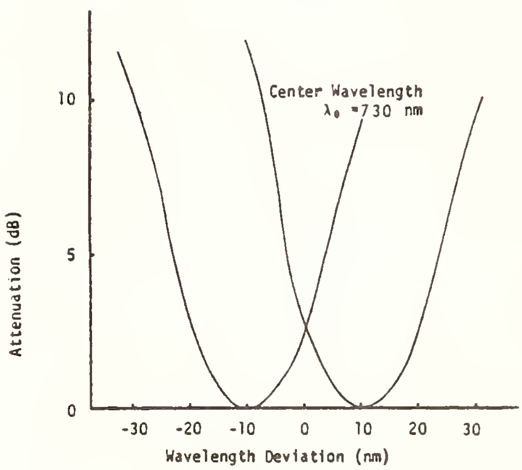


Fig.3 Monochromator Characteristics

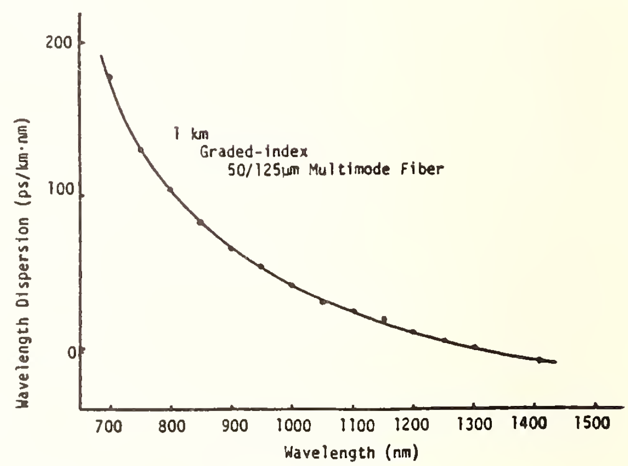


Fig.4 Wavelength Dispersion Data

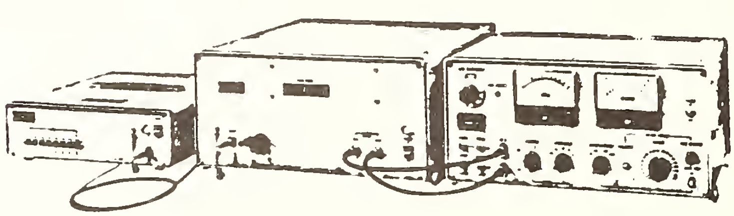

Fig.5 Outside view of Wavelength Dispersion Measuring Equipment

MEASUREMENT OF BANDWIDTH VERSUS IMPULSE RESPONSE WIDTH IN MULTIMODE FIBERS

M. J. Buckler
Bell Telephone Laboratories
Norcross, Georgia, USA 30071

## ABSTRACT

An empirically based relationship, which is simple yet highly correlated, has been found to exist between optical 3dB bandwidth and impulse response RMS pulse width in multimode graded index optical fibers. Experimentation has shown this relationship to be independent of the degree of externally induced mode coupling. Propagation of error analysis was used to find the total $\pm 3\sigma$ limits, and theoretical comparisons are made for three ideal pulse shapes - cosine, raised cosine and gaussian.

## I. INTRODUCTION

Both the time domain and frequency domain fiber transmission characteristics are important for determining maximum and/or optimum bit rate - length systems, for evaluating the possible necessity of line equalization, for fiber parameter optimization, and for engineering fiber routes. Using an empirical approach, we have investigated the relationship between bandwidth and pulse width for graded index multimode optical fibers.

## II. EXPERIMENTAL APPARATUS

Figure 1 shows a block diagram of the impulse response measurement system[1]. A narrow optical pulse (450 psec FWHM) is launched into the fiber; 512 samples are taken per oscilloscope sweep (20nsec full screen) and 64 sweeps are accumulated and averaged. The minicomputer then calculates and stores the Fast Fourier Transform (FFT) for this pulse. A 0.5m reference length is broken off of the launch end of the fiber and similarly measured. The baseband frequency response of the fiber is calculated from the ratio of these two FFTs and the time domain response is found by calculating the inverse FFT of the resultant response. With proper filtering the $\pm 3\sigma$ measurement precision for this measurement set and procedures is $\pm 10$ MHz optical 3dB bandwidth and $\pm 0.01$ nsec RMS pulse width.

## III. RESULTS AND ANALYSIS

A number of experiments were conducted with uncoated fibers (negligible mode mixing), production coated fibers (partial mode mixing), and connectorized cabled fibers ("complete mode mixing") and their respective concatenations. All of the fibers used in these experiments were of the $SiO_2$-$P_2O_5$-$GeO_2$ type with a 0.23 NA. Moreover, for the uncoated fiber experiments low-loss loose tube splices[2] were used so as to achieve minimal modal disturbance. Table I shows the basic fiber and link characteristics for each experiment.

TABLE I EXPERIMENT PARAMETERS

| Fiber Type | Fiber Outer Dia. (μm) | Fiber Core Dia. (μm) | Fiber Length (km) | Maximum Concatenated Length (km) |
|---|---|---|---|---|
| Uncoated | 110 | 55 | 1.0 | 9.0 |
| Coated | 125 | 50 | 1.1 - 2.2 | 8.8 |
| Connectorized Cabled | 110 | 55 | 0.9 | 7.4 |

Evaluation of the data for these three experiments indicated that bandwidth and impulse response width were strongly correlated, regardless of pulse shape. It was found that the best curve fit was a power law of the form

$$y = ax^{b} \tag{1}$$

where y represents optical 3 dB bandwidth (MHz) and x represents RMS impulse response width (nsec). Using a least squares linear regression analysis the best fit values of a and b are given in Table II.

TABLE II BEST FIT POWER LAW CURVE

| Experiment | No. of Data Points | a | b | Correlation Coefficient |
|---|---|---|---|---|
| Uncoated Fiber | 15 | 170.6 | -1.01 | 0.9958 |
| Coated Fiber | 25 | 170.1 | -1.01 | 0.9964 |
| Connectorized Cabled Fiber | 123 | 168.6 | -1.01 | 0.9959 |

Figure 2 shows a plot of the 3 dB bandwidth versus RMS impulse response width data measured for the connectorized cabled fiber experiment.

For ease of application of these results the form of the power law curve fit has been simplified to

$$y = a_1 /x. \tag{2}$$

This is justified in view of the fact that the magnitude of the power law exponent was nearly unity and insensitive to the degree of mode mixing. Refitting the connectorized cable data (since it most nearly approximates the application environment) gives

$$y = (169.1)/x. \tag{3}$$

Using a propagation of error analysis the total $\pm 3\sigma$ uncertainty in $a_1$ due to measurement imprecision and curve fitting was $\pm 11$.

## IV. CONCLUSIONS

These experiments have shown that optical 3 dB bandwidth and RMS impulse response width are highly correlated regardless of the amount of fiber mode mixing. It has been found that for the multimode graded index optical fibers studied here,

$$\text{3 dB Bandwidth (MHz)} = \frac{169 \pm 11}{\text{RMS Impulse Response Width (nsec)}} \qquad (4)$$

with a coefficient of correlation greater than 0.99.

Establishment of this relationship allows the economy of a single simple measurement, while still having the flexibility of making calculations or projections in either the time or frequency domain. For example, using this function, we can now specify with a high degree of confidence, the required 1km bandwidth, for production fibers, necessary to construct various system regenerative repeater spans.

In the presentation, we will discuss the instrumentation, experimental results, and propagation of error analysis which led to this newly found bandwidth versus pulse width relationship. Also, theoretical comparisons will be made for three ideal system response pulse shapes and examples presented to show how this relationship allows us, for the first time, to interrelate transmission system and manufacturing requirements.

### References


1. Dannwolf, J. W., Gottfried, S., Sargent, G. A., and Strum, R. C.: "Optical-Fiber Impulse-Response Measurement System," IEEE Trans. on Instrumentation and Measurement, 1976, IM-25, pp. 401-406.

2. Miller, C. M.: "Loose Tube Splices for Optical Fibers," BSTJ, 1975, 54, pp. 1215-1225.

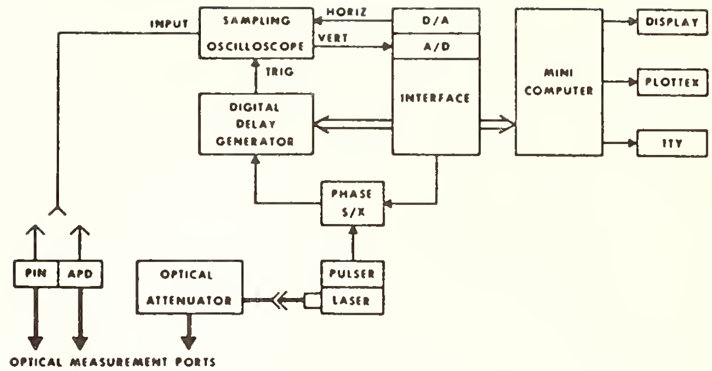


FIGURE 1. IMPULSE RESPONSE MEASUREMENT SET

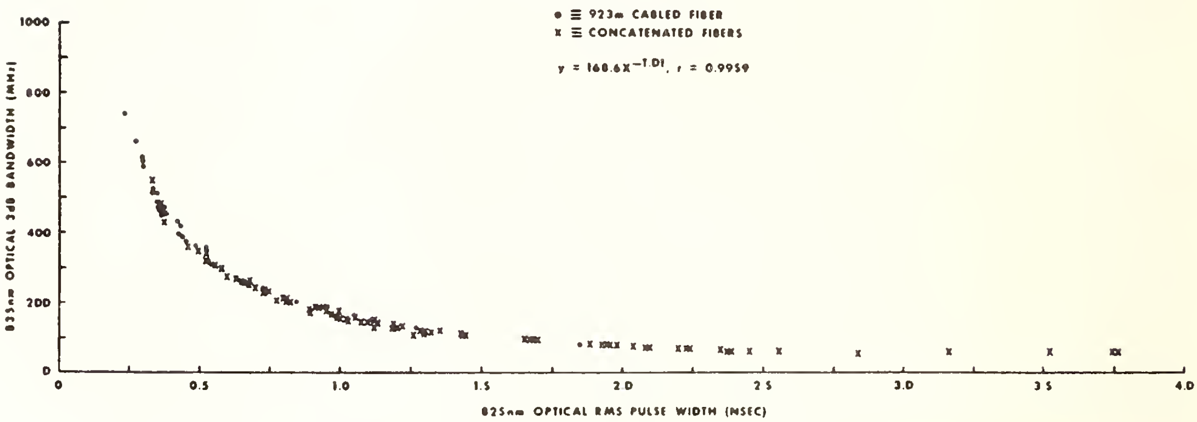


FIGURE 2. BANDWIDTH VERSUS IMPULSE RESPONSE WIDTH DATA FOR THE CONNECTORIZED CABLED FIBER EXPERIMENT

# FIELD MEASUREMENTS OF FIBER OPTIC CABLE SYSTEMS

O. I. Szentesi
Siecor Optical Cable, Hickory, N. C. 28603

## INTRODUCTION

Field testing of fiber optic cable systems is usually performed in order to monitor the fiber splicing process, to ensure that end-to-end transmission specifications (attenuation and bandwidth) are met and to provide baseline data for cable plant maintenance.

A generalized fiber optic transmission system is depicted in Figure 1. It consists of the electro-optical (E/O) interface, the fiber cable system, and the optical-electrical (O/E) interface. The E/O and O/E interfaces and their associated common equipment is often referred to as the Optical Line Terminating Equipment (OLTE). The fiber cable system consists of one or more fiber cables joined with splices and terminated at the ends with optical fiber connectors. In many cases the OLTE and the fiber cable system are connected via the Fiber Distribution Frame (FDF) which is an optical patch panel.

As far as the E/O and O/E interfaces are concerned, the minimum optical measurements are the output power (or rather the power coupled into the fiber) and the minimum required received input power. The only equipment required for these measurements is an optical power meter and a variable optical attenuator. The efficient testing of the transmission medium itself requires additional equipment. This paper discusses the field measurements associated with the optical cable portion of the system. Typical results obtained on over 1200 jointed fiber strings will be discussed.

## FIELD TESTS

The most common field tests before, during and after cable installation are listed in Table 1. For each test one or more methods are given. Selection of the method depends on the availability of test equipment, training of craftsmen, availability of manpower, etc. Obviously, whether one elects to do all or any of the tests depends on the specifications and the margins involved.

Continuity

The continuity of each fiber in an optical cable, either before or after placement may be readily checked with a simple light source, such as a flashlight. Attenuation of optical cables is sufficiently low that this method of checking is possible even after several kilometers have been installed.

On-the-reel Attenuation

For field measurement of attenuation of cables on the reel the optical time domain reflectometer (OTDR) is the most commonly used test equipment. The advantages over insertion loss or two length measurements are obvious in that only one end of the cable needs to be prepared, repeatability (up to about 10 dB) is better, and the measurement requires less time.

Splice Attenuation

The most convenient method of measuring splice attenuation is optical time domain reflectometry. Unfortunately, a single measurement of the loss of a splice can be considerably in error if the backscattering coefficients of the two fibers are different. As a matter of fact, the observation of apparent splice "gains" is not uncommon. Therefore, if an accurate measurement is required the splice loss has to be measured from both directions and the two numbers averaged. This is not usually done. Instead, the OTDR is used to minimize splice losses. A typical field result is shown in Figure 2. The individual numbers may be in error, but the mean value of 0.28 dB for the 88 fiber splices is accurate. It is interesting to note what the effect of splice loss monitoring is in terms of the final mean loss. During the course of splicing, six splices were remade. The effect of the remakes was to lower the mean loss from 0.31 dB to 0.28 dB. In this particular instance, splice loss measurements had no significant impact on the final result. In another installation, however, 240 fiber splices averaged 0.34 dB. Without remakes the average would have been 0.60 dB. More importantly, 11 closures would have had to be reentered and 18 fiber splices remade to meet end-to-end requirements. This later example illustrates the benefits of monitoring of splices as they are made.

Connector/End Splice Attenuation

Connector performance can be assessed by measuring the additional insertion loss introduced by the connector or alternatively with the OTDR. Again the later is more convenient since it is a single-ended measurement.

If the connectors are not installed in the field, connectorized pigtails are spliced on to the fiber cable. The OTDR is the most convenient test equipment for this purpose, but if the pigtail is too short, it may not be able to resolve separately the loss of the connector and the loss of the end splice.

End-to-End Attenuation

Since the final measurements are performed on connectorized systems, non-destructive insertion loss measurements are necessary to determine end-to-end attenuation. The repeatability of the measurements is dominated by the repeatability of the connector losses. To simulate equilibrium mode distribution, a mandrel-wrap EMS can be implemented by wrapping the input pigtail 4-5 times around a 25mm OD mandrel.

Table 2 compares end-to-end measured results with calculations based on on-the-reel cable data and splice losses measured with the OTDR. The agreement of the average values is typically within ±1 dB.

Alternatively, for low attenuation systems, the OTDR can be used to determine end-to-end attenuation.

End-to-End Bandwidth

Bandwidth can be measured either in the frequency domain or in the time domain. In the field, measurements are most often performed in the frequency domain. Repeatability is of the order of ±10%. Both step index or step-graded-step index mode scramblers have been used. We have found that if the end-to-end attenuation is greater than about 15 dB at short wavelength or 10 dB at long wavelength the effect of the mode scramblers is negligible (Table 3).

At short wavelengths, the spectral width of the laser may become important when measuring long systems. For a 12km system, 2nm spectral width at 850nm gives a material dispersion limited bandwidth of 183 MHz.

FIELD TEST EQUIPMENT

A few years ago no satisfactory test sets were available for field use and Siecor had to develop a family of lightweight portable test sets. These include the OTDR (Figure 3), a hand-held digital lightmeter/multimeter, an insertion loss test set (Figure 4) and a bandwidth test set which measures the amplitude response up to 400 MHz in the frequency domain (Figure 5).

Today, including Siecor there are at least three manufacturers offering a complete line of test sets. In addition, there are numerous manufacturers offering one or more test sets suitable for field use.

CONCLUSIONS

Field test sets for fiber optics have become available recently. Siecor has measured over 1200 concatenated fiber strings end-to-end. Agreement between measured and predicted attenuation readings has been excellent. The repeatability of end-to-end bandwidth measurements is about ±10% but predictability of end-to-end bandwidth has not improved over the years.

TABLE 1. Fiber Optic Cable Field Tests

| | TEST | METHOD |
|---|---|---|
| Prior to Installation | Continuity | Visual |
| | Attenuation | OTDR |
| Splicing | Splice Attenuation | OTDR |
| | Connector/End Splice Attenuation | 1. OTDR<br>2. Insertion Loss |
| After Installation | End-to-End Attenuation | Insertion Loss |
| | End-to-End Bandwidth | 1. Swept Frequency<br>2. Pulsed |

TABLE 2. Comparison of Calculated and Measured Attenuation (7.4km)

| Fiber No. | Calculated (Cable & Splice) (dB) | Measured (dB) |
|---|---|---|
| 1 | 26.6 | 26.5 |
| 2 | 23.8 | 28.1 |
| 3 | 25.2 | 25.7 |
| 4 | 26.3 | 26.3 |
| 5 | 25.8 | 25.7 |
| 6 | 26.2 | 25.5 |
| 7 | 24.4 | 24.8 |
| 8 | 23.7 | 24.1 |
| Average | 25.3 | 25.8 |

TABLE 3. Typical End-to-End Bandwidth (11km)

| Fiber No. | -3dB Optical End-to-end Bandwidth (MHz) | | | |
|---|---|---|---|---|
| | Test Set A @ 1321 nm No Mode Scrambler | | Test Set B @ 1283 nm SGS Mode Scrambler | |
| | → | ← | → | ← |
| 1 | 135 | 127 | 120 | 118 |
| 2 | 130 | 137 | 140 | 120 |
| 3 | 139 | 113 | 110 | 110 |
| 4 | 105 | 115 | 118 | 100 |
| 5 | 105 | 115 | 100 | 100 |
| 6 | 167 | 178 | 150 | 150 |
| 7 | 105 | 108 | 110 | 110 |
| 8 | 105 | 114 | 105 | 105 |
| 9 | 115 | 128 | 115 | 108 |
| 10 | 109 | 121 | 120 | 105 |
| Average | 122 | 126 | 119 | 113 |

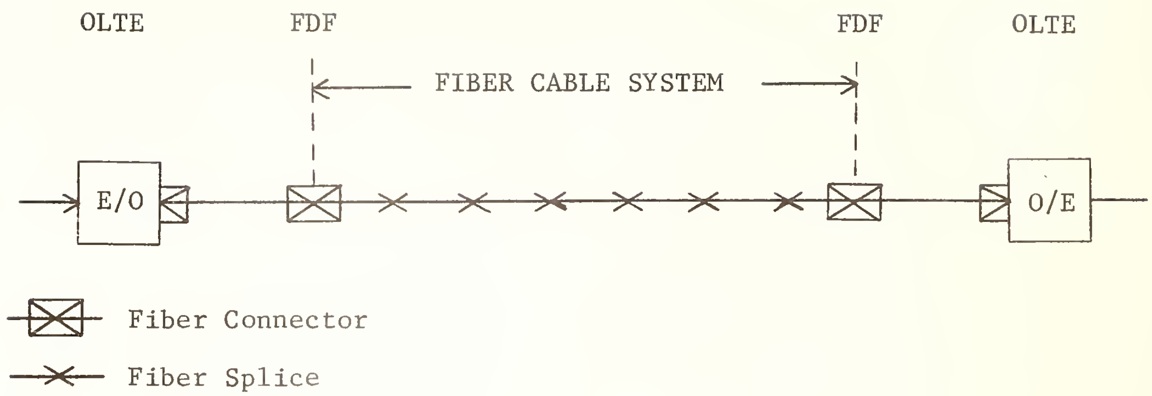


FIGURE 1. Generalized fiber optic transmission system.

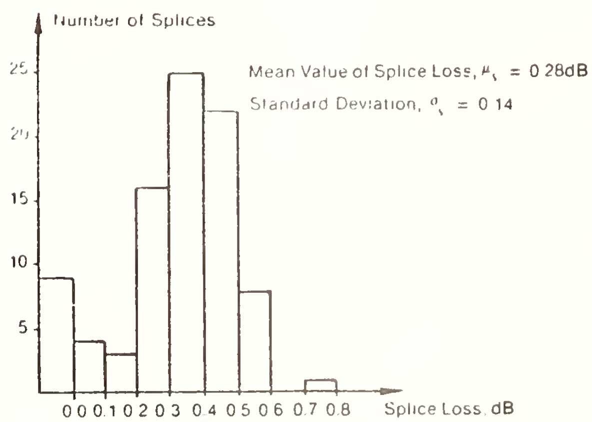


FIGURE 2. Splice losses obtained with OTDR.


FIGURE 3. OTDR for field use.

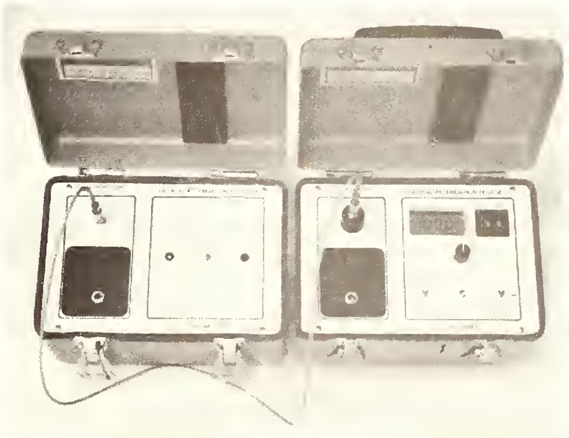

FIGURE 4. Attenuation Test Set.

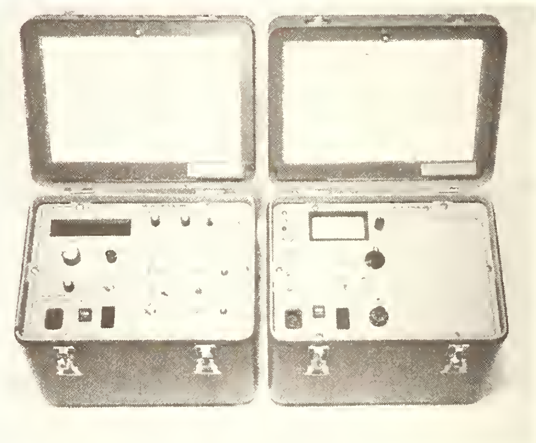

FIGURE 5. Bandwidth test set for both short and long wavelength.

# IMPROVED AUTOMATED LOSS SET FOR OPTICAL CABLES

L. S. Short and R. B. Kummer

Bell Telephone Laboratories
Norcross, Georgia 30071

## INTRODUCTION

An automated loss set for optical cables (ALSOC) has been described previously.[1] A new version (ALSOC III) has been in use in the Western Electric lightguide manufacturing plant since August 1981. The new set has several advantages; it eliminates uncertainty due to connector loss, creates a steady state launch distribution as would occur in the field, measures loss at two wavelengths, and detects crossovers in a fiber ribbon automatically. The set also contains an optical time domain reflectometer (OTDR) and visible HeNe laser for diagnosing high loss or broken fibers. The loss of a 12-fiber ribbon can be measured at 2 wavelengths in 3 minutes with an accuracy of better than 0.1 dB. A laboratory version which includes a time-domain bandwidth measurement will also be described. A loss concatenation experiment indicates that the set can be used to predict accurately system loss.

## GENERAL DESCRIPTION

Figure 1 is a block diagram of the test set. The loss measurement is designed to approximate closely the loss of a cable in an installed system. The optical sources are a GaAlAs laser at 825 nm and InGaAsP LED at 1300 nm. An undersized (small core, small $\Delta$) launch fiber serves two purposes.

Its refractive index and core diameter were chosen to simulate a steady state launch distribution in the cabled fibers. Furthermore, this undersized input fiber together with a large core, large Δ fiber on the detector end eliminates intrinsic splice loss. Computer controlled micropositioner stages determine the optimum measurement coordinates of each fiber in the ribbon under test, and this peaking procedure eliminates extrinsic splice loss. The OTDR and the visible HeNe laser can be used to troubleshoot a high loss or broken fiber. This portion of the test set has been in use at Western Electric since August 1981.

A time-domain bandwidth measurement was added for laboratory system studies. Using the optimum measurement positions from the loss measurement, the fiber under test can be excited with either a pulsed GaAlAs injection laser at 825 nm or a pulsed InGaAsP injection laser emitting at 1278 nm. The output pulse is detected by a Si avalanche photodiode (APD) at the short wavelength or a Ge APD at the long wavelength, then sampled, digitized and averaged by the digital processing oscilloscope (DPO). The microcomputer calculates the fast Fourier transform (FFT) of the output pulse. The transfer function of the cable is obtained by repeating the measurement on the short reference ribbon and taking the ratio of the two FFT's. Both the OTDR and the loss measurement can be useful in the interpretation of bandwidth concatenation results.

## RESULTS

A loss concatenation study was made on a 6 km link consisting of 12 0.5 km 12-fiber ribbons with 11 splices. Individual ribbon loss, splice loss, and total loss were all measured. As shown in Figure 2, the actual concatenated link loss agrees with the sum of the ribbon losses and splice losses to within 0.2 dB. This indicates the test set is simulating a steady state launch distribution and thus that factory measurements can be used to predict accurately system loss.

## ACKNOWLELDGEMENTS

The authors would like to thank C. E. Davis for his work in the construction of the ALSOC III loss test set.

## REFERENCES

1. L. C. Hotchkiss, "Automated Loss Measurement Set for Optical Cables," Symposium on Optical Fiber Measurements, 1980, pp. 23-26.

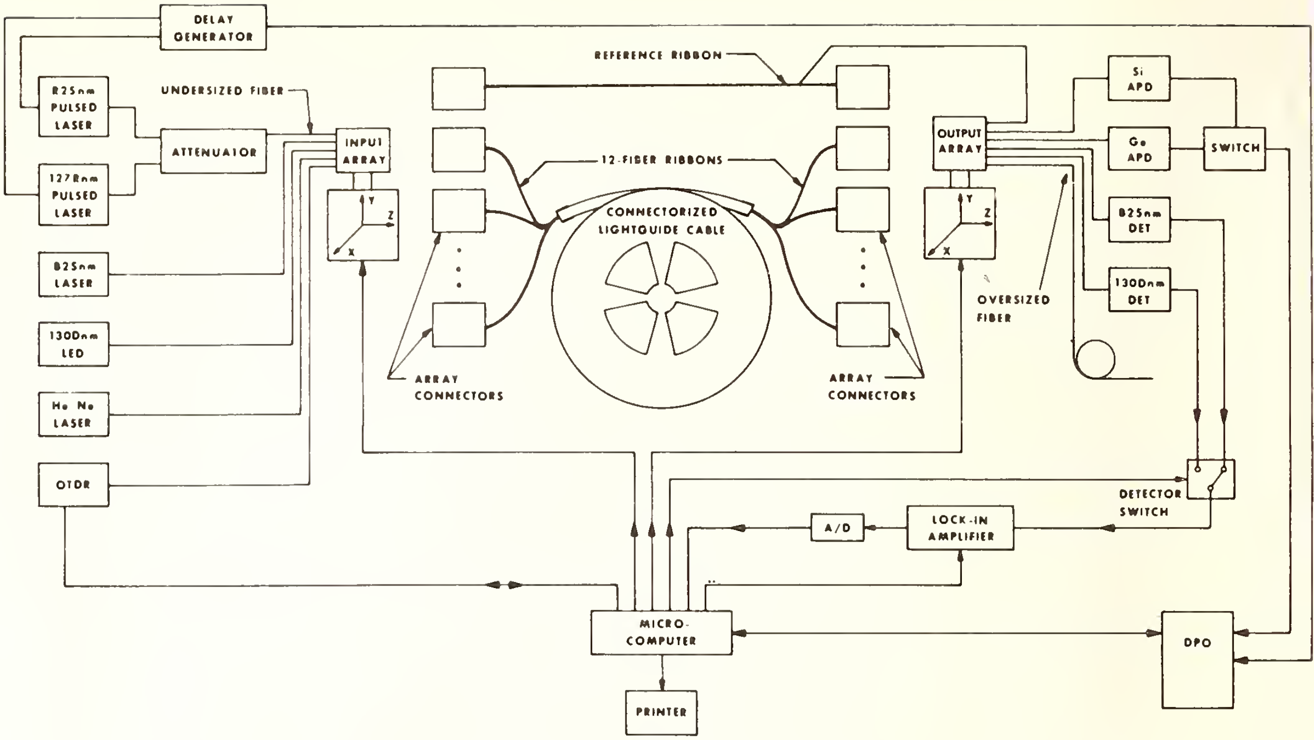


FIGURE 1. AUTOMATIC MEASUREMENT SET FOR OPTICAL CABLES

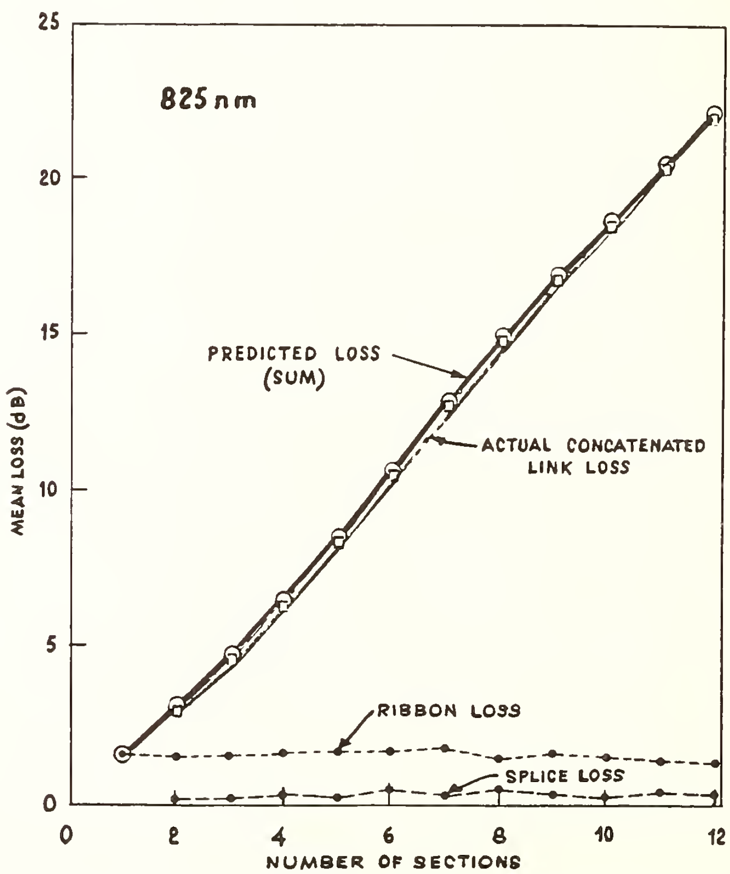


FIGURE 2. 825 nm LOSS CONCATENATION STUDY

# Prototype system for automated measurements of transmission properties of graded index fibres

J.W. Versluis and H.P. de Wert
Optical Fibre Department, Glass development laboratory
N.V. Philips Gloeilampenfabrieken, Eindhoven, The Netherlands

## Introduction

The accepted philosophy to measure all manufactured fibres requires increased measuring speed to keep in step with the expanding production.
For this reason we have developed automated equipment in which we have combined all transmission measurements. Besides man-independent measurement conditions have been effected.
The system measures attenuation at three and bandwidth at two wavelengths, length and numerical aperture in 7 minutes including the fibre cut-back to 2 metres.
The measuring techniques implemented for attenuation as well as bandwidth employ the Philips preferred launch conditions [1)]. For both types of measurement a stable modescrambler, based on microbending[2)], is applied to approximate steady state distribution[3)] of the 50/125 μm graded index fibres.
Several daily checks are built in, while weekly calibration measurements applied to standard fibres ensure quality assessment of the measurements on production fibres.

## System description

A block diagram of the system is shown in fig. 1. The Philips P 851 micro-computer is employed for general control and for part of the measurements. The Tektronix WP 1310 system averages the pulses, stores them and performs the FFT.

## Source and launch optics

Special parts in fig. 2 are the fibre switch SW, the modescrambler MS and the position detector P1, P2.
The switch employs the principle of the ball connector [4)]. The position of the outgoing fibre F1 is controlled by a stepper motor. It turned out that the fibre switch also acts as a modescrambler, limiting the far field distribution from fibre FP1 and increasing those from fibres FP2 end FP3. Three additional sources are possible.

This is a good start for the actual modescrambler employed to obtain a fair approximation of the equilibrium mode distributions of the tested fibres. Measurements over a long period of time showed a stable behaviour of the far field distribution.
The intensity distribution is projected 1 to 1 on the fibre to be measured. This stationary distribution, accepted for attenuation measurements, applied to bandwidth, has shown a repeatability as favourable as for overmoded launching by a step index fibre. Moreover the values thus obtained were fairly well in agreement.
The position detection system P1, P2, determines the axial position of the front end of the fibre as described in the measurement procedure below. One micron stepper motors are employed. Source S2 is applied when the nominal NA is determined using overmoded launching.

## Detection and receive optics, fig. 3

The position of diode D1 as shown (I) is applied for laying the fibre into the vacuum chuck VC, and when pulse sampling or far field scanning takes place. Position II is in use for all intensity measurements, including alignment of the fibre.
The fibre end should be positioned accurately in axial direction, and has to coincide with the centre of rotation of the rotatable stage as well. Again the position detector P1, P2 is applied as described below.
A rotation of $60^{o}$ in either direction allows projecting the output light power on to an APD.

## Measurement procedure

1. Insertion and alignment of the fibre.

   The cleaved [5] ends of the fibre being tested are examined separately on quality with a microscope.
   Experiments showed that a video monitor was insufficient to assess the quality of the cleaves effectively. Primary coatings (with a higher refractive index than that of the cladding) are not removed when cleaved. The accepted fibre ends are simply laid into the vacuum chucks, which are mounted on XYZ-stages moved by stepper motors. After the entry of fibre identification, geometrical data and coating type the program is started. The chucks now move in axial direction until the fibre front ends interrupt a fine light ray. This ray is part of the axial position detection system P1, P2 (fig. 2 and fig. 3 ).

Now the front ends of the fibre are known within $\pm 5\ \mu m$, irrespective of the chuck positions, and are adjusted axially. Part of the launched light is now captured by the launch end of the fibre, which part is aligned for maximum optical output. This automatic procedure has a radial repeatability of one $\mu m$ or better. The repeatability of the fibres in the vacuum chucks and the eccentricity of the coating render additional radial optimation at the detector end unnecessary. Axial movement at the launch end are made to correct any focal dispersion of the 1 to 1 imaging system.

2. Bandwidth

Firstly pulses of the 1300 nm laser are taken in, averaged and stored after manual search and amplitude adjustment. Then a correction for the background level is made while the fibre is being rotated to the silicon-APD.
The fibre switch selects the 850 nm laser source and the same steps are repeated . Besides pulse delay time is measured and the fibre lenght calculated. The WP 1310 now starts calculations using reference pulses that were stored after the daily checks (virtually no deviations in pulse form are found between checks).

3. Attenuation

Meanwhile intensity measurements take place at 850, 1300 and 1600 nm controlled by the P851. The cooled germanium-detector is in position II of fig. 3 and the output of the lock-in amplifier is averaged several times. After the cutting back of the fibre to 2 metre without disturbing the position of the fibre at the launch end, measurements on the above wavelenghts are repeated.

4. Numercial aperture

With source S2 the 2 metre fibre is then used to measure the far field. The 3 % intensity angle determines the nominal NA.

## Results and performance

Manual actions are reduced to simple operations. The only difficulty is the assessment of the quality of the cleave.Qualification tests in conjunction with the use of current measuring equipment have not shown any significant deviations. Spread in bandwidth measurements is small, attenuation showing larger deviations. This deviation is probably due to the fairly low signal-to-noise ration of the germanium detector, and has to be improved.
The manual search during the bandwidth measuremnets will be replaced by the setting of a programmable delay lime in conjunction with the measured delay time.

Literature


1. Wire Industry, 49, no 479 (March 1982), p 164
2. J.W. Versluis, J.G.J. Peelen, Optical communication fibres. Manufacture and properties, Philips Telecommunication Review, 37, no 4 (Sept. 1979), p 215
3. A. Diekema, L.H.M. Engel, G.A.M. Goltstein, P. Mathijsse and J.W. Versluis, Attenuation of optical fibres for the Eindhoven - Helmond field trial, Symposium on Optical Fiber Measurements, 1980, Boulder, Colorado, p 27
4. A. Nicia and A. Tholen, High-efficient ball-lens connector and related functional devices for single-mode fibers, 7th European Conference on Optical Communication, 1981, Copenhagen, 7.5.
5. D. Gloge, P.W. Smith, D.L. Bisbee and E.L. Chinnock, Optical fibre end preparation for low-loss splices, B.S.T.J. 52, no 9, (Nov. 1973), p 1579.


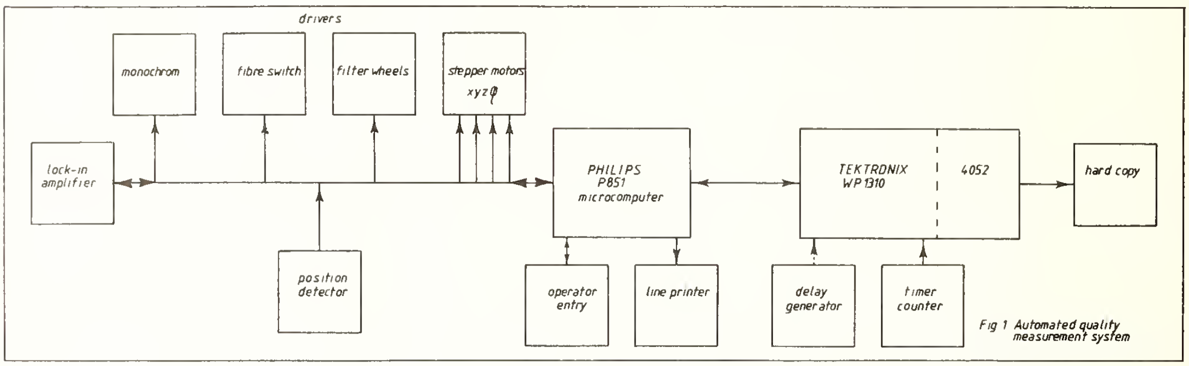

Fig 1 Automated quality measurement system

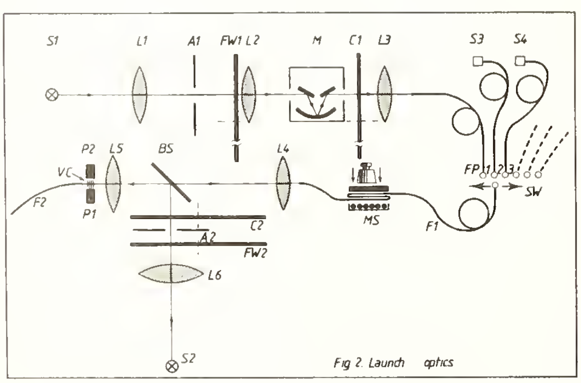

Fig 2 Launch optics

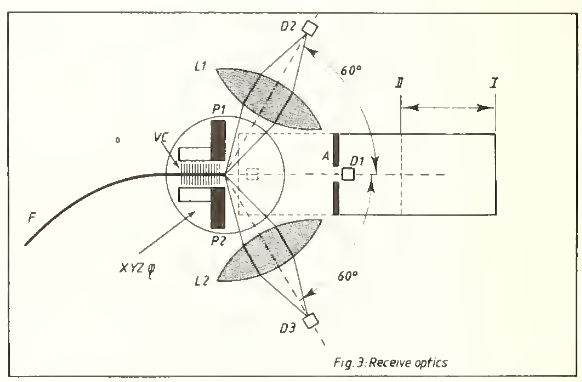

Fig. 3: Receive optics

| | |
|---|---|
| *S1,S2* | *halogen lamps* |
| *L1-6* | *lenses* |
| *A1,A2* | *apertures* |
| *FW1,FW2* | *filterwheels* |
| *M* | *monochromator* |
| *C1,C2* | *choppers* |
| *FP1-3* | *fibres* |
| *S3,S4* | *laser diodes* |
| *SW* | *fibre switch* |
| *MS* | *mode scrambler(adjustable)* |
| *L4,L5* | *objectives 40x0,65* |
| *BS* | *beam splitter* |
| *VC* | *vacuum chuck* |
| *F2* | *fibre under test* |
| *P1,P2* | *position detection system* |

| | |
|---|---|
| *F* | *fibre under test* |
| *VC* | *vacuum chuck* |
| *XYZΦ* | *stages* |
| *D1* | *cooled Ge-diode* |
| *D2* | *Ge-APD* |
| *D3* | *Si-APD* |
| *L1,L2* | *lenses* |
| *A* | *aperture* |
| *P1,P2* | *position detection system* |

Precise Measurement of Optical Fiber Breaking Elongation

K. Matsui, S. Tanaka and M. Hoshikawa

Sumitomo Electric Industries, Ltd.

1, Taya-cho, Totsuka-ku, Yokohama, 244, Japan

## 1. Introduction

In optical fiber technology, it is important to characterize mechanical properties precisely in addition to transmission properties. Especially fiber elongation is one of the important mechanical characteristics in evaluating the fatigue phenomenon and predicting the mechanical lifetime. However the conventional tensile tests based on the mechanical systems are not always sufficient ones for the precise measurement of breaking elongation, due to the following reasons;

(1) There are deviations from linearity in the dependence of glass elongation on stress.[1]

(2) It is difficult to correct the contributions of catenary in the long fiber span during tensile test.

(3) It is difficult to correct the stress relaxation in jacketing materials.

In order to solve these problems we propose a utilization of modulation phase of optical signals for the direct and precise detection of the fiber elongation during tensile tests and at fracture.

## 2. Measurement System

(1) Tensile testing machine

The diagram of the testing machine is shown in Fig. 1. The tensile testing machine is designed to satisfy the following features;

1) Optical fiber is held tightly around the 8 cm diameter mandrels covered with rubber. Optical fiber is wound around them three times

and fixed by adhesive tape. Fig. 2 shows the illustration of the chucks. Slip of fiber during load is 1 mm at most. As fiber elongation is measured directly by modulation phase method described later, the smallest slip mentioned above does not influence the elongation measurement. Thus error of elongation strain is extremely small. Loss increase is not observed during these procedures.

2) Pulling speed is controlled to ensure the constant strain rate by a variable-speed motor.

(2) Fiber elongation measurement by modulation phase method

The measuring arrangement of fiber elongation is shown is Fig. 3. The essence of the measurement is the detection of optical path length change by means of modulation phase change. A sinusoidally modulated optical signal is transmitted through the test fiber, and the phase change of the received signal, which is related to the optical path length change, is continuously monitored by a vector volt meter during the tensile strength test. The physical fiber elongation $\Delta \ell$ is calculated from the observed phase change $\Delta\theta$ (deg) by the following equation,

$$\Delta \ell = \frac{1}{\{1 - \frac{N^2}{2}[p_{12} - \nu(p_{11} + p_{12})]\}} \times \frac{c}{Nf} \times \frac{\Delta\theta}{360} , \qquad (1)$$

where N is the group index $(= n - \lambda\frac{dn}{d\lambda})$, f the modulation frequency, c the velocity of light, $p_{11}$ and $p_{12}$ the strain optic tensors, and $\nu$ is the Poisson's ratio of the glass fiber. At a frequency of 800.000 MHz, which is usually used in our measurement, equation (1) becomes 0.884 mm/deg, yielding the high accuracy of fiber elongation measurement.

## 3. Experiment

Fig. 4 shows an example of tensile breaking strain measurement of optical fibers. The experiment was conducted under the fiber gauge length of 10 meter and the strain rate of 5% a minute. The modulation frequency is 800.000 MHz, and the change in detected modulation phase was recorded within 1 degree up to the instance of fiber fracture. Consequently the measurement accuracy of tensile strain against the whole fiber length was within 0.01%. Fig. 4 clarifies the fine difference in fiber breaking strains with different coating structure.

## 4. Conclusion

The elongation of optical fiber at fracture was measured with high accuracy (below 0.01%), by optical modulation phase method. Thus it becomes possible to characterize the mechanical properties of optical fibers precisely upon the basis of these data and to predict the lifetime of optical fibers with high precision.

## Reference

[1] J.T. Krause, L.R. Testardi, and R.N. Thurston, Physics and Chemistry of Glasses, 20, 135 ~ 139 (1979).

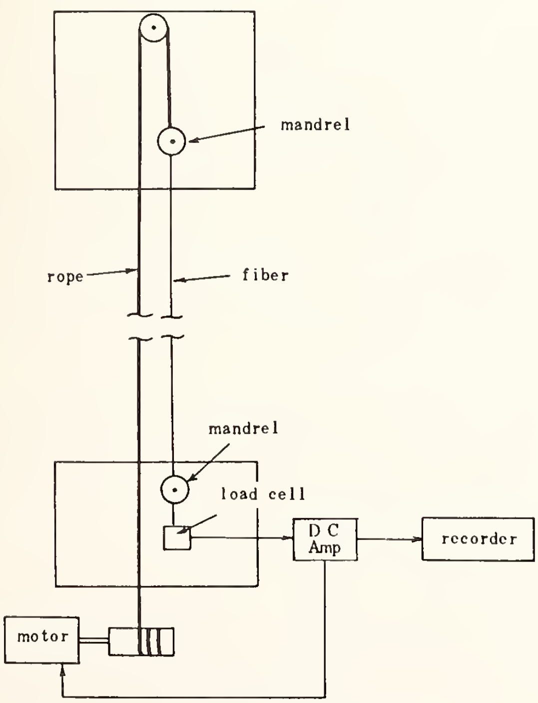


Fig. 1 Over view of tensile testing apparatus.

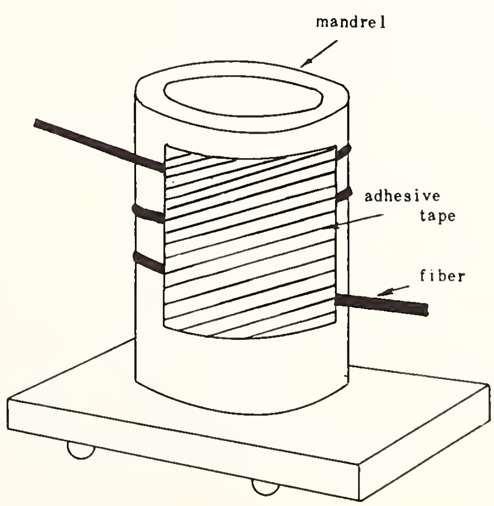


Fig. 2 Illustration of fiber chuck.

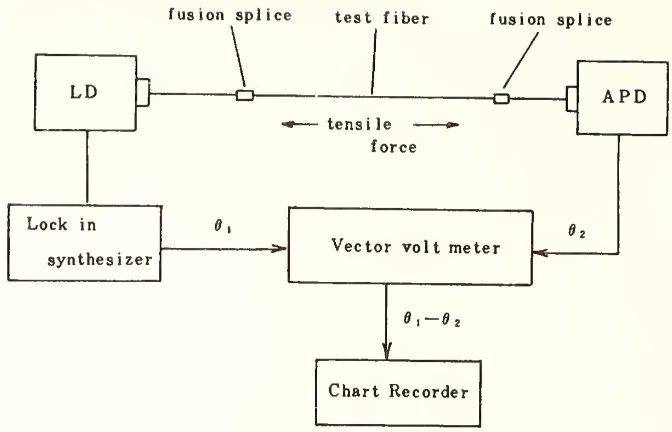


Fig. 3 Measuring arrangement of fiber elongation by modulation phase method.

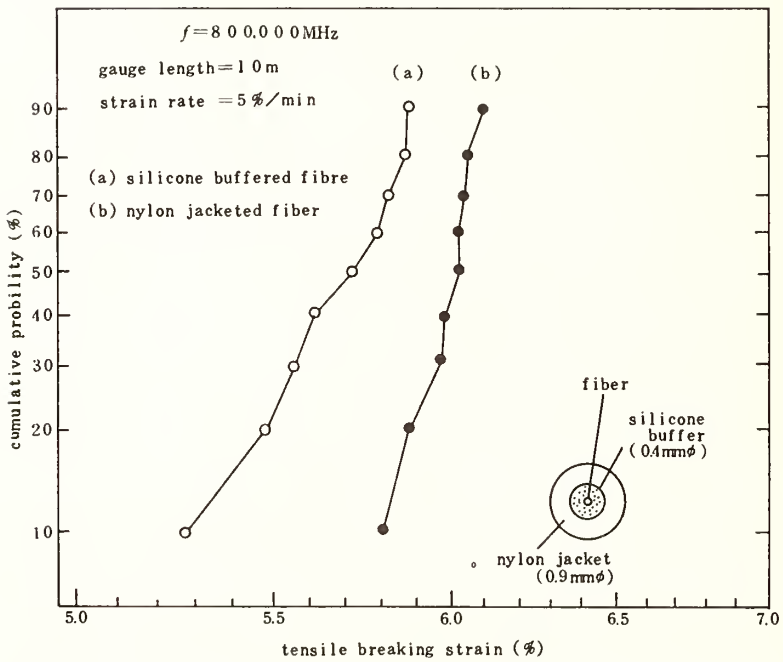


Fig. 4 Tensile breaking strain of optical fiber

These fibers were produced by the VAD method and the diameter of the cladding, which consists of silica, is 125 μm and the diameter of the core, which consists of silica doped with Ge, is 50 μm. The fibers were coated with silicone resin and jacketed with nylon further.

# PRECISE MEASUREMENT OF STEADY-STATE FIBER ATTENUATION

P.J. Vella, K. Abe and F.P. Kapron*
Bell-Northern Research, Ottawa, Ontario
Canada, K1Y 4H7

## INTRODUCTION

Various light launching techniques [1] have been employed to measure fiber attenuation accurately and reproducibly. One of the reasons behind such efforts stems from the need for accurate prediction of fiber link attenuation (as well as fiber bandwidth). In this paper, the 'steady-state' attenuation is recognized as a unique fiber parameter and problems associated with its exact measurement are addressed. Furthermore, link attenuation predictability is evaluated based upon the steady-state measurements of individual fiber sections.

## STEADY-STATE ATTENUATION

It is well known [2] that, in general, the power decay, P(L) in dB, along an optical fiber is not a linear funcion of the distance, L, from the light source. This is illustrated in Fig. 1 where observed light power decay curves are shown for fibers excited with a LED and an injection laser diode (ILD). The output power observed by cutting back the fiber every 50~100 m was fitted to the following equation:

$$P(L) = P(0) - \alpha_s L - P_t \, [1 - \exp(-L/L_t)].$$

where all powers are in dBs, and attenuation rates in dB/km.

This equation was derived by assuming that the net attenuation rate could be written as the sum of the steady-state (quasi-equilibrium) attenuation rate $\alpha_s$ and a transient attenuation rate $\alpha_t \exp(-L/L_t)$, the latter contribution decaying with a characteristic length $L_t$. In the equation, $P_t$ $(=\alpha_t L_t)$ is a transient loss whose existence gives rise to the following problems in attenuation measurements. (1) A conventional two point cut-back method may give attenuations that depend on fiber lengths and light launch conditions. Therefore the measured attenuation is not a unique fiber parameter. (2) The multiple cutback method of measuring $\alpha_s$ is a destructive way of determining the expected unique fiber parameters. Therefore, it is imperative to devise light launch conditions that do not give rise to transient effects and to ascertain that the steady-state attenuation is really a unique fiber parameter independent of launch conditions, lengths, etc.

Experimentally, it was established that the transient loss arises from the following two effects: incomplete cladding mode stripping (found to occur even with fibers coated with higher index plastics) and leaky and/or lossy higher order modes. In order to eliminate the transient loss, an approximately 15 cm long section of the fiber coating was stripped near the launch end, shaped into a loop and immersed into oil whose refractive index was 1.514 ($N_d$). With the above stripping technique, several multiple cutback measurements have shown that transient losses of less than 0.05 dB were consistently attainable regardless of the light sources and launch conditions employed. The steady-state attenuation was thus precisely measurable within 0.05 dB using this simple stripping technique and the two point cut-back method.

LINK PREDICTABILITY

The steady-state attenuation of nine fiber sections was measured using the above "loop" stripping technique. Then the fibers were spliced together to form a 17 km link. Using an ILD source, the optical power was sequentially measured at the output and input ends of individual fiber sections. A conventional stripping technique, which consists of removal of the coating for a 10 cm long section followed by immersion into the oil, was used for the power measurements at the output ends. For the input end measurements, both the conventional and the "loop" stripping methods were used. The measurement results are summarized in Table 1 listing insitu steady state attenuations ($A_1$), two point cut back attenuations measured with the conventional stripping method ($A_c$), splice losses including the transient loss ($S_1$) and splice losses measured with the conventional stripping method ($S_c$) (See Fig. 2). The good agreement between the steady-state attenuations measured individually ($A_s$) and in the links ($A_1$) shows that the steady-state attenuation is indeed a unique fiber parameter which, together with the average splice loss $\bar{S}_1$ (which includes transient loss), can be used to accurately predict link attenuation.

CONCLUSION

In summary, a simple method for measuring the steady-state attenuation of optical fibers has been demonstrated. The technique was found to give attenuation values consistent with measurements within a concatenated link. Good link predictability was achieved based on the steady-state attenuation by including the attenuation transient loss into the net splice loss.

REFERENCES

[1] M. Tateda et al, Appl. Opt., 18, 3272 (1979); M. Eve et al, Opt. Quant. Electr., 10, 253 (1978); G.T. Holmes, Techn. Digest, 6th ECOC, p. 144, York 1980; T. Le Hiep and R. Th. Kersten, Opt. Comm. 40 (2), 111 (1981).

[2] V.V. Grigor'yants et al, Sov. J. Quant. Electron., 8 (9), 1161, (1978); M.J. Adams et al, Opt. Comm., 17 (2), 204, (1976).

*Current address, ITT, EOPD, Roanoke, Virginia, 24019.

Table 1: Measured in situ attenuations ($A_1$, $A_c$) and splice losses ($S_1$, $S_c$).

| Link Length (km) | $A_s$ (dB) | $A_1$ (dB) | $A_c$ (dB) | $S_1$ (dB) | $S_c$ (dB) |
|---|---|---|---|---|---|
| 0 | | | | | |
| | 5.61 | 5.43 | 5.72 | | |
| 2 | | | | 0.25 | 0.01 |
| | 5.53 | 5.57 | 5.81 | | |
| 4 | | | | 0.24 | 0.09 |
| | 5.51 | 5.54 | 5.69 | | |
| 6 | | | | 0.19 | 0.05 |
| | 5.73 | 5.82 | 5.96 | | |
| 8 | | | | 0.15 | 0.08 |
| | 5.65 | 5.77 | 5.84 | | |
| 10 | | | | 0.25 | 0.15 |
| | 5.51 | 5.42 | 5.52 | | |
| 12 | | | | 0.07 | 0.05 |
| | 3.42 | 3.40 | 3.42 | | |
| 13.3 | | | | 0.14 | 0.05 |
| | 4.95 | 4.97 | 5.06 | | |
| 15.1 | | | | 0.15 | 0.20 |
| | 5.31 | 5.49 | 5.44 | | |
| 17 | | | | | |
| TOTAL LOSS(dB) | 47.22 | 47.41 | 48.46 | 1.44 | 0.68 |

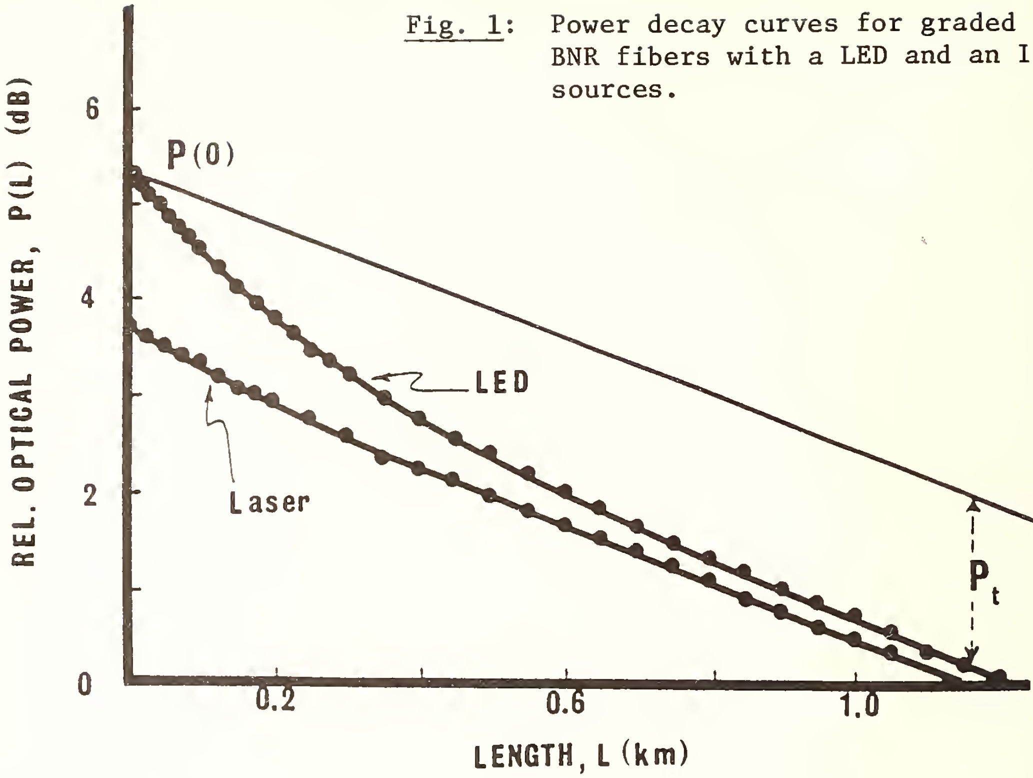


Fig. 1: Power decay curves for graded - index BNR fibers with a LED and an ILD light sources.

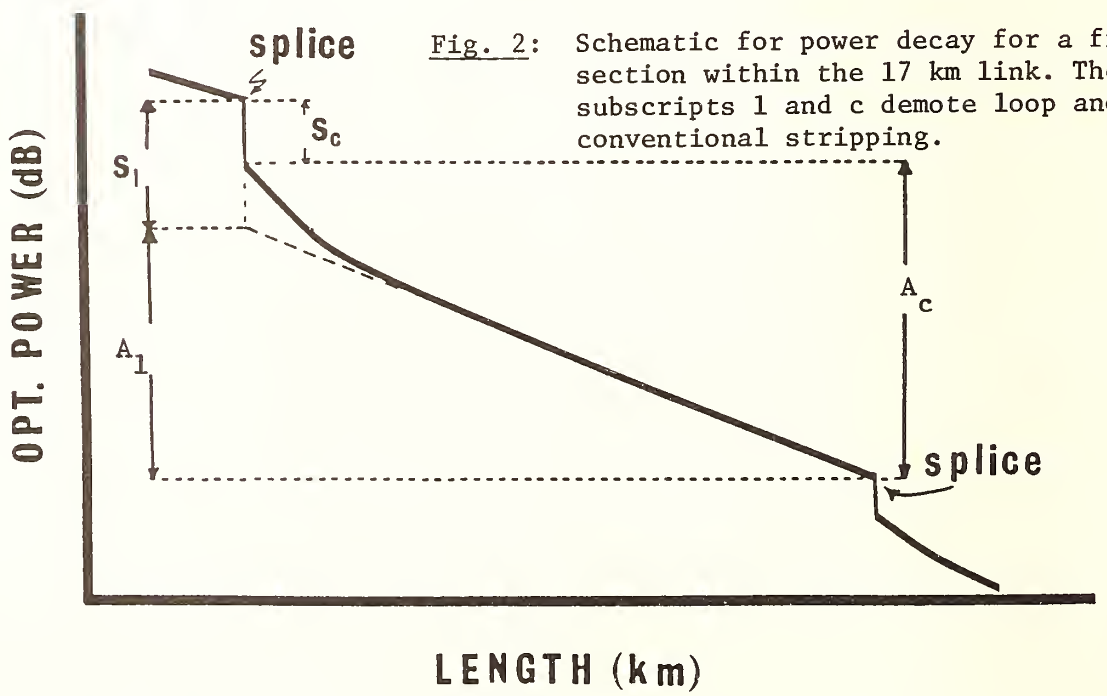


Fig. 2: Schematic for power decay for a fiber section within the 17 km link. The subscripts l and c demote loop and conventional stripping.

# MODAL BEHAVIOUR OF VARIOUS MODE MIXERS AND MODE FILTERS FOR OPTICAL FIBER MEASUREMENTS

A.K. Agarwal, H. Karstensen, U. Unrau
c/o Institut für Hochfrequenztechnik, Techn. Univ., P.O. Box 3329, D-3300 Braunschweig, Germany (Fed. Rep.)

ABSTRACT
A bearing-ball-bed mode mixer is compared with mandrel wrap, 70% excitation and newly developed taper mode filters in the approximation of the stationary mode group power distribution (SMPD) of different fibers. The mode group power is computed from the near-field intensity pattern (NFP) and compared with results from differential mode delay measurements.

## 1.0 INTRODUCTION

Because of differential mode attenuation and delay, the characteristics of multimode fibers depend strongly on the mode power distribution (MPD). Fiber data can be extrapolated with sufficient accuracy to arbitrary lengths only if the fiber carries its SMPD which is the statistical mode of lowest attenuation. Unfortunately, SMPD is reached in low loss fibers with low microbending only after several kilometers.

Standardized measurements require SMPD excitation. Various techniques have been proposed to approximate SMPD at the fiber input by restricted mode volume launching /1,2/, mode filters /3,4/ and mode scramblers /5,6/. SMPD check was made either by radiation pattern comparison or by concatenation experiments. The last method gives a good feeling for the accuracy of attenuation measurements but not necessarily for the accuracy of SMPD launch because of extra mode mixing at splices. The radiation pattern inspection is highly inaccurate: the main information on the power carried by higher order mode groups is contained in the slope of the radiation pattern at its low intensity boundaries and cannot be extracted properly by simple pattern inspection.

SMPD is characterized by its insensitivity to variations in launching conditions. MPD`s of typical low loss MCVD fibers 2-3 km in length are still dependent on excitation. However, most measurements have to be made on such or even shorter pieces of fiber. Generally, two excitations are prevalent: a) incoherent uniform excitation for attenuation, and b) small mode volume excitation by laser diodes for pulse delay measurements. In both cases the MPD profile has to be shaped by mixers or filters to approximate SMPD. It is the aim of this contribution to show the degree of SMPD approximation achieved by various devices in both cases.

## 2.0 MEASUREMENTS

We used a computerized measurement set-up /7,8/ which derives the mode group power distribution from the derivatives of the NFP. Assuming equal power distribution between the modes belonging to a mode group the MPD is known. The experiments were performed on three different fibers of which the manufacturer specs are given in Table 1. Figs. 1a, b, c show results for fibers no. 1, 2, 3, respectively, in case of uniform excitation by a halogen lamp filtered to 820+/-10 nm wavelength. We depict the difference $\langle \Delta \rangle$MPD between the actual MPD and an ideal uniform MPD vs. the relative mode group number m/M. Three well known arrangements were compared: the PHILIPS bearing-ball-bed mode scrambler /6/, BELL s mandrel wrap mode filter /3/ and the 70% mode volume launch. In addition, curves for a new taper mode filter are given. All devices were measured with 10 m of fiber.

Fibers 1 + 2 are quite alike, and so are Figs. 1a + b. Fiber 1 was found to exhibit slight deformations; this obviously causes less power content of the lower mode groups and a steeper roll-off of the MPD-curve after 2.2 km in comparison to fiber 2. However, as it will be explained later, it is felt that both curves already approach SMPD quite closely. Compared to the quasi-SMPD curves the mandrel wrap filter shows a more sharp cutoff in higher mode groups. Shown here are curves for a mandrel of 12 mm O.D. with 5 turns of loosely wrapped fiber. Larger O.D.`s shift the cutoff to higher m/M values but the slope remains nearly constant (curves at the conference). On the other hand the restricted mode volume excitation (70% $A_N$ and spot size) causes a too gentle roll-off, as already noted in /9/.

Only the scrambler and the taper filter match the quasi-SMPD curves quite closely. It was found that the scrambler always produces quasi-SMPD if set for approx. 1.6 dB loss, independent of the inserted fiber length. (For construction details see /6/). If integral power comparisons are made it must be reminded that the mode content increases with mode group order. The scrambler not only converts guided to radiation modes but also converts power from higher to lower mode groups. Thus it has a good loss budget. The biconical taper filter was made by heating the fiber under tension. Tens of tapers with different diameter ratio and length were produced. It was found that a ratio of 0.6 and 1 - 2 mm of length always give quasi-SMPD in 50/125 µm GI-fibers. Mainly, the ratio determines the cutoff, length and smoothness have further influences on cutoff an slope. Fig. 1c shows generally the same results with only 900 m of a different fiber.

Fig. 2a gives similar curves for fiber 2, but now for laser-diode excitation at 900 nm. The far-end MPD shows still the same low-order mode group dominance as the input MPD; only the higher mode groups are more attenuated. Obviously, intrinsic mode mixing on 2.2 km did not make up for the SMPD. The mandrel wrap filter again provides only an even sharper cutoff. Only the mode scrambler, now set to approx. 3.0 dB attenuation for central excitation, fills the mode volume to a certain extent but not up to the quasi-SMPD of Fig. 1b.

Nevertheless, the effect is quite substantial as it can be checked by pulse delay measurements. For that purpose LD pulses were fed to a monomode fiber (a=3.0 µm, $A_N$=0.11) which excited the test fiber at various radii. From the measured pulse broadening a mode group bandwidth distribution (MGBD) was calculated by Fourier transform. Fig. 2b depicts MGBD vs. m/M. The bare fiber shows a large bandwidth spread over 1.2 GHzkm which reduces to 0.7 GHzkm if it is wrapped 5 turns around a 12 mm O.D.

mandrel. The use of the scrambler flattens the variation to 0.3 GHzkm around 1.2 GHzkm which exceeds the specs by 35%. If the scrambler always produced a SMPD at its output independent of the monomode fiber position at its input, no variation in MGBD would be noted.

## 3.0 DISCUSSION

SMPD in a fiber is reached if due to mode mixing and attenuation the average power distribution among the mode groups remains constant. At SMPD in average all modes are attenuated and delayed uniformly (statistical mode). Because of the actual loss of higher order modes the SMPD decreases as a function of m/M. By comparing the 3 curves in Figs. 2a and 2b it is seen that the scrambler should show a more gentle roll-off to produce SMPD. Going back to Fig. 1b with this information one sees that the far-end, the taper and the scrambler curves approach SMPD quite closely. Since the scrambler is set here for low loss, SMPD is obviously reached more easily by tailoring a uniform excitation instead of mixing up a low mode volume.

The usefulness of the mandrel wrap filter for standardized attenuation measurements has already been proven /3/ despite of its too steep MPD slope. It can therefore be concluded that attenuation measurement accuracy does fortunately not depend on a very precise SMPD launch. The ball-bed scrambler and the taper should give even better comparability of measurements; especially a prefabricated taper to be connected to the fiber under inspection would be a very handy precision device. In pulse delay measurements the ball-bed scrambler is so far the only candidate to achieve comparable results.

## 4.0 ACKNOWLEDGEMENT

The authors wish to thank Ir. J.W. Versluis of PHILIPS/Eindhoven for providing the scrambler and fiber 3, Dipl.-Ing. G. Maltz of KABELMETAL/Hannover for lending fibers 1 and 2 and, the German Research Foundation DFG for funding this work.

## 5.0 REFERENCES

/1/ Kaiser, P., Trans. IECE Japan 61 (1978), 225 - 229.
/2/ Eve, M. et al., Opt. and Quant. Electron. 10(1978), 253.
/3/ Cherin, A.H. et al.,Fiber and Integr. Optics 4(1982), 49 - 65.
/4/ Le Hiep, T. and Kersten, R.Th., Opt. Comm. 40(1981), 111 - 116.
/5/ Kaiser, P., Symp. on Opt. Fiber Measurements, Boulder 1980, 11 - 14.
/6/ Versluis, J.W. et al., Philips Telecom. Rev. 37(1978), 215 - 230.
/7/ Unrau, U. et al., Conf. Messtechnik in der optischen Nachrichtentechnik, Berlin 1980, 173 - 175.
/8/ Agarwal, A.K. et al., 3rd IOOC, San Francisco 1981, 74 - 75.
/9/ Calzavara, M. et al., Electron. Lett. 17,No. 15. 1981. 543 - 545.

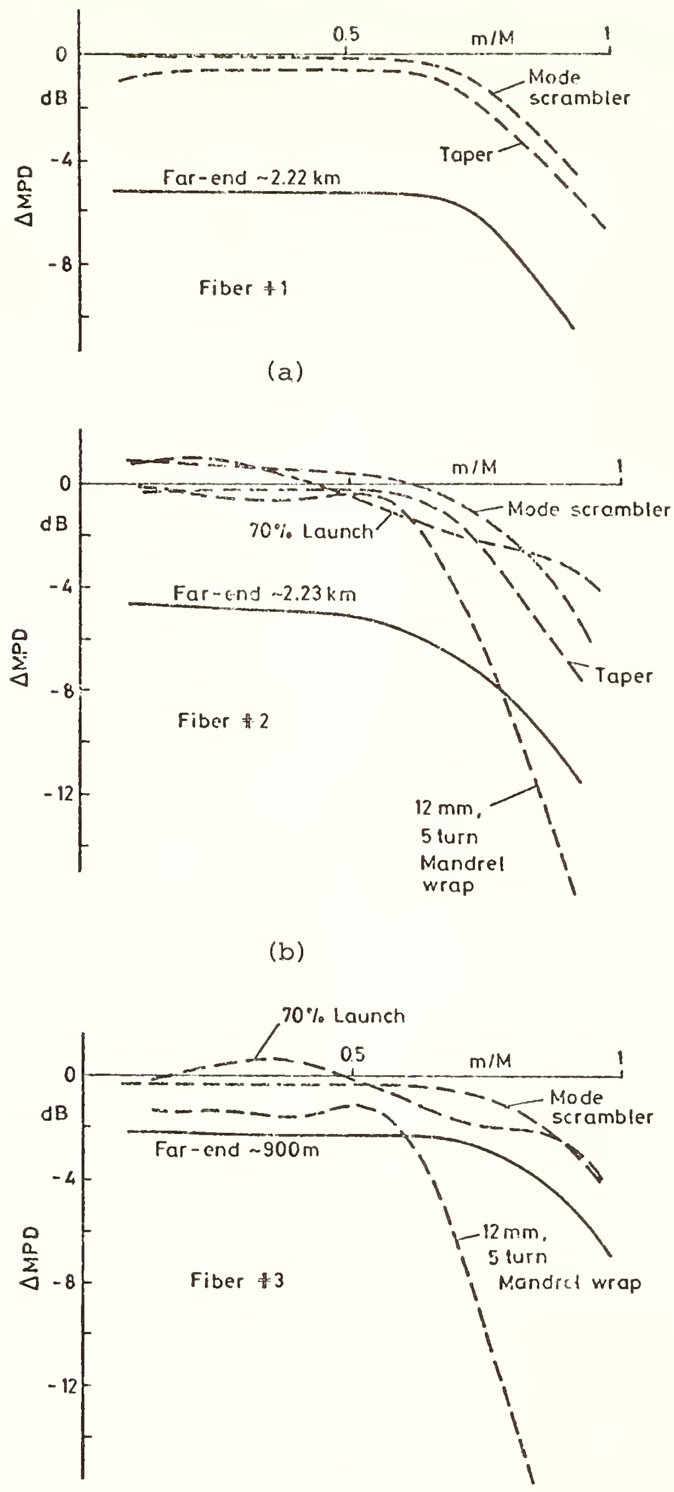


Fig.1 Difference in mode power distribution ΔMPD to equal excitation vs. relative mode group number m/M with uniform input excitation

| Manufacturers | Fiber 1 CLTO, France | Fiber 2 CLTO, France | Fiber 3 Philips, Holland |
|---|---|---|---|
| Length (m) | 2220 | 2230 | 900 |
| $A_N$ | 0,19 | 0,20 | 0,17 |
| Loss (dB/km) | 2,1 | 2,1 | 2,4 |
| Core/Clad (μm) | 50/125 | 50/125 | 50/125 |
| Bandwidth (MHzkm) | 884 | 874 | 641 |

Table 1

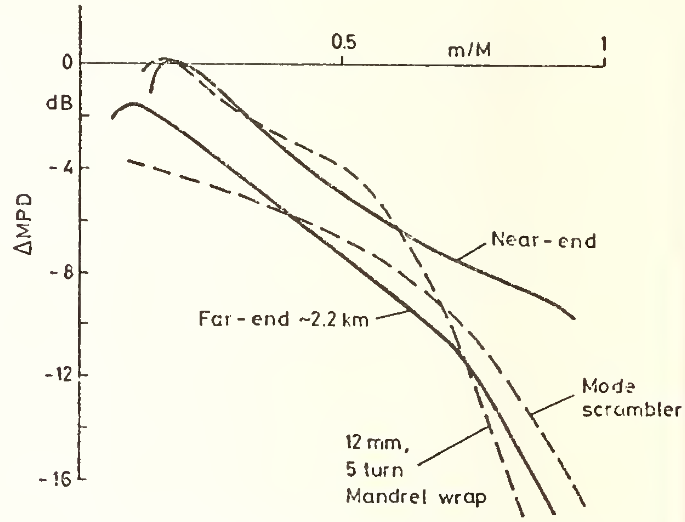


Fig.2a ΔMPD vs. m/M with LD input excitation (fiber 2)

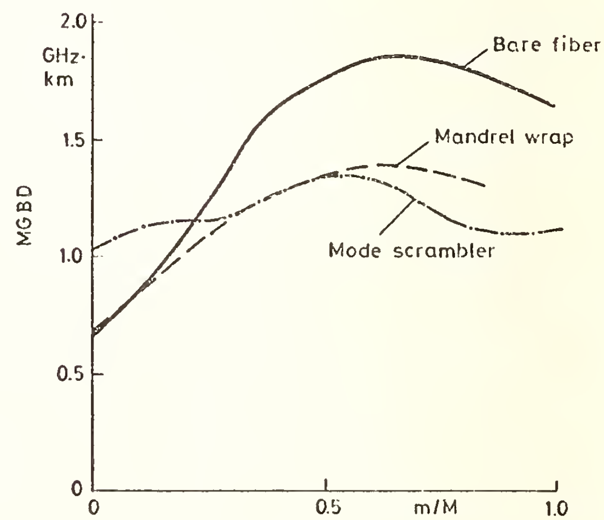


Fig.2b Mode group bandwidth distribution (MGBD) vs. m/M with LD input excitation (fiber 2)

# INFLUENCE OF DIFFERENTIAL MODE ATTENUATION ON BACKSCATTERING ATTENUATION MEASUREMENTS

M. Eriksrud, A.R. Mickelson, S. Lauritzen, N. Ryen

Electronics Research Laboratory
Norwegian Institute of Technology
N-7034 TRONDHEIM-NTH, NORWAY.

Although there have been laboratory tests of the repeatability of backscattering attenuation measurements[1], there has yet been no careful assessment of the sensitivity of the backscattering technique to launching conditions. It has been shown[2-3] that a mode-filtering technique can be used to eliminate power fluctuations due to slowly varying fiber parameters. The resulting power decay function then represents a measure of the actual fiber loss. However, graded index multimode fibers can also exhibit rapid parameter variations and differential scattering and absorption effects which cause excess loss. The present work applies some simple modelling of the differential mode attenuation process to interpret the results of backscattering and cut-back measurements of the variation of attenuation of telecommunication grade fibers with launching conditions.

Fig. 1.a illustrates a set of backscattering attenuation curves (loss functions) obtained from measurements from either end of a 50 μm/0.21 NA graded index fiber. As can be seen, slight changes in attenuation values are observed with different mode-filters. The mode-filter which most heavily supresses higher order modes (in forward and backward directions) yields the highest loss value. This is in agreement with the cut-back attenuation measurements (Fig. 2.a)

which indicate that lower order modes of this fiber have higher loss than the medium order modes. The excess loss due to lossy high-order modes is not present on the backscattering curves.

Fig. 1.b illustrates a similar set of curves obtained from a 50 μm/0.2 NA fiber of another manufacturer. This fiber has very different differential mode attenuation characteristics than the fiber of Fig. 1.a, as is shown in Fig. 2.b. Higher and medium order modes have substantially higher loss than lower order modes, and therefore, by employing mode-filters of successively smaller mode volumes, the loss, as measured by backscattering, is reduced.

As is illustrated by the above example, the measured attenuation of different fibers can be affected in different ways by changes in the launching conditions. Backscattering attenuation measurements performed with various mode-filters can effectively be used to evaluate the distribution of losses within the fiber. Further discussion of this point will be presented at the conference.

## References


1. B. Costa, B. Sorda, U. Menaglia, L. Piccari and G. Grasso: "Attenuation measurements performed by the backscattering technique", Electron. Lett., Vol. 16, pp 352-353, 1980.

2. A.R. Mickelson and M. Eriksrud: "Theory of the backscattering process in multimode optical fibers", Appl. Opt., Vol. 21, pp 1898-1909, 1982.

3. M. Eriksrud and A.R. Mickelson: "Application of the back-scattering technique to the determination of parameter fluctuations in multimode optical fibers", to appear in the October issue of IEEE J. Quantum Electron.

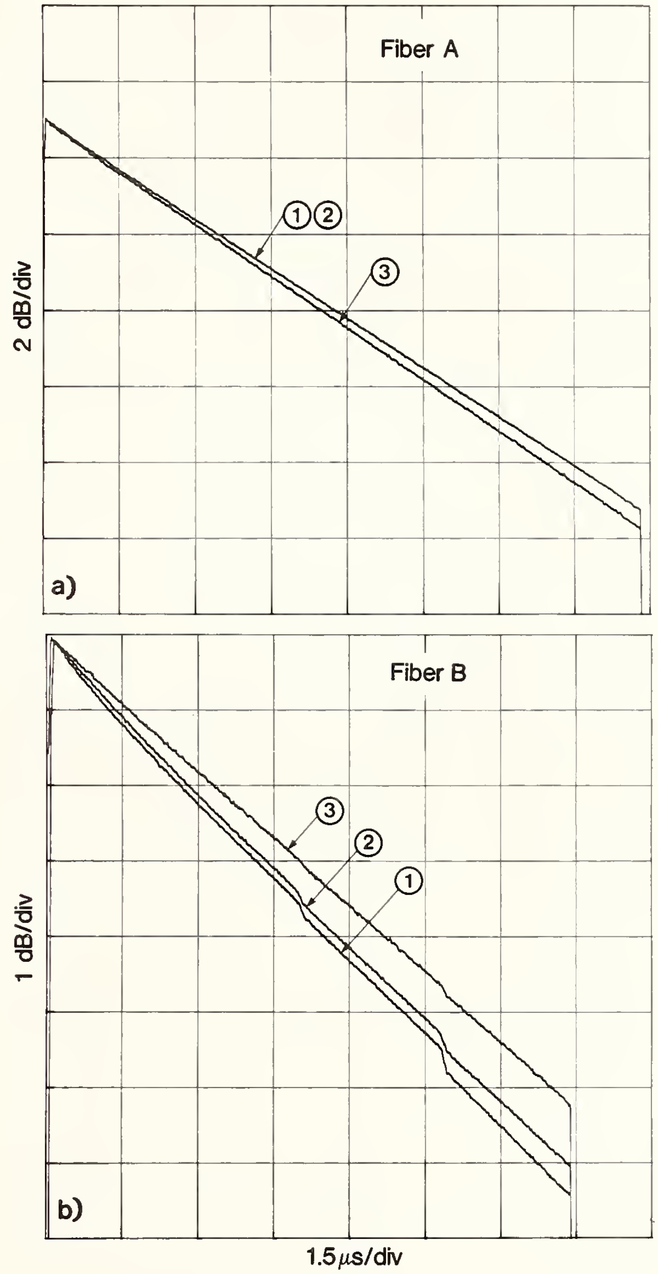


Fig. 1. Backscatter power loss function (λ=840 nm) obtained from the backscattered power curves, measured from either end of the fiber

1) without a mode-filter,
2) with a 100 m long fiber pigtail with a minimum 45 μm core and 0.20 NA as a mode-filter,
3) with a 100 m long fiber pigtail with a minimum 30 μm core and 0.18 NA as a mode-filter.

The corresponding average loss values are indicated in Fig. 2.

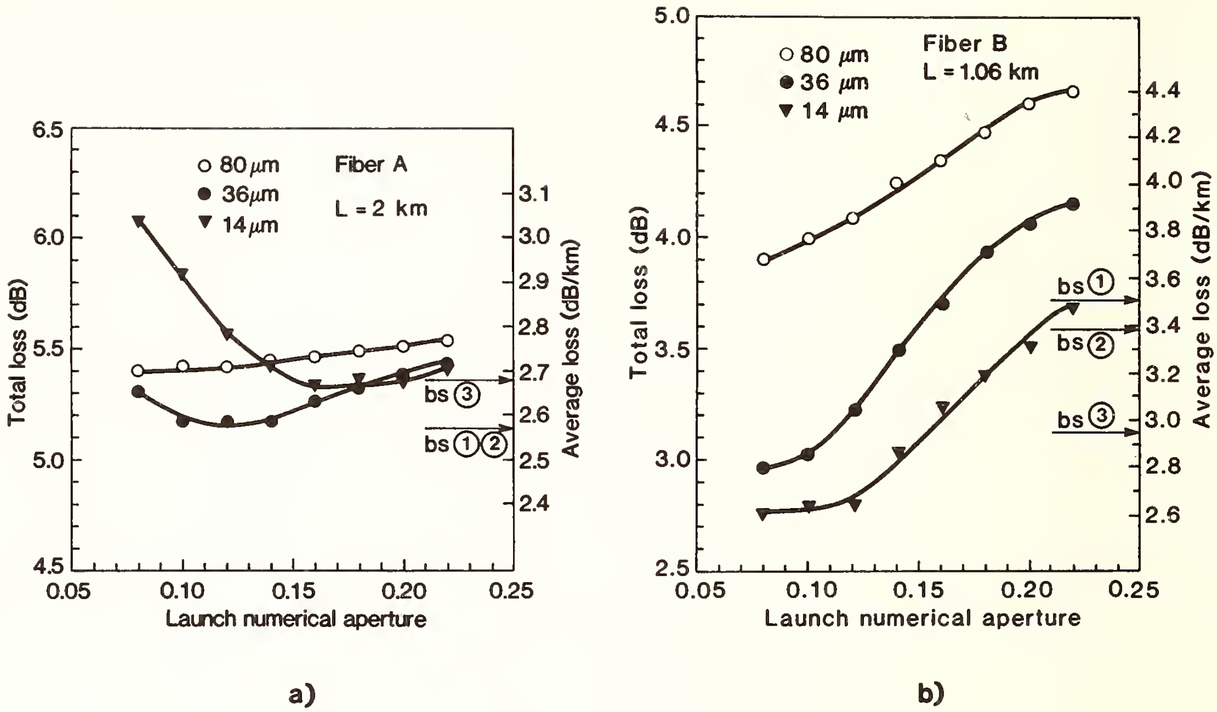


Fig. 2. Attenuation (λ=840 nm) measured as a function of launching conditions with a reference (cutback) length of 2 m, using beam optics launch with spot centered on the fiber core (50 μm diameter). Spot diameters of 80, 36 and 14 μm were employed.

# MEASUREMENT OF OPTICAL FIBRE ABSORPTION LOSS: A NOVEL TECHNIQUE

R. KASHYAP and P. PANTELIS

BRITISH TELECOM RESEARCH LABORATORIES, MARTLESHAM HEATH, IPSWICH, IP5 7RE, UK.

INTRODUCTION: There is increasing evidence that absorption loss between 1 and 1.6 μm is not negligible in OH free single mode fibres [1]. However, the absorption loss contribution to total attenuation in optical fibres has become difficult to assess with the achievement of lower losses. There are a number of reports [2-5] on methods of measurement, with one achieving a loss of less than one dB/km using a calorimetric method. We present a novel calorimetric technique, using a pyroelectric sensor material, polyvinylidene fluoride ($PVF_2$), which has the advantage of having a large pyroelectric coefficient and can be shaped to ideally suit this application. Using this material it is possible to measure sub-dB/km absorption losses with increased sensitivity with a few hundred milliwatts of laser power.

SENSOR: This consists of a tube of $PVF_2$, appropriately poled to produce a large pyroelectric coefficient, which is made at BTRL (Patent applied for). The tube used was 500mm long, with an OD of 1.409 mm and ID of 0.941 mm. It had a measured pyroelectric coefficient [6] of 29 $\mu C\ m^{-2}\ K^{-1}$. It is coated with conductive paint and held horizontally in a close fitting copper tube. Intimate thermal contact between the two is ensured by further filling the space with silver loaded conductive paint. This assembly is thoroughly lagged in a rigid insulating polyurethane foam box to isolate it from environmental effects. Access is easily available to both ends in order to allow the filling of the tube with water. The water performs two functions. Firstly, heat is conducted from the fibre to the sensor by the water, and secondly, it acts as the inner conductor for the accumulation of the charge. Since the sensor is an electrical insulator, water has a comparatively low enough resistance to introduce no significant errors in the measurement. The charge from the inner surface is picked up by a 50 micron diameter wire, one end of which is inserted into the tube to make contact with the water, and the other end fixed to a standard 50 ohm co-axial connector. The signal pickup end is enclosed in a small aluminium box to act as the earth terminal in conjunction with the copper tube. A low noise co-axial lead takes the signal to a simple charge amplifier (Kistler 5007), capable of measuring charges below one pC. The output of the amplifier is displayed on a chart-recorder. Piezoelectric effects in $PVF_2$ are easily filtered by a low pass filter.

MEASUREMENT TECHNIQUE: Since the measurement relies on the pyro-electric effect in a $PVF_2$ tube, a large surface area is desirable. Hence, for a given tube diameter, a longer tube will produce a larger charge per unit rise in temperature. Since the temperature rise is the same for every point in the short length of a low loss fibre (when the absorbed power << input power), for a given input power there is a linear increase in sensitivity with length. The sensor was chosen to be 0.5m long, on grounds of convenience and physical constraints. Precautions similar to those in Ref. 4 are taken to remove cladding modes to minimise errors. The tube is filled with water prior to insertion of the fibre. The far end is also mode stripped and terminated at a power-meter. The laser is switched on and the charge generated measured by the charge amplifier. Since this is essentially a quasi-static charge measurement which requires care, well established techniques are exploited [7,8].

THEORY: The absorption in the fibre is transmitted through the water to the inside wall of the sensor. The sensor tube detects a temperature difference across its walls. In order to ensure that the outside wall is unaffected by scattered radiation from the fibre, it is thermally clamped in a copper tube of thermal capacity much greater than the $PVF_2$ tube. This would otherwise pose a problem owing to absorption in the conductive paint. In addition, the copper tube defines the boundary condition for the solution of the heat flow equation. An approximate analysis of the structure shows that for the dimensions of the sensor:

$$\text{Absorption Loss, } \alpha = 3.384 * 10^7 * X / ( \mu * P) \text{ dB/km} \quad ...1$$

where, $\mu$ is the charge response of the sensor in pC/K, X is the initial slope of the generation of charge curve in pC/s, P is the measured optical power in mW at the output of the fibre. Using a value of 52.81 nC/K for $\mu$, we get:

$$\alpha = 640.8 * X / P \text{ dB/km} \quad ...2$$

RESULTS: To calibrate the sensor, a silica tube of 200 micron OD with a resistance wire through an 80 micron hole was used to dissipate a known amount of power using an ac current. Fig 1 shows the charge build-up with time after the current is switched on. The form is exponential in agreement with theory. Since the measurements are quasi-static, it is preferable to measure the initial rate of charge build-up than the final value of charge. Fig 2 shows the linear relationship of the initial slopes (as in Fig 1) vs. the power dissipated. The slope of this graph is 11.5 (nC/s) per watt of absorbed power. It also shows that a measurement of 0.1 pC/s is possible where the Johnson noise for this sensor (with a 1Hz BW) is about 8%. Using the data on the sensor and the calibration slope, the equivalent measured value for loss is:

$$\alpha = 755.2 * X / P \quad dB/km \quad ...3$$

which compares reasonably with the theory.

Optical measurements were made on a high loss fibre to investigate the performance of the technique. A Nd:Yag laser operating at 1.06 microns with a 1.5 W CW output was launched into a low-moded high $\Delta$ fibre. Fig. 3 shows a typical output. The measurements were performed for various input powers to simulate fibres of varying losses. A spurious effect was noticed at the start of the charging curve for all the measurements. The origin of the sharp initial rise, which is independent of input power, is currently under investigation. Fig. 4 shows the result of the subsequent slopes plotted against input power. The slope gives an absorption loss of 3.1 dB/Km. for this fibre. The lowest loss measurable for an input power of 1 W, and a best measurement of 0.1 pC/s, is 0.08 dB/km, which corresponds to a temperature rise of about 2 μK/s. This value can be improved by increasing the length of the sensor, by a higher pyroelectric coefficient and by reducing the tube wall thickness.

CONCLUSION: We have demonstrated a novel technique for measuring low absorption losses, with a present measurement capability of 0.08 dB/km for 1 W launched power. It is simple and reasonably easy to use. Further results on single mode fibres will be presented.

REFERENCES:


1. I. GARRETT, C.J. TODD, Opt.Quant.Electron. 14 (1982)95-143
2. T.C. RICH, D.A. PINNOW, Appl. Phy. Letts 20 (1972) 264-266
3. K.I. WHITE, J.E. MIDWINTER, Opto-electronics 5 (1973) 323-334.
4. K.I. WHITE, Opt. Quant. Electron. 8 (1976). 73-75.
5. K.I. WHITE et. al., Symp. on Opt. Fibre Meas., Boulder, 1980
6. G.R. DAVIES, University of Leeds, Private communication.
7. "Electrometer Measurements", Keithley Instruments.
8. G.S. SPESCHA, E. VOLLE, "Kistler Piezoelectric Measuring Instruments".

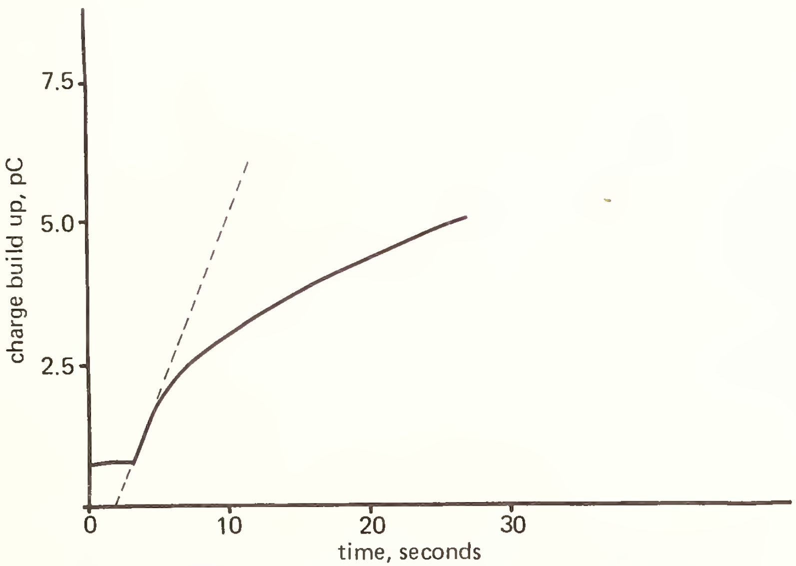


Fig 1 Charge build up for 54 μW electrical dissipation

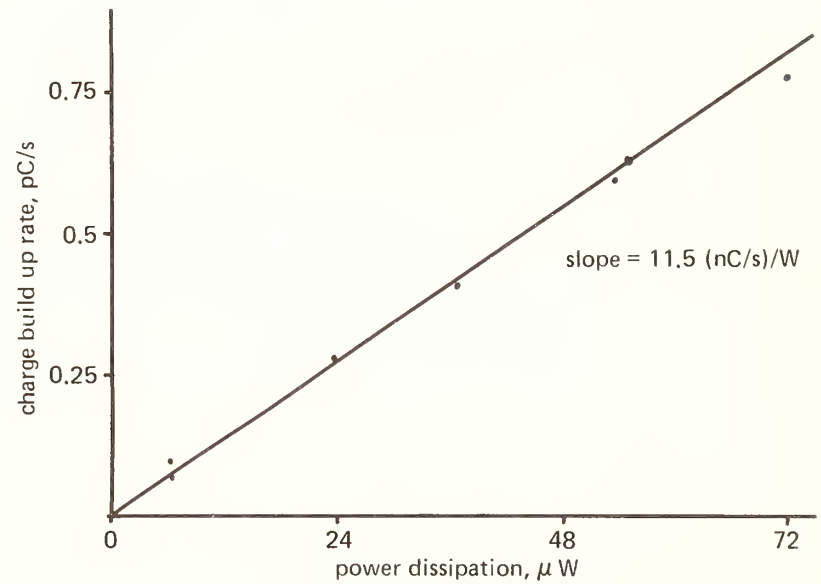


Fig 2 Sensor calibration

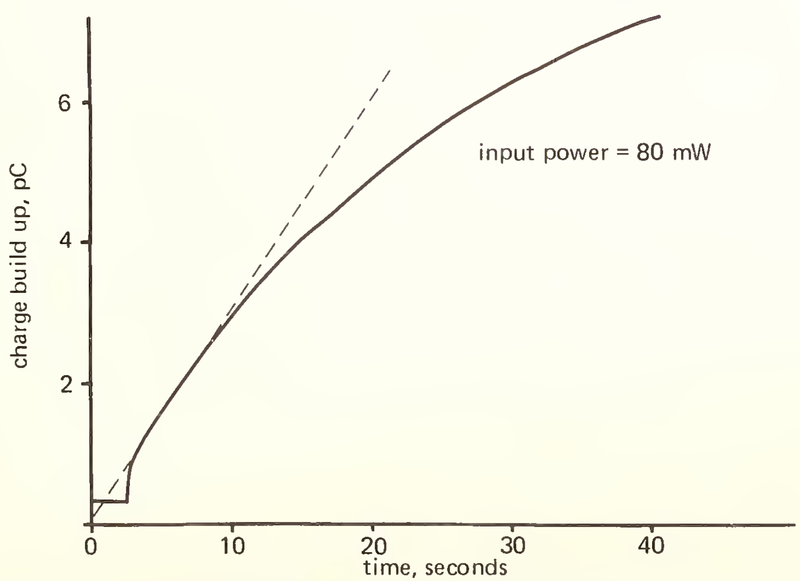


Fig 3 Charge build up for fibre

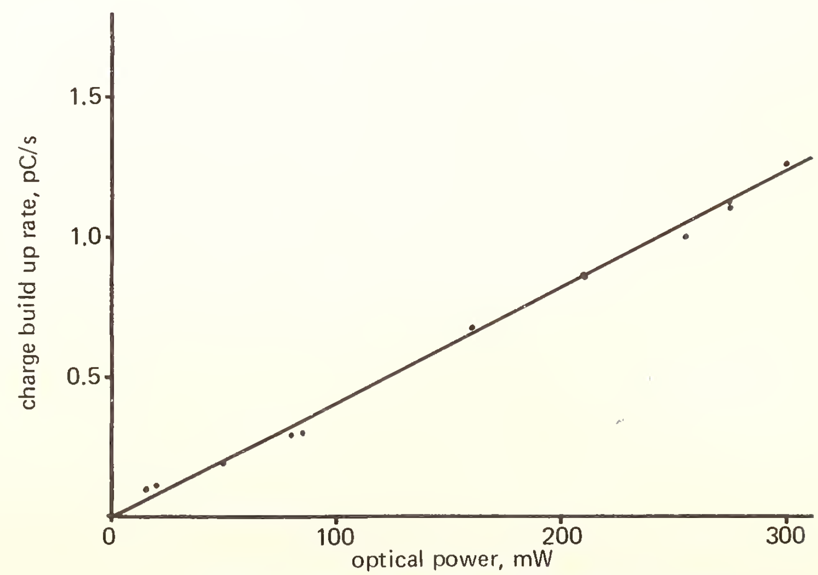


Fig 4 Charge rate vs. input power for fibre

# Single-mode Fiber Measurement in Japan

Kiyoshi Nosu

Yokosuka Electrical Communication Labovatory, NTT

1-2356 Take Yokosuka-shi Japan

## 1. INTRODUCTION

In recent years, single-mode fiber manufacturing technique has made a remarkable progress in producing low-loss fibers. The mass production of low-loss single-mode fibers stimulated the progress in peripheral techniques surrounding single-mode fiber transmission. The establishment of low-loss light coupling into a single-mode fiber, low-loss connecting, and splicing supports the large-capacity transmission through a single-mode fiber for the longer repeater spacing. In Japan, a 400Mb/s fiber transmission system is now on a field trial conducted since 1980 by NTT[1].

On the system design of single-mode fiber transmission, it is essential to establish the measurement techniques for fiber transmission characteristics and device performances. This paper reports the measurement techniques for single-mode fibers in Japan.

## 2. FIBER LOSS MEASUREMENT

Fiber loss is the most important factor to determine a repeater spacing in single-mode fiber transmission. For single-mode fiber loss measurement, it is unnecessary to apply an exciter or a dummy fiber, which is popular in multimode fiber loss measurement, as a single-mode fiber guides only one fundamental mode. The measurement is raher simpler. Neverthless, in order to keep a wide dynamic range with high resolution in loss measurement, a light source is required to output a high power and to couple it efficiently with a single-mode fiber, keeping power level stable. In our measurement systems, the dynamic range is about 70 dB at 1.3 µm and 1.5 µm bands by using a laser diode light source. The temperature dependence of an light source output level is less than 0.1 dB over the range of 10°C to 40°C. The light source adopted the confocal lens system [2] for efficient coupling and output level stableness. A Peltier effect device were applied to LD temperature control and APC loop to the output power stabilization.

For wide wavelength range loss measurement, a halogen lamp is a popular light source. Figure 1 shows an example of single-mode fiber loss spectra spreading from 1.2 µm to 1.7 µm, measured by the lamp. The dynamic range is more than 15 dB over the whole wavelength range.

Another way to measure fiber loss like OTDR will be discussed later.

## 3. INSERTION LOSS MEASUREMENT

Fundamental configuration for insertion loss measurement is the same as for fiber loss measurement. There are, however, some issues concerning measurement accuracy or reproducibility. One is whether a measurement object is polarlization sensitive or not. The sensitivity causes measurement errors when source light is polarized. Figure 2 shows a principal structure of depolarizer[3]. This device was designed to get reproducible measurements in the insertion loss measurement sensitive to polarization. In this device, birefringence material gives the path length difference to ordinary and extraordinary rays so as to remove the coherency between the rays. As a result, the depolarized output light is composed by combining the two rays which are already unable to interfere with each other. This device is effective to remove the polarization sensitivity from the measuring systems.

Other issue appears in connecter loss measurement. Figure 3 shows connector loss measurements in two cases of LD and LED light surces. The connectors are of FA-type[4] designed to be applicable both to single- and multi-mode fibers. There are large variances of loss measurements in an LD case, although an LED case shows reproducible measurements. A main cause is a gap, working like an etalon,formed between connector faces. Therefore, it will be unavoidable that a variance remains when an LD light source is used in loss measurement of devices with connectors as well as in connector loss measurement.

## 4. OPTICAL TIME DOMAIN REFLECTOMETRY

An Optical Time Domain Reflectometer (OTDR) is a powerful tool for supporting the cable installation and system supervisary, because the OTDR provides not only the optical cable fault location but the distribution loss measurement.

The OTDR configuration for single-mode fiber is essentially similar to that for multi mode fiber although the smaller level of backscattering in single mode fiber makes the measurement difficult[5]. The coupling efficiency of laser diode (LD) is smaller into a singl-mode fiber than into a multi mode fiber.

LD is adequate to the light source of the OTDR from the view points of easy-handling and reliability. The Burried Hetero-structure(BH) LD developed at the ECL is fit to the OTDR of its high output power and high coupling efficiency[6]. Figure 4 shows an example of backscattered waveform from single-mode fiber. The BH-LD launchs +9dBm peak power into fiber under the test. A polarization-separated-type optical directional coupler prevents the power leak of a source light into a sensor. A high speed digital averaging processor is effective to widen the measurable dynamic range. This OTDR can achieve up to 17.5dB one way dynamic range for fault location.

Figure 5 shows the backscatted waveform of a 19km long fiber. Sharp drops and rises appear on the exponentical decay slope. The drops and rises are caused by not only splice loss but fiber parameter mismatch at splice points. The results indicate that bidirectional observation is essential to evaluate the splice loss. It is necessary to adopt a kind of scrambler against polarization, as polarization dependence of backscat-tered light causes the OTDR measurment error.

The OTDR is also applied to estimate the birefringency in a single-mode fiber[7].

## 5. CHROMATIC DISPERSION MEASUREMENT

The bandwidth of single-mode fiber is limited by the chroma-tic dispersion. So it is significant to evaluate the chromatic dispersion in the high speed transmission systems.

Time domain pulse delay measurement have been reported not to have so good resolution as to measure the dispersion accurately. Figure 6 shows the schematic view proposed for chromatic dispersion measurement[8]. In Figure 6 , LDs oscillate at slightly different wavelength, and two phase shifters are set up to minimize the composite signal level demodulated in the receiver. The result at 1288nm wavelength is -2.48ps/km·nm in a 16km long single-mode fiber.

Wavelength-variable optical source is required to measure the dispersion over the wide wavelength region. The measurement covering 1.0-1.6μm has been reported where optical parametric oscillator and difference method is used[9].

[Acknoledgement]

The auther thanks Drs E.Iwahashi and M.Koyama for their encouragement, and thanks Yokosuka ECL members for their cooperation.

[Reference]

(1) E.Iwahashi, IEEE J.QE., vol.QE-17, NO.6, 1981.

(2) M.Saruwatari et al, ibid.

(3) Y.Fujii et al, presented at Nat.Conf.IECE Japan, March,1982.

(4) K.Nawata, IEEE J.QE., vol.QE-16, NO.6, June, 1980.

(5) K.Aoyama et al, IEEE, J.QE., vol.QE-17, NO.6, 1981.

(6) Y.Nakano et al, Electron. Lett., vol.17, NO.21, Oct., 1981.

(7) M.Nakazawa et al, IEEE J.QE., vol.QE-17, NO.12, Dec., 1981.

(8) K.Aoyama et al, presented at 1981 Nat.Conf.IECE Japan, Mar., 1982.

(9) A.Sugimura et al, IEEE J.QE., vol.QE-16, NO.2, 1980.

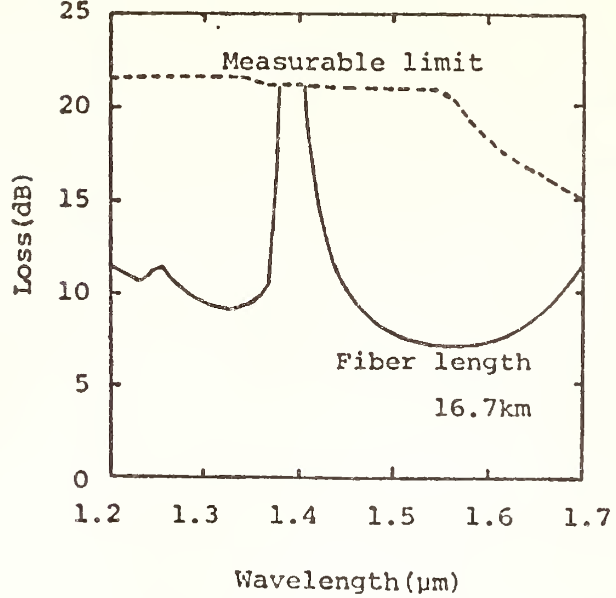


Fig.1 Single-mode fiber loss characteristics with loss measuring equipment

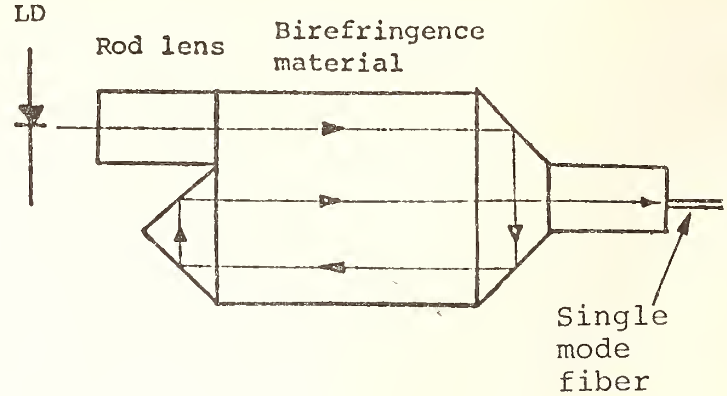


Fig.2 Depolarizer

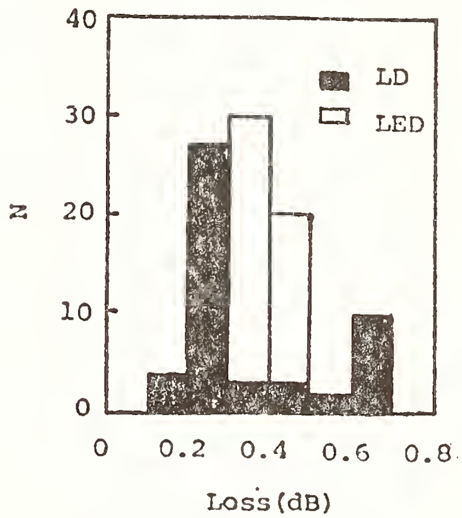


Fig.3 Connector losses dependent on optical sources

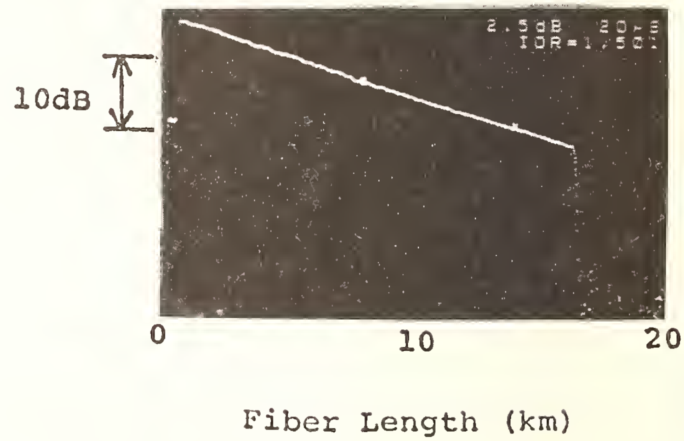


Fig.4 OTDR with LD

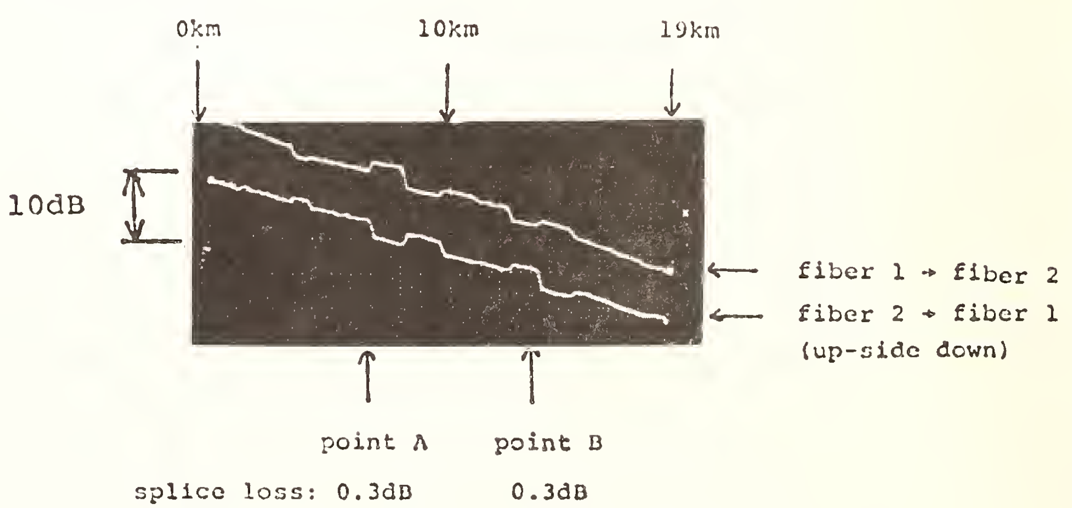


Fig. 5 OTDR measurements of spliced fibers (with LD)

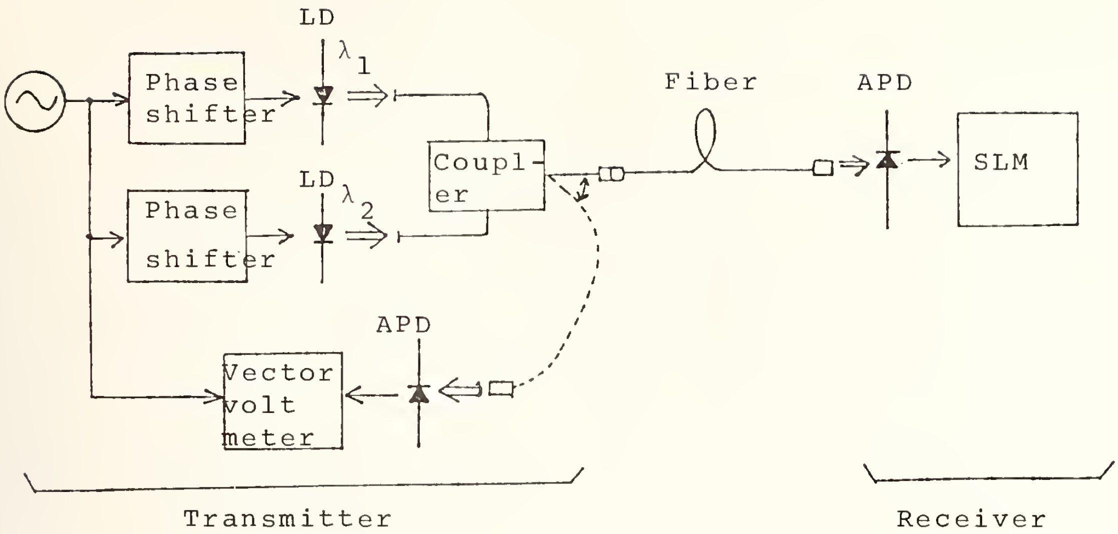


Fig.6 Chromatic dispersion measurement with baseband phase comparison method

# The Characterization of Monomode Fibre Links Installed in Operational Duct

J R Stern, D B Payne, T D S Wood and C J Todd
British Telecom Research Laboratories, Martlesham Heath, UK.

1 Introduction During the past year a number of experimental monomode optical fibre links have been assembled at British Telecom Research Laboratories in order to aid transmission performance studies and to provide test bed links for system trials. These links include a 102 km laboratory link[1], a 31.6 km cabled laboratory link[2] (containing 15 splices), a separate 31.5 km cabled link[3] (containing 30 splices) and a 61.3 km cabled link[4] (containing 37 splices). The last 2 links have been installed in operational duct in the vicinity of the Research Laboratories to form a complex of cables linking Martlesham to telephone exchanges at the nearby towns of Woodbridge and Ipswich. The 31.5 km field installation, cable manufactured by Telephone Cables Limited (TCL), has been successfully operated at a bit rate of 650 Mbit/s[3]. Installation of the 61.3 km cabled link, manufactured for BT by Standard Telephone Laboratories[4], has recently been completed at the time of writing. System trials[5] have now been successfully conducted at 565 Mbit/s (1300 nm) over the full 61.3 km and at 140 Mbit/s (1550 nm) over an unrepeatered 90 km link formed by splicing the 2 installed cable routes together.

The planning and assembly of these links has posed interesting problems in fibre characterization, both in the laboratory and field, and the purpose of this paper is to outline the approaches we have adopted. Emphasis here is on data taken from the 31.5 km field installation although preliminary data is presented for the 61.3 km installation. Fuller information and analysis will be available at the conference. Implications for the future field testing and specification of monomode fibre systems will be discussed.

2 Fibre Measurements The fibre used in our trials has been produced to a matched cladding design previously described[6] with the zero chromatic dispersion point in the region of 1320 nm. During the planning and assembly of the laboratory links and the 31.5 km installed cable route, equivalent step index (ESI) profiling[7] was extensively used to characterize and select the individual link fibres and, as we shall see below, predict splice loss performance. In this technique, the mode spot size variation with wavelength

is measured for a short length of fibre, and the ESI profile which gives the best fit to the experimental data is selected as a good approximation for the behaviour of the true, complex profile shape. The equivalent profile is then used to characterize key parameters for the fibre - eg. microbending (cabling) losses and splice losses (arising due to ESI profile mismatches). ESI profiling allows monomode fibre to be specified by only 2 parameters: equivalent core radius and equivalent index difference. The additional parameters of fibre outside diameter, concentricity error and spectral loss enabled the individual lengths of fibre for the trial links to be fully specified. The ESI measurements were carried out using a simple automated apparatus[8] based on a standard spectral loss apparatus. The mean values of the ESI parameters and the concentricity error of the individual fibre ends spliced together in the 31.5 km trial were as follows: Core radius ($a_s$) = 4.81 μm; std.dev = 0.42 μm, index difference ($\Delta n_s$) = 0.0031; std.dev = 0.00053, and concentricity error = 0.52 μm; std.dev = 0.26 μm.

In the 61.3 km trial an alternative approach to ESI profiling was adopted by the manufacturer (STL). The refracted near field technique[9] was used to obtain full index profile measurements. Values of peak index difference ($\Delta n_p$) and core radius were read from the index plots. The mean values obtained for the fibre batch were: $\Delta n_p = 5.03 \times 10^{-3}$, a = 4.34 μm. ESI (and concentricity error) data is currently being measured at BTRL for a representative batch of the fibres. The 2 approaches to fibre profile characterization will be discussed at the conference. Currently, we believe that the ESI approach should prove of particular importance to the fibre user as a simple means of characterizing and specifying both cabling and splicing performance. The alternative approach of full profile measurement, however, is likely to continue to be of major interest to the fibre manufacturer.

3 Cable Measurement Both spectral and point loss (1300 nm and 1550 nm) measurement techniques have been used in the laboratory and field programmes. Point loss measurements have proved of particular value in the field environment where compact equipment and speed of measurement are at a premium. The main difficulty experienced with both types of measurement has been accuracy. Typically fibre losses have been in the range 0.2-0.3 dB/km at 1550 nm and, for measurements made on 1-2 km lengths of fibre, errors are ~0.05 dB/km even when great care is taken. A statistical approach is

therefore necessary to establish the magnitude of cable incremental losses to sufficient accuracy. Only be measuring over a large batch of fibres with a range of ESI parameters can 'safe' criteria be established for a given cable structure. Earlier work carried out by Hornung and Reeve[10] at this laboratory was used to guide fibre selection for the 31.5 km field installation. The cable for this trial, manufactured by Telephone Cables Ltd (TCL), employed a loose tube structure and introduced negligible microbending loss in the critical, long wavelength (1500 nm) window where cabling incremental loss is most likely to occur. Indeed several low $\Delta n_S$ fibres, which had shown significant microbending loss on reel showed a marked reduction in loss at 1550 nm when packaged and cabled in this structure (see Table 1).

The cable for the 61.3 km link, manufactured by STL, was of the tight secondary package design. In cables of this type the fibre can, in principle, be subject to differential strain from other cable components introduced during stranding and sheathing. However, with appropriate manufacturing control, these problems can be minimized and the final cables for the 61.3 km link showed no incremental loss in the 1550 nm range compared with the secondary packaged fibre loss. Further it was established by direct strain measurement that no significant remnant fibre strain was introduced during duct installation of the 61.3 km tight packaged link.

An important objective of our field measurement programmes was to establish the magnitude of any change in cabled fibre loss on installation in duct. It was decided that "remoted ended" loss measurements in the field would be inaccurate and the following "loop splicing" strategy was therefore adopted for both field trials. Two splices were made at one end of each of the installed, 4-fibre cables to form looped fibre pairs. Loop loss measurements were then performed from a test vehicle, the loop splices being cut out and returned to the laboratory for subsequent assessment. In this way it was possible to establish that the average cable loss had not changed on installation for the 31.5 km link (see Table 1). Final conclusions for the 61.3 km link await measurement of the loop splices but present indications are that, no change in average cable loss has occurred. An extremely useful feature of the loop splicing strategy was that, after measurements on the individual cables had been completed, all subsequent link measurements could be made from the laboratory as the installed cables were cumulatively spliced together.

A second method has also been used to characterize the loss performance of our experimental links; Optical Time Domain Reflectometry (OTDR). This technique proved to be of key importance in allowing the rapid and convenient assembly of spliced, monomode links, a complete loss "finger-print" being obtained at 1300 nm. A particular advantage is that splices and fibres can be individually measured without the need for cutback measurements. The photon counting OTDR apparatus developed at BTRL has a range of around 20 dB (one way fibre loss) for detecting a fibre break (cessation of Rayleigh scatter) but can be used as an effective measurement tool over much of that range[11]. A 0.1 dB measurement precision is possible over a range of about 10 dB. Some care in interpretation of the OTDR traces is necessary. For example, significantly different splice losses can be measured for light incident in opposite directions at the splice. Occasionally a negative splice loss is observed for one direction of propagation. These effects are thought to be due to ESI profile mismatches on either side of the splice leading to different back scattering coeffficients. Under these conditions, an average loss for the 2 directions should yield the true splice loss, and the loop splicing strategy described above allowed this to be conveniently obtained.

Good agreement has been obtained between OTDR measurements of fibre loss and splice loss in comparison with conventional cutback techniques. The splice loss distribution as measured by OTDR (1300 nm) is shown in Fig 1 for the 31.5 km installed system and the mean value of 0.22 dB agrees extremely well with the mean splice loss of 0.215 dB obtained by subtracting the sum of the cable losses from the total link loss (Table 1).

Lower average splice losses have been obtained on the 61.3 km link. The splice loss histogram for the installed route, measured by OTDR at 1300 nm, is shown in Fig 2. Comparison with the average splice loss obtained by the 'cutback' technique awaits the loop splice loss evaluation mentioned above.

4 Splice Loss Interpretation Theoretical calculations of the intrinsic losses due to profile mismatch and to concentricity error show that a 0.15 dB mean loss is expected for the 31.5 km field installed link. These calculations use as input data the measured tolerance values for the fibre pair at each splice. A computer programme accounts for the statistical nature of the azimuthal orientation of the concentricity error vectors. Average loss due to the splicing machine itself (core deformation) has been shown to be around

0.08 dB for low concentricity error fibre. Thus the sum of the mean losses due to the splicing technique and the fibre tolerance amounts to around 0.23 dB which agrees well with the mean value actually measured. The splice loss for this particular link is clearly significantly influenced by fibre production tolerances and improvements should lead to a lower mean value. Present indications are that the lower splice losses achieved on the 61.3 km link are in fact due to better tolerances - particularly concentricity error. Firmer conclusions should be possible by the time of the conference.

5 Conclusions Techniques for characterizing the performance of monomode fibre links have been discussed with particular reference to experience gained on 2 installed cable routes. The link performances obtained have significantly exceeded our original expectations and have enhanced the prospects for early deployment of operational monomode systems in the UK network. The 2 trials have enabled conventional multimode cable structures, of both the loose tube and tightly jacketed type, to be successfully tested for monomode operation. No major cabling problems have emerged even at the more sensitive wavelength of 1550 nm. In the link characterization programmes, a loop splicing strategy was adopted in order to overcome loss measurement problems encountered in the field. ESI profiling and OTDR techniques have featured prominently. The former technique may provide a basis for the complete specification of monomode fibres from the point of view of cable incremental losses and, in conjunction with concentricity error measurements, splice losses. The latter shows promise as an important tool for the characterization of monomode links as well as for fault location.

Acknowledgments The authors wish to gratefully acknowledge the contributions of their many colleagues at BTRL involved in the assembly and characterization of the monomode links. Acknowledgment is also due to staff at Standard Telephone Laboratories for provision of data under a British Telecom Development Contract, to Telephone Cables Ltd, GEC Optical Fibres and the Director of Research, BTRL, for permission to publish this paper.

References

1 Malyon, D et al: Elec Lett, 18, (1982), pp 445-447.

2 Payne, D B et al: Elec Lett, 18, pp 82-84.

3 Stern, J R et al: The field installation of a 31.5 km monomode optical fibre system operated at 140 Mbit/s and 650 Mbit/s, Elec Lett, 18, (1982), pp 631-632.

4 Irvine, J et al, 8th ECOC, Cannes, Sept 1982.

5 J E Midwinter, to be published.

6 Ainslie, B J et al: Proc 7 ECOC, Copenhagen 1981, 2.5.1.

7 Millar, C A: Elec Lett, 17, (1981), pp 458-460.

8 Millar, CA: Proc OFC 82, Phoenix, Arizona 1982, ThEE3.

9 White, K I, Opt and Quant Elec, 11, (1979), pp 185-196.

10 Hornung, S and Reeve, MH: Elec Lett, 17, (1981), pp 774-775.

11 Healey, P: ICC June 1982, Philadelphia, USA.

Table 1

MEAN FIBRE LOSSES dB/km

| | 31.5 km Installed Link | | 61.3 km Installed Link | |
|---|---|---|---|---|
| | 1300 nm | 1550 nm | 1300 nm | 1550 nm |
| Primary coated (on reel) | 0.45 | 0.77* | - | - |
| Tubed/secondary coated | 0.45 (0.02) | 0.25 (0.02) | - | - |
| Cabled | 0.47 (0.02) | 0.25 (0.02) | 0.44 | 0.29 |
| Installed | 0.46 (0.03) | 0.26 (0.03) | - | - |
| Spliced | 0.68 (0.01) | 0.51 (0.01) | 0.49 | 0.33 |

*this result indicates tension on the primary coated fibre on reel. Figures in brackets are standard errors in the mean for each measurement.

-indicates data not yet available.

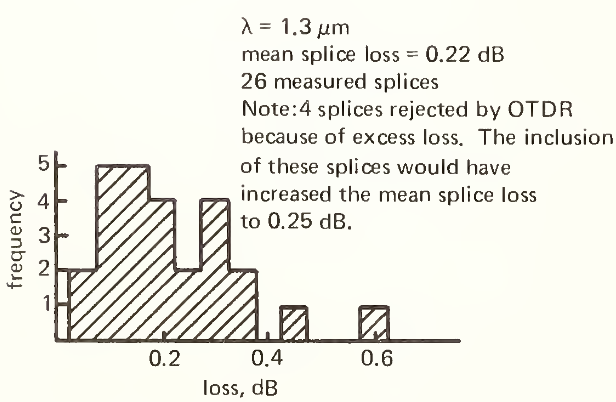


Fig. 1. Splice histogram GEC/TCL

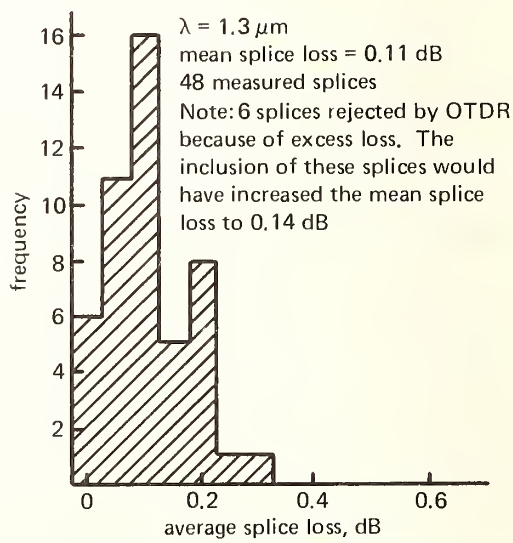


Fig. 2. Splice histogram STL/STC

# SINGLE MODE FIBER LOSS ROUND ROBIN

W. B. Gardner
Bell Telephone Laboratories
2000 Northeast Expressway
Norcross, GA 30071

Obtaining good agreement between multimode fiber loss sets has proven difficult. The standard deviation between locations (i. e., test sets) is limited to about 0.2 dB/km by the problem of reproducing test set launch conditions.[1,2] This particular problem should not exist with single mode fibers, since only one mode can propagate. Consequently, one would expect the interlocation standard deviation to be less than 0.2 dB/km when measuring single mode fiber attenuation. Indeed, because the loss of single mode fibers is frequently only a few tenths of a dB/km, a loss measurement accuracy of a few hundredths of a dB/km will be necessary. We have recently completed a loss measurement round robin involving seven Bell System test sets. The results indicate that this level of accuracy is indeed attainable with single mode fibers.

Three fibers were circulated among seven Bell Labs and Western Electric locations. The fibers were wound under low tension with multiple layers on six inch diameter plastic spools. They were of the depressed cladding design[3], having core diameters in the 7.5 - 9.0 μm range, and $LP_{11}$ mode cutoff in the 1.26 - 1.31 μm range. Each location measured each fiber twice; the means of the two measurements are listed in Table I. The cutback technique was used, with a loop approximately 40 mm diameter present to suppress unwanted modes. Location 5 used a 1.30 μm laser diode; all other locations used a tungsten lamp with a monochromator.

The interlocation standard deviation $\sigma$ is seen in Table I to be typically about .03 dB/km. The one exception is the measurement at 1.55 $\mu$m wavelength of Fiber 3. The large $\sigma$ in this case is the result of a steeply rising spectral loss curve. The rise occurs at this wavelength in Fiber 3 because this fiber has a more deeply depressed cladding[4] than Fibers 1 and 2. Since the 1.55 $\mu$m loss is very large in this case, the larger $\sigma$ is not of great concern.

In conclusion, an interlocation standard deviation of .03 dB/km has been demonstrated for single mode fiber loss measurements. This is nearly an order of magnitude better than the $\sigma$'s achievable with typical multimode fibers.

I would like to thank my colleagues W. T. Anderson, J. S. Nobles, P. D. Lazay, J. Stone, A. R. Tynes, A. Tomita, and J. Sanchez for performing the measurements reported here.

REFERENCES

1. A. H. Cherin and W. B. Gardner, Laser Focus 16, #8, 60 (1980).

2. D. L. Franzen, G. W. Day, B. L. Danielson, G. E. Chamberlain, and E. M. Kim, Appl. Opt. 20, 2412 (1981).

3. P. D. Lazay, A. D. Pearson, W. A. Reed, and P. J. Lemaire, CLEO, Washington, June 10-12, 1981, paper WG6.

4. P. D. Lazay, A. D. Pearson and M. J. Saunders, Topical Meeting on Optical Fiber Communication, Phoenix, April 13-15, 1982, paper ThCC2.

# TABLE I

## BELL SYSTEM SINGLE MODE LOSS ROUND ROBIN
## (ALL LOSSES IN dB/km)

| | $\lambda$ = 1300nm | | | $\lambda$ = 1550nm | | |
|---|---|---|---|---|---|---|
| FIBER NO. → | 1 | 2 | 3 | 1 | 2 | 3 |
| FIBER LENGTH → | 2km | 2km | 1km | 2km | 2km | 1km |
| LOCATION 1 | .51 | .41 | .49 | .54 | .23 | 9.91 |
| 2 | .52 | .46 | .51 | .54 | .29 | 8.09 |
| 3 | .51 | .41 | .42 | .52 | .21 | 10.00 |
| 4 | .53 | .40 | .44 | .57 | .24 | 8.40 |
| 5 | .55 | .43 | .45 | — | — | — |
| 6 | .58 | .43 | .52 | .60 | .29 | 9.15 |
| 7 | .60 | .42 | .52 | .60 | .26 | 8.77 |
| | | | | | | |
| INTERLOCATION $\mu$ | .53 | .42 | .47 | .56 | .25 | 9.05 |
| INTERLOCATION $\sigma$ | .03 | .02 | .04 | .03 | .03 | .78 |
| | AVG. INTERLOCATION $\sigma$=.03<br>FOR MULTIMODE FIBERS, $\sigma$=.20 | | | | | |

CHARACTERIZATION OF THE BEND SENSITIVITY OF SINGLE-MODE FIBERS USING THE BASKET-WEAVE TEST

By A. Tomita, P. F. Glodis*, D. Kalish*, and P. Kaiser
Bell Laboratories, Holmdel, N. J. 07733; *Norcross, GA, 30071

Presently, extensive research and development efforts are under way to optimize the index profile, geometry, coating, and cable-structure of single-mode (SM) fibers [1-5]. The optimization includes keeping the core diameter as large as possible for ease of splicing and connectorization, while still maintaining a high resistance against macro- and microbending (MB) losses. As in case of multimode fibers, MB losses depend on the fiber parameters, the plastic coating, and the cable structure. In contrast to MM fibers, however, MB losses in SM fibers are wavelength dependent and can be eliminated in the short-wavelength region of the SM domain as has been demonstrated previously[7]. While a truly satisfactory test regarding the MB resistance of a SM fiber can only be made with a cabled and deployed fiber, simulated tests must be used to facilitate the fiber optimization process. One such test, which has become known as the 'Basket Weave" (BW) test, consists of multi-level winding the fiber on a spool, and measuring the spectral losses for different winding tensions[7]. A high immunity against the ensuing stresses is a measure of a superior jacketed-fiber structure. In addition to possibly incurring MB's due to the transverse pressure exerted by adjacent windings, the fiber may suffer losses due to winding crossings, and macrobends due to the curvature of the spool. Because of the relaxation of the rewind stresses of the plastic-coated fiber, the excess losses generally decrease with time, and meaningful comparisons of data can only be made if the measurements are performed a specific time after the rewind process.

The SM fibers used for this study were of the depressed-cladding type, which permits a nearly independent optimization of the core size and minimum dispersion wavelength[1-4]. Specifically, core diameters ranged from 8.0 to 9.3μm, and index differences $\Delta/\Delta^-$ (Fig. 1) from 0.31/0.06 to 0.49/0.19%, respectively, as obtained with the refracted-near-field technique. Fiber o.d.'s were 125μm, a/b ratios approx. 6.0, and cut-off wavelengths ~1.22μm. The spectral losses of the fibers wound under <3 to 75g tension on 15-cm-diam. spools are shown in Figs. 2 to 4. The SM wavelength region is bounded by the cut-off band of the 1st higher ($LP_{11}$) mode on the short-wavelength side, and by a loss edge at longer wavelengths. The long-wavelength edge (LWE) may be due to the IR absorption tail, macro- or micro-bending losses, and in case of the depressed-index fibers, also due to the leakage of the fundamental mode through the inner cladding layer[2-4]. Characteristic for fiber A with small index depression (0.31/0.06%) and large core (9.3μm), excess losses were observed throughout the SM domain even for moderate winding tension, and the LWE rapidly moved to shorter wavelengths with increasing tension (Fig. 2). While the LWE of fiber B with intermediate index depression also moved to shorter wavelengths (Fig. 3), the loss in the 1.3μm wavelength region was constant and independent of the various bending forces exerted. The BW test thus revealed the superiority of fiber B in regards to resisting MB stresses, and a good correlation was found to exist between the excess losses encountered in the BW test, and added-losses measured during the various cabling stages of an experimental submarine cable design[8,9].

While the spectral loss was independent of the winding tension for fiber C which had the smallest core and the lowest cladding index (Fig. 4), a LWE appeared immediately after the

1.385μm OH band. After rewinding onto a 35cm diameter spool, however, the LWE moved further into the IR, and until now unknown loss bands appeared in the long-wavelength region (Fig. 5). We tentatively attribute these bands to the coupling of the core-guided mode to discrete outer cladding modes. Additional results concerning the intensity, location, and curvature dependence of these bands will be presented at the Symposium.

In summary, the basket-weave test provides rapid and valuable information concerning the macro- and microbend sensitivity of different types of SM fibers. Because of the wavelength dependence of the bending losses, BW tests should generally be performed in conjunction with spectral loss measurements. A properly-designed SM fiber does not exhibit MB -induced excess losses in the short-wavelength region of the SM domain, which can be extended to longer wavelengths with an improved jacket and/or cable structure.

ACKNOWLEDGEMENTS:

The index profile data were provided by M. J. Saunders whose cooperation was very much appreciated.

REFERENCES:

1. P. D. Lazay, A. D. Pearson, W. A. Reed, and P. J. Lamaire, CLEO '81, WG6-1, Washington, D. C. (1981)
2. P. D. Lazay, A. D. Pearson, and M. J. Saunders, OFC '82, Phoenix, THCC2 (1982)
3. L. G. Cohen, D. Marcuse, and W. L. Mammel, Ibid., THCC1
4. B. J. Ainsley, K. J. Beales, C. R. Day, H. P. Girdlestone, and J. D. Rush, Ibid., THCC 3
5. V. A. Bhagavatula, D. B. Keck, R. A. Westwig, and P. E. Blaszyk, Ibid., THCC4
6. Y. Katsuyama, S. Mochizuki, K. Ishihara, and T. Miyashita, Appl. Opt. 18, 2232 (1979)
7. P. Kaiser, W. G. French, D. L. Bisbee, and J. W. Shiever, IOOC '79, 7.4-1, Amsterdam (1979)
8. R. E. Wagner, S. M. Abbott, R. F. Gleason, R. M. Paski, A. G. Richardson, D. G. Ross, and R. D. Tuminaro, ICC, Philadelphia '82
9. R. D. Tuminaro, private communication

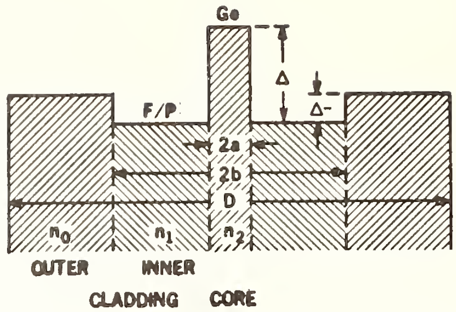


Fig. 1

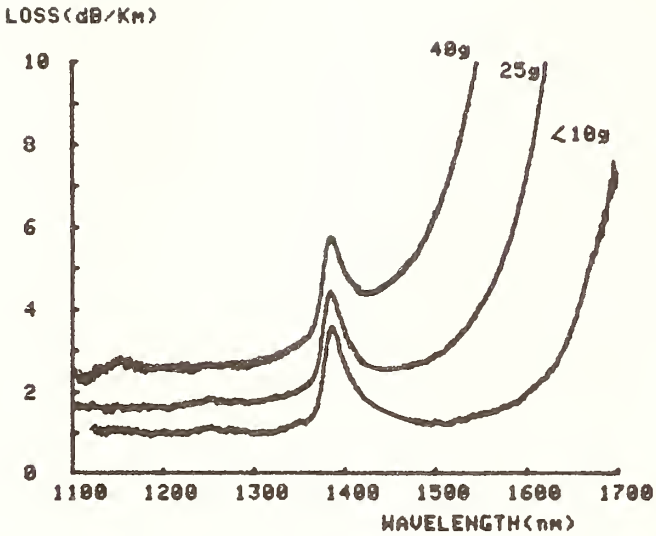


Fig. 2

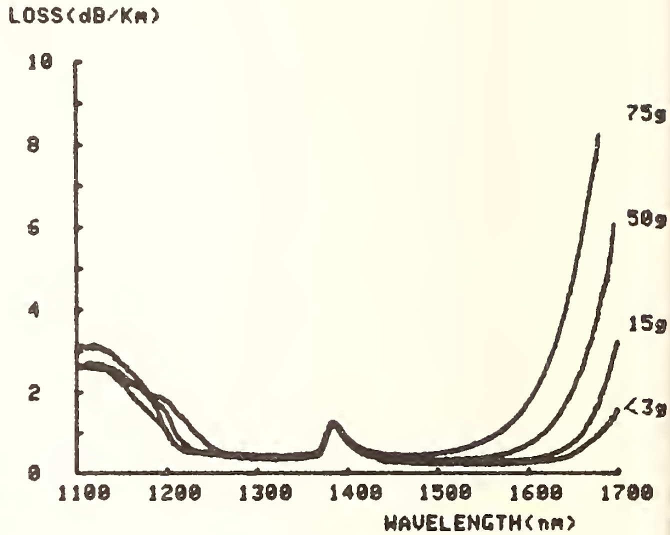


Fig. 3

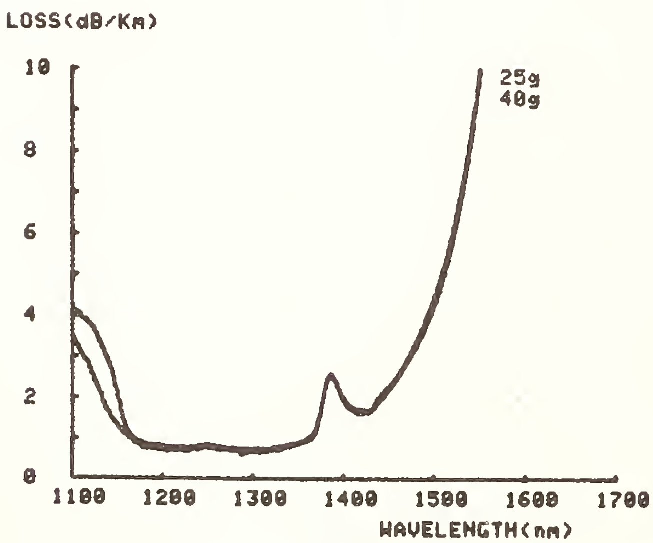


Fig. 4

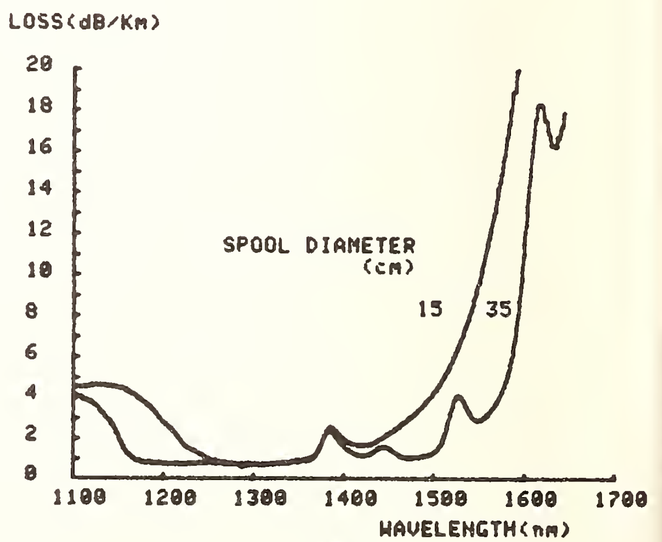


Fig. 5

# CALCULATION OF EQUIVALENT STEP-INDEX PARAMETERS FOR SINGLE-MODE FIBRES

M. FOX

BICC Research & Engineering Ltd, London, England

Introduction It is desirable to represent the propagation behaviour of a single-mode fibre by a few key parameters. A method currently in favour is to define an "equivalent-step-index" fibre, whose core radius a and relative refractive index difference $\Delta$ should lead to reasonably accurate calculations of cut-off wavelength, spot size (and hence of losses at joints or due to microbending) and waveguide dispersion, using standard formulae. The approaches used are either to calculate suitable average values of a and $\Delta$ from the refractive index profile, or to find the values from the cut-off wavelength and the relation between spot size and wavelength in the single-mode region. The data used would usually be experimental. In the present paper, however, they are calculated from an assumed parabolic profile, for which a spot size formula has been published by Marcuse.[1]

Calculations from the refractive index profile This method is given by Stewart[2] and Bhagavatula.[3] For a parabolic-index fibre, of core radius a and relative refractive index difference $\Delta$, with maximum refractive index n, the equivalent step-index values are

$$a_{ES} = 3a/4, \qquad \Delta_{ES} = 8\Delta/9, \qquad \lambda_{ES}(\text{cut-off}) = 2\pi n a \Delta^{1/2}/2.4048$$

The last result may be compared with the correct value

$$\lambda(\text{cut-off}) = 2\pi n a \Delta^{1/2}/2.4877$$

Calculations from curves of spot size V wavelength An experimental plot of spot size against wavelength[4] shows a sharp fall due to cut-off of the second mode and then a slow increase; both sections of the curve are extrapolated to give the cut-off values. Millar[4] uses two procedures: either (a) the calculations are based on the cut-off values of wavelength and spot size alone; or (b) they also use the slope of the curve in the single-mode region. A third method, (c) (Alard et al,[5] Millar[6]) involves the fitting by least squares of an empirical formula due to Marcuse[1] to the single-mode region of the curve. The values of 2a and $\Delta$ that give the best fit are accepted.

Marcuse[1] quotes his results in terms of the field radius $w_f$, defined in terms of the Gaussian approximation to the field in the fibre: $E = E_o \exp(-r^2/w_f^2)$. He derives formulae for $w_f/a$ in terms of V, for both step and parabolic index profiles. Snyder[7] gives a less accurate formula for step-index fibres.

The various procedures then involve the following calculations:-

(a) $\lambda$ and $w_f$ are known at cut-off, viz $\lambda_o$ and $w_o$:

Assuming the maximum refractive index to be 1.45,

$$2a_{ES} = 1.8198 w_o \quad \text{and} \quad \Delta_{ES} = 0.13935\ (\lambda_o/2a_{ES})^2$$

(b) $\lambda$, $w_f$ and $dw_f/d\lambda$ are known at cut-off, viz $\lambda_o$, $w_o$ and $w_o'$:
Millar[4] shows that $2a_{ES} = 3.3039(w_o - 2\lambda_o w_o'/3)$. $\Delta_{ES}$ is found as above.

(c) $w_f$ is known for a range of values of $\lambda$ in the single-mode regions: Marcuse's step-index formula may be written in terms of $w_o$ and $\lambda_o$, and of $\lambda$. By fitting the result to the data using least squares, "best values" of $w_o$ and $\lambda_o$ and hence of $2a_{ES}$ and $\Delta_{ES}$, are found.

Simulated results For a parabolic index fibre with 2a = 11.0134 μm, n = 1.45, and 100 $\Delta$ = 0.3388, the cut-off wavelength is 1.174 μm. Spot sizes have been calculated from these parameters and Marcuse's parabolic-index formula, and the ESI values were calculated by the various methods. The results are:

| | No. of data pairs | Wavelength range ($\mu$m) | Cut-off $\lambda_o$ ($\mu$m) | Diameter $2a_{ES}$($\mu$m) | % RI diff $100\,\Delta_{ES}$ |
|---|---|---|---|---|---|
| From profile | - | - | 1.214 | 8.2601 | 0.3012 |
| From spot size curve: | | | | | |
| method (a) | 1 | 1.174 | 1.174 | 8.0000 | 0.3000 |
| method (b) | 1 + slope | 1.174 | 1.174 | 8.6260 | 0.2582 |
| method (c) | 11 | 1.174-1.761 | 1.326 | 8.6003 | 0.3311 |
| " | 21 | 1.174-2.348 | 1.271 | 8.2686 | 0.3295 |
| " | 31 | 1.174-2.935 | 1.226 | 7.8112 | 0.3431 |

The simulation is inexact in that experimental data at cut-off are open to doubt. The extrapolations are to some extent subjective, even using polynomial fits to both sections of the curve.[8] There may also be a systematic error in the cut-off wavelength; though Millar[8] finds good reproducibility. Millar shows that the least squares method is sensitive to the formula used for fitting.

The closeness of the least squares fit was tested; Using the ESI values from 21 data pairs, the estimated values of spot size agreed with the simulated data to within 1.8%. This may be contrasted with the use of the parameters from the profile method, which gave deviations up to 9.8%. Marcuse[1] shows that the power transmitted through a joint with offset d is proportional to $\exp(-d^2/w_f^2)$. The loss in dB is thus $4.34d^2/w_f^2$; hence the percentage error in the calculated loss is twice the percentage error in the spot size. The profile method thus underestimates the joint loss by up to 20%.

Comments It is evident that there are discrepancies between the ESI values of the parameters calculated by various methods. The dependence of the results on the range of wavelengths used in the least squares method is particularly disturbing. Admittedly the parabolic profile is quite different from the step profile, but so are practical profiles.

The least squares method, (c), does, however, provide an excellent representation of the curve of spot size v wavelength. Methods (a) and (b) represent the experimental value of the cut-off wavelength as well as possible. The question of whether any of the derived values give useful values of dispersion remains open.[3,9]

Conclusions The best method of deriving ESI values of parameters depends on the use to which they are to be put.

It is strongly recommended that, if ESI values of parameters are quoted as results or in specification, the method of calculation should be stated in detail.

Acknowledgement The author thanks the directors of BICC Research and Engineering Ltd for permission to publish.

References

1. Marcuse,D., Bell Syst.-Tech. J., 56, 703-718, 1977

2. Stewart,W.J., Electron. Lett., 16, 380-382, 1980

3. Bhagavatula,V.A., Electron. Lett., 18, 319-320, 1982

4. Millar,C.A., Electron. Lett., 17, 458-460, 1981

5. Alard,F., Jeunhomme,L., and Sansonetti,P., Electron. Lett., 17, 958-960,1981

6. Millar,C.A., paper ThEE3 at OFC '82, Phoenix, Ariz., April 1982

7. Snyder,A.W., Proc. IEEE, 69, 6-13, 1981

8. Millar,C.A., Electron. Lett., 18, 395-396, 1982

9. Nelson,B.P., and Hornung,S., Electron. Lett., 18, 270-272, 1982

# COMPARISON OF CUTOFF WAVELENGTH MEASUREMENTS FOR SINGLE MODE WAVEGUIDES

C. C. Wang, C. A. Villarruel and W. K. Burns
Naval Research Laboratory
Washington, DC 20375

The determination of a single mode fiber's cutoff wavelength, characteristic of the fiber's index profile, is an important consideration both to verify fiber design and to avoid modal noise[1] in applications such as communication systems and sensors. The use of an effective cutoff wavelength which is characteristic of a particular fiber length, or condition of curvature, can be in error by hundreds of nanometers and can lead to system design errors. After considerable research and experimentation, three types of experiments have evolved to measure the cutoff wavelength of the $LP_{11}$ mode on a single mode fiber: the far-field measurement of Gambling, et al.,[2] the near-field transmission measurement of Murakami, et al.,[3] and the refracted power measurement of Bhagavatula, et al.[4] The far-field measurement of Ref. 2 provides the normalized frequency V from experimental characterization of the $LP_{01}$ far-field diffraction pattern, based on the assumption of a step-index profile. The cutoff wavelength can then be obtained by extrapolating from the experimental wavelength to the wavelength which corresponds to the cutoff frequency of a step-index profile. The transmission experiment in Ref. 3 points out the fiber length dependence of the effective cutoff wavelength due to increasingly large propagation losses as cutoff is approached. However, the authors conclude that a transmission measurement made on a short (10-20 mm) length of fiber gave a result within $\pm$ 5 nm of theory. Ref. 4 reported a refracted power technique in which they show that a measurement of refracted power, while the $LP_{11}$ mode passes through cutoff, avoids the complication of cladding modes and fiber length which are present in any transmission experiment, and is thus suitable for a measurement on a much shorter fiber length (few mm). This approach was shown to yield discrepancies of up to 100 nm for the cutoff wavelength compared to transmission experiments on 5 cm long fibers. To resolve the apparent contradiction between Refs. 3 and 4 we carefully conducted measurements using each of the three methods on the same ITT single mode fiber. We conclude that the refracted power technique is the best direct experimental method.

Our experimental arrangement required for the far-field and near-field transmission approaches are similar to those described in Refs. 2 and 3, respectively. In Fig. 1, we show the setup which allows both near-field observations of the transmitted mode pattern and refracted power measurements at the input end of the fiber. We adapted the approach of Ref. 4 by placing the stripped fiber in an etched Si groove and coupling out both cladding modes and the cutoff $LP_{11}$ mode through index-matching liquid and a prism. The fiber radiation length was adjusted by coating the remainder of the fiber with black paint.

The data from the far-field measurement, taken with a source wavelength of 0.845 μm, yielded a normalized frequency $V = 1.88 \pm 0.09$, $2a = 4.92 \pm 0.14$ μm and, $NA = 0.103 \pm 0.002$, implying a cutoff wavelength of $660 \pm 33$ nm with the assumption of a step index profile. The results of the transmission measurements are shown in Fig. 2. In these measurements we demonstrated the effective cutoff wavelength dependence on fiber length and condition of curvature by constraining the fiber in decreasing diameter tubes. We could not make this measurement on a fiber shorter than 2 cm because of interference from cladding modes which could not be stripped in shorter lengths. The observed cutoff wavelength for all fiber curvatures converges near 690 nm at the 2 cm length. This is probably due to intrinsic fiber stiffness. The typical data from the refracted power technique with a fitted curve are shown in Fig. 3 for radiation length of 0.25 mm. Fig. 4 shows the curves for four radiation lengths. The normalized refracted power is defined as the ratio of the radiated power when the core is excited preferentially with the $LP_{11}$ mode to the radiated power when only cladding modes are excited and is plotted as a function of wavelength. As was noted in Ref. 4, we observed no sudden change in normalized refracted power at the cutoff wavelength, but rather a broad transition region of 60-70 nm or more for each radiation length. We associate the long wavelength boundary of the transition region with the cutoff wavelength, assuming that the boundary is the point at which the $LP_{11}$ mode is no longer guided. The cutoff wavelengths show no marked dependence on radiation length, with an average value near 830 nm. The large discrepancy among the results of three independent measurements leads us to believe that the transmission measurement on a 2 cm fiber is not representative of a much shorter fiber. This is likely due to the large propagation losses the $LP_{11}$ mode experiences near cutoff. We conclude that an experiment of the refracted power type is necessary to determine cutoff wavelength with the best available experimental accuracy.

References


1. S. Heckman, Electron. Lett. 17, 499 (1981).

2. W. A. Gambling, D. N. Payne, H. Matsumura, and R. B. Dyott, IEE J. Microwaves, Opt. and Acoust., 1, 13 (1976).

3. Y. Murakami, A. Kawana, and H. Isuchiya, Appl. Opt. 18, 1101 (1979).

4. V. A. Bhagavatula, W. F. Love, D. B. Keck, and R. A. Westwig, Electron. Lett. 16, 695 (1980).


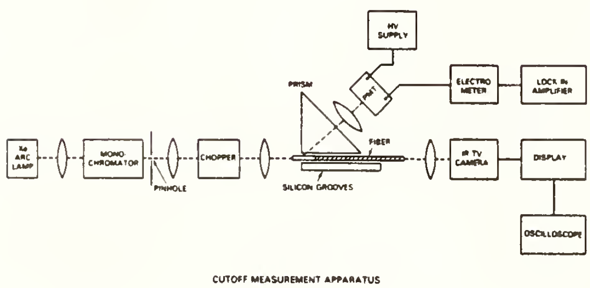


Fig. 1

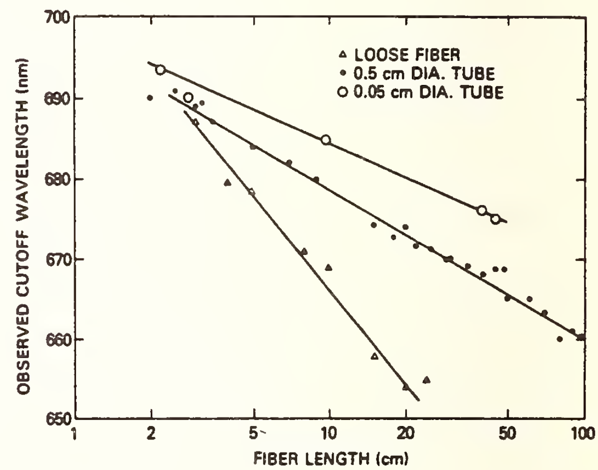


Fig. 2

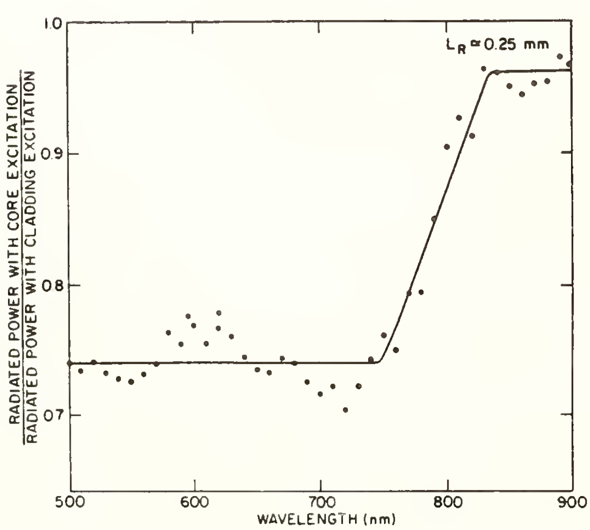


Fig. 3

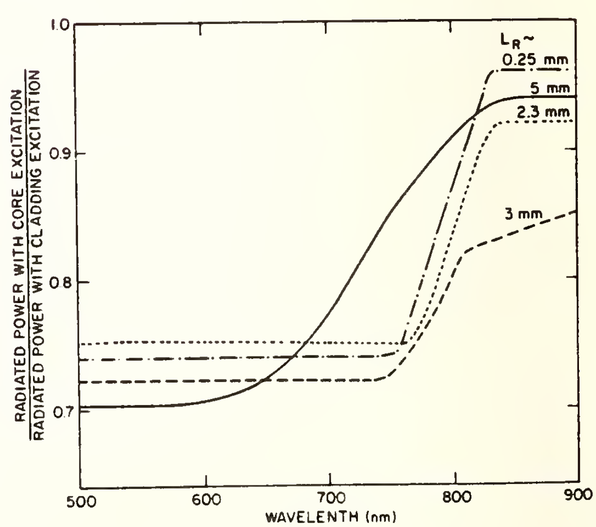


Fig. 4

# MEASUREMENTS OF FIBRE POLARISATION PROPERTIES USING A PHOTO-ELASTIC MODULATOR

A.J. Barlow and D.N. Payne
Department of Electronics, University of Southampton, Southampton, England.

## INTRODUCTION

Single-mode fibres with controlled polarisation properties are required for many fibre applications. For example, high-birefringence fibres are able to transmit linearly-polarised light, a property which is useful in interferometric fibre sensors and in coherent transmission systems. Low-birefringence fibres, on the other hand, have negligible intrinsic birefringence and are suited to conventional communications, polarisation-control devices and polarimetric sensors.

Precise measurements of fibre polarisation properties are an essential prerequisite for the development of fibres which exhibit extremes of birefringence. Conventionally, measurements are made using standard polarimetric techniques (polariser and analyser) or, in the case of very high birefringence fibres, by visual observation of the beat pattern. Neither technique is entirely satisfactory, since for low-birefringence fibres with retardations of $<10^{o}$/m the sensitivity is low, whereas for high-birefringence fibres, measurements are inaccurate and are limited to the visible region.

A dramatic improvement in measurement sensitivity can be obtained by employing dynamic photoelastic modulation of the birefringence, rather than static measurement. We report here the details of the technique and its use in the development of fibres with both the highest and the lowest birefringence yet recorded. Furthermore, the sensitivity of the measurement has permitted an accurate determination of the wavelength dispersion of the stress-optic coefficient in fibres, together with its temperature dependence. These parameters are of considerable importance in the interpretation of birefringence measurements and in the design of fibre devices which employ bends or twists to achieve controlled birefringence.

## MEASUREMENT TECHNIQUE

The photo-elastic modulator consists of a glass plate element vibrated at a frequency f by an acoustic transducer. The acoustic vibration sets up an oscillatory photo-elastically induced retardation in the plate. As shown in figure 1, linearly-polarised light is launched into the fibre and the output polarisation state is analysed by the combination of the photoelastic modulator and an analyser, which rotate as a unit. A demodulator provides d.c. signals proportional to the amplitude of the light-intensity modulation at frequencies f and 2f($S_1$ and $S_2$ respectively). These relate directly to the fibre birefringence properties.

In use, a Soleil compensator (Fig.1) is adjusted to null the fibre retardation, as shown by a zero modulation component $S_1$ and a maximum in $S_2$. In this way, direct birefringence measurements are obtained with a high sensitivity. The use of the modulation permits much faster and more accurate measurements than existing polarimetric methods, and considerably less dependence on polariser extinction efficiency when measuring ultra-low birefringence values. The lowest measurable birefringence is in fact limited largely by the finite birefringence of the input lens.

## RESULTS

1) Low-birefringence fibre measurements.

Ultra-low birefringence fibres can be reproducibly manufactured using the fibre spinning technique.[1] The residual birefringence present in a spun fibre is extremely small (typically $<1^{\circ}$) and its variation with temperature is negligible. The modulator system has been used to perform several measurements which confirm the properties of these fibres. Furthermore, since the fibres are virtually polarisation transparent they can be used to perform a number of measurements of fundamental polarisation parameters without fear of interference from intrinsic birefringence. As an illustration of this and of the accuracy obtainable with the photo-elastic modulator technique, we have performed a series of measurements of the stress-optic coefficient and its dispersion in germanium-doped spun single-mode fibres. The stress-optic coefficient is of importance in several forms of fibre birefringence, such as the thermal-stress birefringence used to advantage in high-birefringence fibres[2], and the bending birefringence used in the fibre isolator[3].

The technique used is to measure the rotation of the plane of polarisation produced by twisting a vertically-hung fibre. When a fibre is twisted at a rate $\xi$, a stress-optic rotation $\alpha = g'\xi$ is introduced, where $g'$ is the photo-elastic rotation constant and is directly proportional to the stress-optic coefficient C. The measured values of $g'$ as a function of wavelength $\lambda$ are shown in Fig. 2, with the computed value for pure silica shown for comparison. From the fibre curve we calculate a value of the stress-optic coefficient C(1 μm) in doped silica of $-3.23 \times 10^{-11} m^2 kg^{-1}$ and its wavelength dispersion $dC/d\lambda = 2.4 \times 10^{-15} m^2 kg^{-1} nm^{-1}$. The dispersion in C is significant and can contribute substantially to polarisation mode dispersion (∿ 10%) and to measurements of high-birefringence fibre beat length as a function of wavelength.

The variation of $g'$ with temperature T is shown in Fig. 3 and leads to a value for dC/dT of $-4.31 \times 10^{-15} m^2 kg^{-1} K^{-1}$. This is sufficient to cause a change in fibre bending birefringence with temperature of 0.01% $K^{-1}$, an effect which limits the stability of fibre birefringent filters or sensor devices which use controlled bend birefringence.

2. High-birefringence fibre measurements.

The modulator technique is also useful in measurements on fibres with very high birefringence, where, for example, it can be used to determine very small changes due to temperature or aging. In Fig. 4, the variation of fibre beat-length with temperature is shown for a fibre whose birefringence resulted primarily from core ellipticity. From the slope of the curve it is evident that about 15% of the birefringence was produced by thermal stress. From measurements such as these, an understanding of the birefringence-producing mechanisms in the fibre has been obtained and this has led to the development of a fibre with a novel stress-inducing structure. Beat lengths as low as 0.6 mm at a wavelength of 0.633 μm are now regularly obtained. Measurements of the properties of these fibres, as a function of temperature and wavelength will be reported.

## CONCLUSION

We have implemented a sensitive technique for birefringence measurement which uses a photo-elastic modulator. A range of measurements of fibres with extremes of birefringence have been conducted.

## REFERENCES

1. A.J. Barlow, J.J. Ramskov-Hansen and D.N. Payne, Appl. Opt., 20,2962-2968,1981
2. R.H. Stolen,V.Ramaswamy,R.Kaiser and W.Pliebel, Appl.Phys.Lett.,33,699-701,1978
3. G.W. Day,D.N.Payne,A.J.Barlow and J.J.Ramskov-Hansen, Opt.Letts.7,238-240(1982)

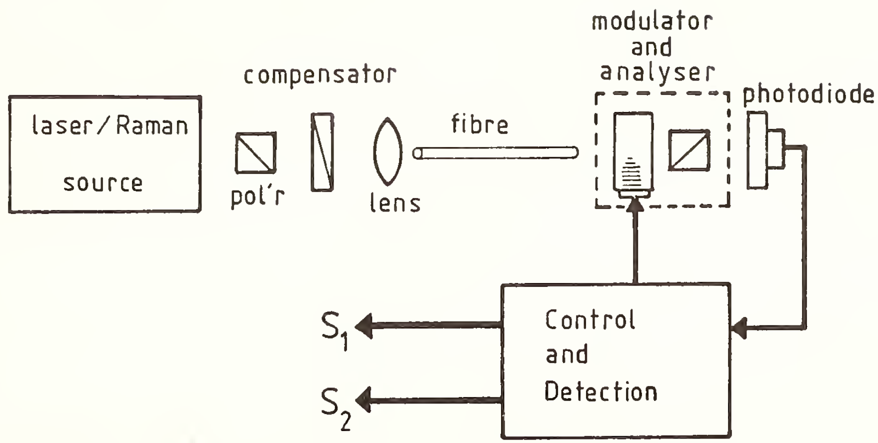


Fig. 1. Experimental arrangement

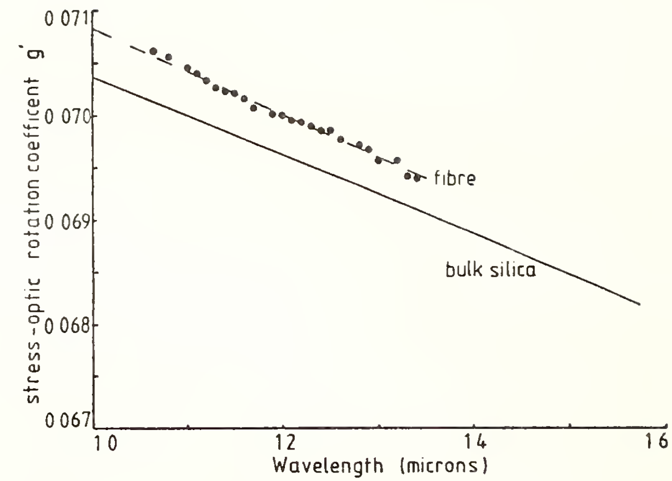


Fig. 2. Variation of stress-optic rotation coefficient with wavelength in a twisted fibre

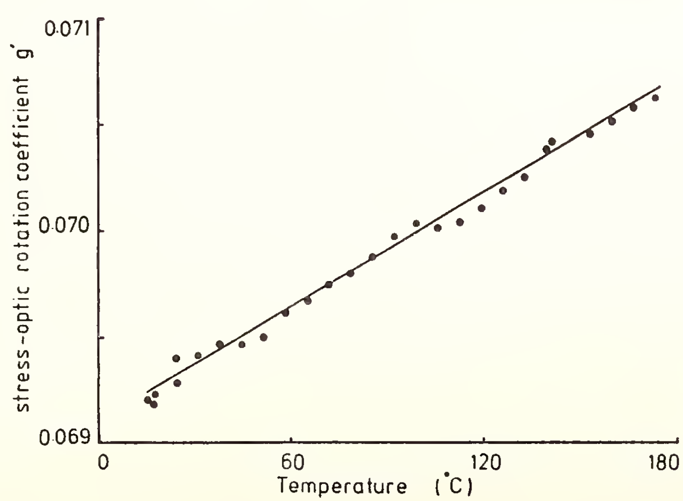


Fig. 3. Variation of stress-optic rotation coefficient with temperature in a twisted fibre

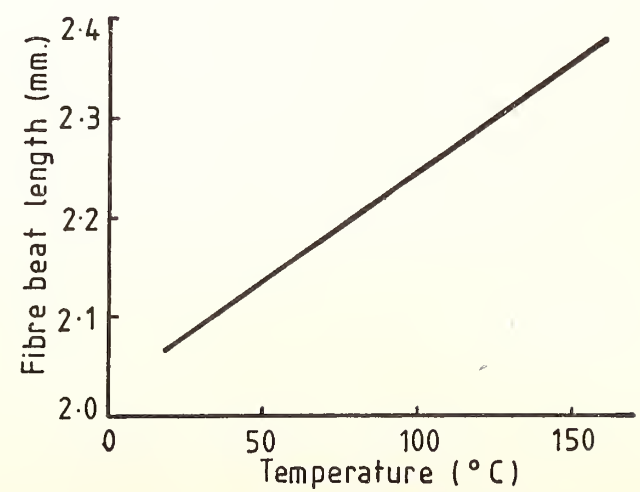


Fig. 4. Temperature dependence of polarisation beat length in a high-birefringence fibre.

Measurements of strain in cabled monomode fibre

S. Hornung and M.H. Reeve
British Telecom Research Laboratories, Martlesham Heath, Ipswich, U.K.

Introduction: It is expected that, over the next decade, large quantities of optical fibre cable will be installed into the British Telecom inland long haul telecommunications system. Most of this cable will be installed into underground duct. Fibre in this system is required to have a lifetime of 20 years or more. Fibre life is greatly influenced by humidity and residual strain. Moisture ingress can be controlled by an aluminium-polyethylene laminate (APL) water barrier in the cable, but little is known about residual fibre strain levels in the ground. The level of residual strain is required as an input to any realistic calculation of fibre lifetime from stress corrosion effects.

This paper reports the measurement of this residual fibre strain on 15km of monomode fibre cable, installed into occupied duct using conventional installation practice. Strain levels were measured on the fibres themselves by means of pulse delay before and after installation. A wide variety of duct conditions were encountered. However, in spite of this, residual strain levels remained low throughout. It is felt that this result will be typical of that found for future system installations, giving great confidence in fibre life.

Route: Measurements were performed on 10 cables (plus a spare) comprising a trial monomode system being installed between British Telecom Research Laboratories, Martlesham Heath and the telephone exchange in Ipswich, a distance of 15km. Each cable contains 4 fibres to provide $2\times30$km loops operating at 140MBits at 1.3µm and 1.55µm. The fibre parameters were all in the region of 9µm core, 125µm outer diameter with peak $\Delta n$ of order $5.3\times10^{-3}$. The average fibre attenuation was 0.44 and 0.29dB/km at 1.3 and 1.55µm respectively. All $LP_{11}$ mode cut-offs were in the region of 1.1-1.2µm. Final details of the installed system will be available by the time of the symposium. Average joint losses of 0.11dB at 1.3µm were achieved in a laboratory pre-installation trial. (1,2)

The cable was a tight-coated helical lay structure, in which fibres directly extruded with nylon to 0.85mm were stranded around a 1.8mm coated steel wire. A polyethylene sheath with an APL water barrier gave a final outer diameter of 7mm. The secondary coated fibre had been proof tested to 0.6% strain.

Technique: The basis of the technique was to measure the length of the fibres before and after installation by timing a laser pulse travelling the length of the fibre. Pulse delay was measured for each fibre in the laboratory before installation whilst both ends were accessible. Once installed the fibres were loop-jointed into pairs at the far end. The combined delay was then measured for the entire loop from a measurement vehicle. The combined delay was then compared ( after suitable corrections) with the sum of the measurements before installation. Measurements after the installation were done once the cable had been made fast at all intermediate manholes. The lengths of cables pulled-in varied from 1km to 2.5km. All were installed in at least two stages, pulling-in from a middle manhole in two directions. In some cases where high friction was encountered, the cable would be pulled-in in more stages. The installation followed established practices. A mechanical fuse inserted between the pulling rope and cable limited the maximum tension to 1KN (local cable strain of 0.17%).

The apparatus used for the measurements is shown in fig.1. A solid state single heterostructure laser produces a short (2-3ns) pulse at 850nm, which is launched into the fibre by means of lenses. The laser pulse is detected by a silicon avalanche photo-diode, and displayed on a sampling oscilloscope. The laser is triggered by the prompt output of a digital delay generator, whilst the oscilloscope is triggered by the delayed output of the delay generator, allowing time for the laser pulse to reach the far end of the fibre. The laser is fired at 10kHz rate by an oscillator connected to the external trigger port of the delay generator. The pulse is recorded on graph paper by an XY plotter. An accurate delay may then be obtained from the position of the pulse on graph paper and from the delay of the generator. A pulse reflected from the launch end of the fibre provides a t=0 position by similar means, in order to eliminate any delays in the equipment used. The technique may be used "double ended" if both ends of a fibre or fibre loop are accessible, or "single ended" in which case a chemically deposited mirror is used to reflect the signal at the far end.

Corrections: The measurements before and after installation reveal a change of delay. The source of this change is the residual strain experienced by the fibres. Several corrections are required however in order to calculate the accurate level of strain. These are:-

a. Length of fibre cut off in installation and measurement preparation. This is done by means of marks on the outer sheath. The length of steel strength member cut off provides a further check which also reveals any shrinkage of the outer sheath.

b. Temperature. The temperature was measured in the laboratory and in the underground cable ducts, the difference was 5 to 10 degC. The fibre temperature coefficient in this type of cable is known to be 0.103ns/km/degC.(3).

c. Strain measured by pulse delay is the result of two competing effects. The physical extension to a fibre increases the delay by 48.91ps/km/MPa. Strain however decreases refractive index, causing a decrease in delay of 9.12ps/km/MPa (4). Therefore final strain ($\Delta L/L$) is calculated by multiplying the relative increase in delay ($\Delta T/T$) by the ratio 48.91/(48.91-9.12)=1.23.

Results: Fig 2 shows the histogram of results. Each cable is represented by two points corresponding to two loops. The distribution appears to be bi-moded. The majority of results are around 0.01% positive strain, with a further group at around 0.03%. The higher group suggests some snagging in the already occupied ducts. The error is estimated to be ±0.01% per measurement.

Discussion: The above strains are averaged over the length for each cable, and thus some parts of the cable may experience higher strains than others. The worse case would arise if a section of cable was held under strain between two points where jamming occured. The upper limit is set to 0.17% by the mechanical fuse. Strain here would then be a maximum of 0.17/2=0.085%. The highest residual strain measured was 0.036%, which gives the length of the section under maximum strain as 40% of cable length. However as some slack has been manually pulled into each manhole (100-200m apart) to allow the cable to be tied to support brackets, it is felt that any residual strain will be evenly distributed over the entire cable length.

Conclusion: Previous work (5) has shown that fibre proof tested at 0.6% has a high probability of surviving a strain of 0.2% for 20 years.

Our measurements have shown that monomode cable can be installed in long lengths using conventional techniques with considerably lower residual strains, giving a large safety margin on fibre life.

References:

1. J. Leach et. al. Low Loss Splicing of a 64.2km Single Mode Fibre Link. To be published, Electronics Letters.
2. J. Irven et al. Single Mode Optical Fibre Cables for Landline Systems. To be presented at 8th ECOC, Cannes, September 1982.
3. J. Russell, (STL) private communication.
4. R. Kashyap, to be published.
5. W. Duncan et al. Effect of Service Environment on Proof Test of Optical Fibres. 7th ECOC, Copenhagen 1981

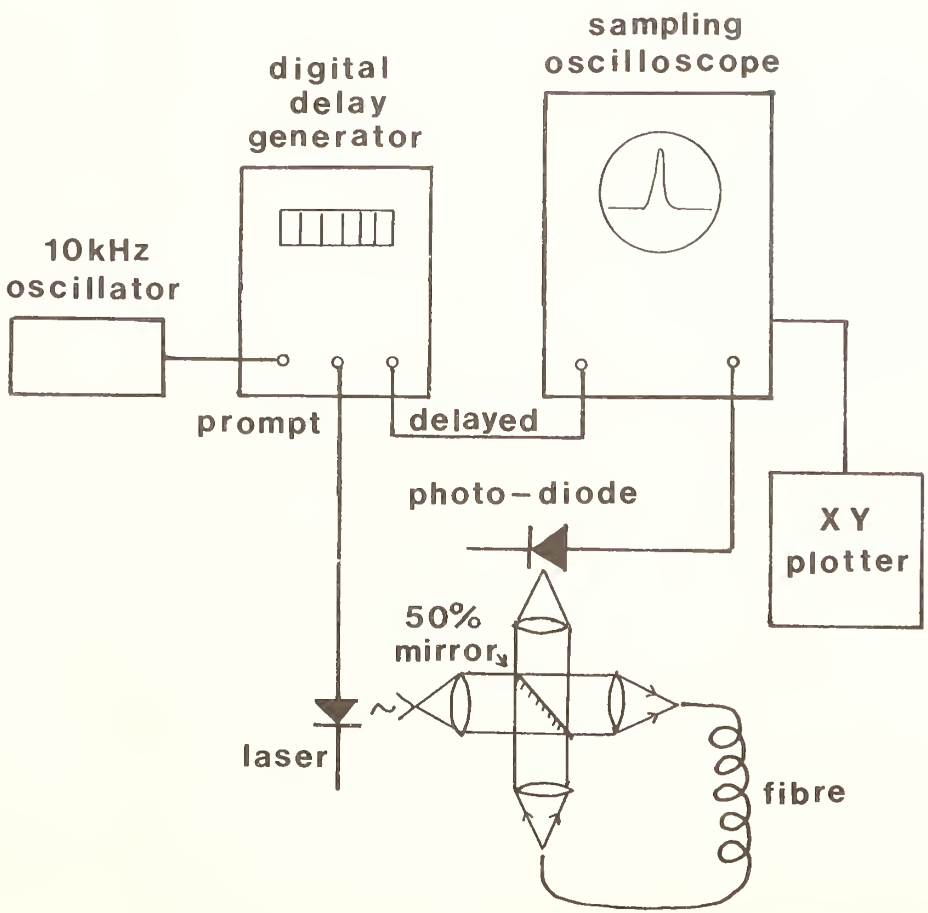


Fig. 1. Experimental apparatus.

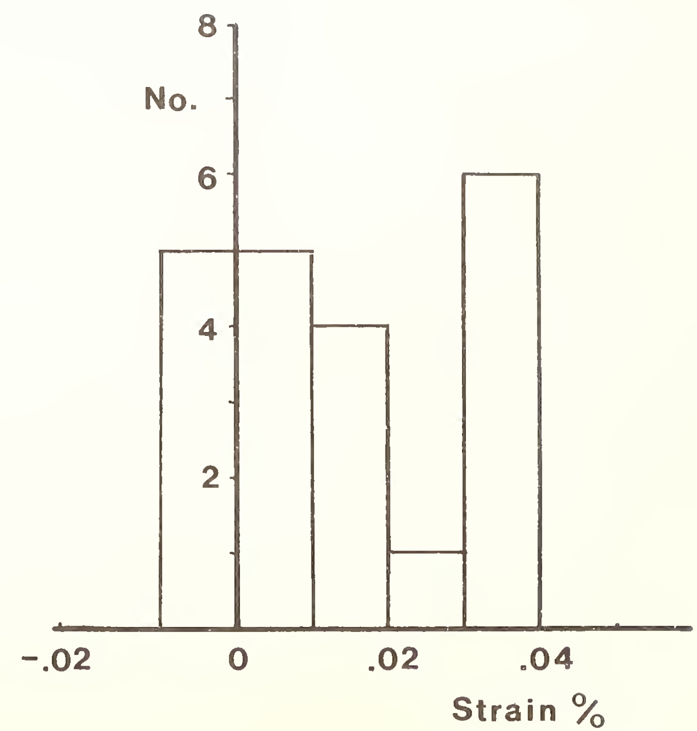


Fig. 2. Histogram of measured residual strain.

# FIELD AND LABORATORY TRANSMISSION AND OTDR SPLICE LOSS MEASUREMENTS OF MULTIMODE OPTICAL FIBERS

R. B. Kummer
A. F. Judy
A. H. Cherin

## INTRODUCTION:

All practical optical fiber systems require the use of interconnection devices such as splices and connectors. Their losses can be a very significant factor in the design of fiber optic systems, particularly multi-kilometer telecommunication links. This paper describes the fundamental parameters affecting splice loss measurements. The relationships between transmission and OTDR (optical time domain reflectometry) splice loss measurements are developed and laboratory data is presented to illustrate how intrinsic and extrinsic splice loss parameters influence these relationships. In addition, recent field data, obtained with an OTDR, is included to show both the utility and limitations of OTDR splice loss testing of installed fiber optic systems.

## TRANSMISSION LOSS MEASUREMENTS:

The measured transmission loss of a splice in a fiber optic system can be significantly affected by the type of source used, the source's location relative to the splice, and the characteristics of the fibers on either side of the splice.[1-3] Let us consider the transmission loss measurement arrangement shown in Figure 1. If the length of the output fiber is short enough (so that the output fiber loss can be neglected), a "short length" splice loss can be defined as:

$$L_S = 10 \log \left(\frac{P_2}{P_1}\right) \qquad (1)$$

For multimode fibers, $L_S$ may be dependent upon the proximity of the splice to the source. If there is a long input fiber with sufficient mode mixing between the splice and the source, $L_S$ is the splice loss measured under near steady state conditions; in this case the input fiber isolates the splice from the source. If the input fiber is short, however, $L_S$ is strongly dependent upon the source launching conditions. Figure 2 shows the dependence of splice loss on source location and numerical aperture of the launch beam. A large variation in the measured value of $L_S$ (greater than a factor of 3 in this case) can occur if the source launching conditions are not isolated from the splice by a long input fiber.[1] An additional splice effect exists when a long length of fiber follows a splice. The modal power distribution along a multimode fiber is generally disturbed by a splice. This can cause the output fiber to have a loss that is different from its loss measured under steady state conditions. Since this difference in fiber loss is a direct result of the splice, it can be considered as part of the total splice loss. We may define a "long length" splice loss, $L_L$ as:

$$L_L = L_S + \delta L_R \qquad (2)$$

where $\delta L_R$ is a change from its steady state value of the output fiber's loss caused by the splice. The total loss of the splice plus the output fiber may be expressed either in terms of the measured powers $P_1$ and $P_3$ (see Figure 1) or in terms of the steady state fiber loss $(L_R^{SS})$ and the long length splice loss $(L_L)$; that is:

$$10 \log \left(\frac{P_3}{P_1}\right) = L_R^{SS} + L_L \qquad (3)$$

thus,

$$L_L = 10 \log \left(\frac{P_3}{P_1}\right) - L_R^{SS} \qquad (4)$$

For a splice with extrinsic misalignment loss between identical fibers, $L_L$ will be greater than $L_S$. For a splice in which intrinsic parameter mismatches exist between fibers, $L_L$ can be less than or greater than $L_S$. In fact, $L_L$ can even be less than zero. This can occur when the input fiber underfills the numerical aperture of the receiving fiber, as for example, when a small $\Delta$, small core fiber is spliced to a large $\Delta$, large core fiber.[3] Where $\Delta$ is the relative refractive index difference between the core and the cladding. In general, $L_S$ is a well-defined localized quantity for a given splice, whereas $L_L$ is a function of the length, the degree of mode mixing and the differential mode attenuation of the receiving fiber. For evaluating the quality of splices and connectors in a laboratory or manufacturing facility, $L_S$ is typically measured under either steady state conditions (using a long input fiber and identical short output fiber) or overfilled conditions (uniform excitation conditions at input with short length of identical transmitting and receiving fibers). $L_S$ is usually quoted as the loss of a splice or a connector.[4]

OTDR LOSS MEASUREMENTS:

Consider the basic arrangement for OTDR measurements[5] consisting of a pulsed laser and detector connected to the same end of a fiber through an optical coupler as shown in Figure 3. A narrow optical pulse is launched into Fiber A, after which backscattering and reflections are detected versus time. The signal reflected or backscattered from a given point along the fiber is detected after a round trip delay time proportional to the distance from the source. Thus, the detected signal versus time represents backscattering versus length along the fiber. If we assume that both attenuation and backscattering are uniform along the length of a fiber and independent of the direction of propagation, then the power after a length $\ell$ in meters is given by $P(\ell) = P_0 \exp[-\alpha\ell]$, where $P_0$ is the initial power level and $\alpha$ is the fiber attenuation coefficient in nepers/m. Some fraction, S, of this power is backscattered and captured by the fiber. It undergoes a further $\exp[-\alpha\ell]$ attenuation before reaching the detector where its detected power is given by

$$P'(\ell) = P_0 S \exp[-2\alpha\ell] \qquad (5)$$

If the backscattering is predominantly Rayleigh, then for multimode fibers the quantity S is given by the following equations:[7,5]

$$S = (3/4)\,\Delta\,\alpha_r\,W/2 \text{ for step-index fibers}$$

$$= (1/2)\,\Delta\,\alpha_r\,W/2 \text{ for near-parabolic graded index fibers}$$

where: $\alpha_r$ = the component of attenuation caused by Rayleigh scattering, $\alpha_r = A/\lambda^4$ where A is a wavelength independent term that is a function of the glass compositional variations.

W = the length of the incident pulse

For a typical graded index fiber measured with a 100 ns pulse, $S = 4 \times 10^{-5}$ when the following typical parameters are assumed: $\Delta = 0.013$, $\alpha_r = 0.00062$ nepers/m @820 nm, and W = 20 meters.

If we assume that a very narrow pulse is used to excite the two fibers shown at the top of Figure 3, then the logarithm of the detected backscattered power versus time will typically be given by the plot shown at the bottom of Figure 3.

From Equation (5), the detected backscattered power from a point immediately preceeding the splice is

$$P_1' = P_0 S_A \exp[-2\alpha_A \ell_A]. \qquad (6)$$

Similarly, the detected power backscattered from a point immediately following the splice is

$$P_2' = P_0 \, S_B \, T_{AB} \, T_{BA} \exp[-2\alpha_A \, \ell_A] \qquad (7)$$

where $T_{AB}$ and $T_{BA}$ are the splice transmission values in the forward and reverse directions, respectively (e.g., the forward splice loss in dB is $L_{AB} = 10 \log T_{AB}$). The OTDR splice loss $(L^o_{AB})$ is determined from the ratio of these two power levels:

$$\begin{aligned} L^o_{AB} &\equiv \frac{1}{2} \cdot 10 \log \left(\frac{P_2'}{P_1'}\right) \\ &= (5 \log T_{AB} + 5 \log T_{BA}) + 5 \log\left(\frac{S_B}{S_A}\right) \qquad (8) \\ &= \left(\frac{L_{AB} + L_{BA}}{2}\right) + 5 \log\left(\frac{S_B}{S_A}\right). \end{aligned}$$

From Equation (8), we see that the splice loss determined by OTDR is equal to the <u>average</u> of the transmission splice loss values in the two propagation directions, <u>plus</u> a term which depends on the ratio of scattering coefficients of the two fibers. This latter scattering term is a measurement artifact which can lead to erroneous splice loss results if not properly accounted for. As shown in the next sections, this term can be plus or minus several tenths of a dB.

If access to the far end of Fiber B is available, then the scattering term can be eliminated by making an OTDR measurement from Fiber B to Fiber A and averaging the splice loss values obtained in the two directions. From Equation (8)

$$\left(\frac{L^o_{AB} + L^o_{BA}}{2}\right) = \left(\frac{L_{AB} + L_{AB}}{2}\right) . \qquad (9)$$

Similarly, the backscattering term itself may be determined by subtracting the two unidirectional OTDR loss values:

$$\left(\frac{L^{o}_{AB} - L^{o}_{BA}}{2}\right) = 5 \log \left(\frac{S_B}{S_A}\right) \quad (10)$$

EXPERIMENTS COMPARING TRANSMISSION LOSS AND OTDR MEASUREMENTS

A series of experiments were performed using the test set shown in Figure 4 to compare OTDR and transmission loss measurements on fibers of either similar or mismatched intrinsic parameters (core radius, delta, scattering coefficient) that were spliced together.

The first step in measuring splice loss was to determine the steady-state loss, $L_B^{SS}$, of the output fiber. This was done by using the transmission set to measure the loss of Fiber B when excited by a steady-state power distribution from an identical fiber, B' (B and B' were actually two sections of the same fiber). Next, a series of long length transmission and OTDR splice loss measurements was made using either B' or a nonidentical fiber, A, as the input fiber. Measurements were made at several different transverse offsets from 0 to 15 μm. At each offset the optical switch was used to alternately connect to the two measurement sets without disturbing the splice. Finally, after the long length measurements were complete, Fiber B was broken approximately 1 meter from the splice, and a series of short length transmission splice loss measurements was made at the same offset values (see Equation (1)).

Five different fibers were used in this study. Each fiber was broken into two sections of approximately 1 km each. Two of the fibers had reasonably large deviations from the nominal core diameter and Δ values but similar scattering coefficients, while another pair had a larger scattering coefficient difference with smaller intrinsic parameter deviations. The fifth fiber was chosen to have nominal parameters.

These five fibers were spliced together in nine different combinations. Three were identical-fiber splices, two had primarily intrinsic parameter mismatch, two had primarily scattering level mismatch, and one was a "typical" splice. The splice loss results are discussed below.

(a) Identical Fibers

A plot of splice loss versus transverse offset for an identical fiber splice is shown in Figure 5. For this case the long length transmission loss is greater than the short length loss, and the difference increases for larger offsets. This result shows that the changes in modal power distribution caused by an offset splice tend to increase the loss of the output fiber. The OTDR splice loss is in good agreement with the transmission results and is bounded by the long and short length curves. OTDR measurements are most accurate for identical-fiber splices since there is no scattering coefficient mismatch and extrinsic splice loss is the same in both directions (i.e., $L_{AB} = L_{BA}$).

(b) Core Radius and Δ Mismatch

The two sets of curves in Figure 6 are for a nonidentical fiber splice with a large core radius and Δ mismatch and a small scattering coefficient mismatch. The splice in Figure 6a is between a large core, large Δ input fiber and a small core, small Δ output fiber, and Figure 6b is for the same splice with the input and output fibers reversed (i.e., measured from the opposite end).

For the "large into small" splice (Figure 6a), there is an intrinsic short length transmission loss of 0.37 dB with zero offset, and a long length zero offset loss of 0.61 dB. In this case, the "large" input fiber overfills the local numerical aperture at every point on the output fiber core causing both an immediate (short length) splice loss and an increase in the loss of the output fiber above the steady-state value.[3] This increase in fiber loss is due to the increased excitation of high-order fiber modes which have a high loss because of mode coupling into nonpropagating modes.

For the "small into large" splice (Figure 6b), the situation is reversed. Here, because the local numerical aperture of the "large" output fiber is underfilled for small offsets, there is zero short length loss. Furthermore, the output fiber loss for small offsets is <u>less</u> than the steady-state loss and gives rise to an apparent <u>negative</u> long length splice loss. This negative loss implies that the modal power distribution excited in the output fiber by the "small" input fiber with no offset contains less power in the lossy high-order modes than the steady-state distribution for that particular fiber. As the splice offset is increased, there is an increasingly large region of the output fiber core where the local numerical aperture is overfilled, resulting in a nonzero short length splice loss and an increase in the output fiber loss. Eventually, the offset effects dominate, and the long length splice loss exceeds the short length value.

(c) Scattering Coefficient Mismatch

The splice loss results for two fibers with a large difference in scattering coefficient, S, are shown in Figures 7a and 7b, with the high-S fiber as the input and as the output fiber, respectively. The relatively small index profile parameter mismatch between these fibers leads to transmission splice loss effects qualitatively similar to those discussed in the previous section, but with a much smaller magnitude. Thus, the transmission splice loss curves for the two directions of propagation are only slightly different.

There is a significant difference, however, in the two OTDR splice loss curves - the OTDR curve for the "high-S to low-S" splice (Figure 7a) indicates a considerably higher loss than either the long or short length transmission measurement, while the OTDR measurement in the opposite direction (Figure 7b) is generally too low. This difference is due to the fact that the scattering term in Equation (8) <u>increases</u> the measured loss for $S_A > S_B$ as in Figure 7a, but <u>decreases</u> the measured loss for $S_A < S_B$ as in Figure 7b. This effect may also be seen in Figure 6, where the scattering coefficient mismatch increases the measured OTDR splice loss in Figure 6a and decreases it in Figure 6b.

The actual OTDR signal with zero splice offset is shown in the insert of Figure 7b. The distinct increase in received scattered power following the splice results in a <u>negative</u> OTDR splice loss. It should be emphasized that the negative OTDR splice loss in this case is a measurement artifact due to a difference in scattering coefficients, whereas the negative long length transmission splice loss discussed in the previous section is a real quantity which affects the end-to-end loss of a system.

From Figure 7, we see that scattering coefficient mismatch can lead to significant errors in OTDR splice loss measurements. Scattering mismatch error may be eliminated by averaging the OTDR splice losses measured in the two propagation directions. Figures 8a and 8b show the directional averages of the splice loss curves from Figures 7 and 6, respectively. In both cases, the OTDR directional average curve is in reasonable agreement with the average of the long length transmission splice loss.

## V. TYPICAL FIELD SPLICE LOSS RESULTS

Recently we measured 142 fiber splices in the field with an OTDR. A histogram of their losses measured from only one cable end is shown in Figure 9. It is apparent that while the mean loss is a respectable 0.12 dB, the data has a large standard deviation ($\sigma$) of

0.24 dB as well as 41 "negative" splice losses. To determine the amount of $5\log(S_B/S_A)$ measurement error, the same splices were measured in the reverse direction and their average difference found as in Equation 10. A histogram of the results (Figure 10) shows that this scattering error has essentially a zero mean but a substantial $\sigma$ of 0.21 dB. Subtracting the scattering error from each splice using Eq. 9, we find in Figure 11 the true splice loss distribution has a $\sigma$ of 0.11 dB - much less than the unidirectional value. Note that, as statistics predicts, the $\sigma$'s add on a root-sum-square basis.

In the field it is difficult to measure splices in both directions due to the OTDR's limited range. So field measured splice loss data is usually distorted by the scattering error term. Unfortunately, in order to design accurate transmission systems, one must determine the true splice loss distribution with a minimum of uncertainty. This dilemma can be moderated by the following technique. Consider Figure 12 which shows N splices joining N+1 uniform fibers. If all the splices are measured from the same end, then the error in measuring their sum will equal the scattering difference between only the first and last fibers. Assuming that the scattering error has a standard deviation of $\sigma'$, then the $\sigma$ of the sum of the N splices will be only $\sigma'$ rather than the $\sigma'\sqrt{N}$ that would occur if no correlation existed. Thus the uncertainty in determining the mean splice loss will be improved by $1/\sqrt{N}$. Note that this technique is only valid if the fibers' backscattering is uniform with length.

## SUMMARY

The measured transmission loss of a splice in a fiber optic system can be significantly affected by the type of source used, the source's location relative to the splice, and the characteristics of the fibers on either side of the splice. We have defined the terms short length and long length splice loss and have shown that a splice can change the loss of the output fiber following the splice. The output fiber's loss will increase from its steady state value if the splice loss is due to transverse offset. The output fiber loss can either increase or decrease if the splice loss is due to intrinsic parameter mismatch. In any event, the long length splice loss can differ from the short length value. Likewise OTDR measurements of splice loss will often differ from transmission measurements. A principal reason for this difference is that the OTDR measures round trip rather than one way loss. In addition the OTDR measurement is also affected by scattering error. When these differences are eliminated by comparing OTDR measurements made from both ends of a transmission path with two way transmission measurements, the OTDR agrees reasonably well with transmission splice loss.

## REFERENCES


1. Cherin, A. H., Rich, P. J., Appl. Opt., Vol. 17, No. 4, (1978), p. 642.

2. Kummer, R. B., BSTJ, Vol. 59, No. 3 (1980).

3. Kummer, R. B., Proc. 6th Eur. Conf. on Opt. Comm., York (1980), p. 302.

4. Cherin, A. H. and Dalgleish, J. F., ITÜ Telecom Jour. Vol. 48, No. XI, (1981).

5. Personick, S. D., BSTJ, Vol. 56, (1977), p. 355.

6. Kummer, R. B., Mettler, S. C. and Miller, C. M., Proc. 5th Eur. Conf. on Opt. Comm., Amsterdam (1979), p. 6.4-1.

7. E. G. Newmann, Elec. Comm., Vol. 34, (1980), p. 157.

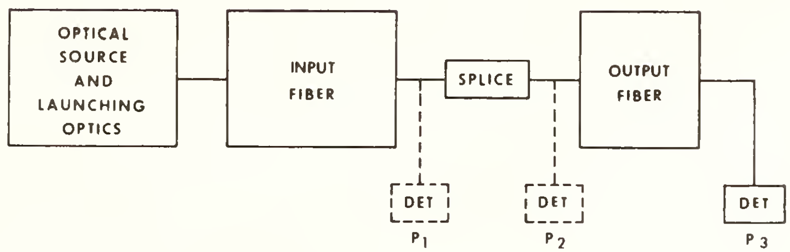


TRANSMISSION SPLICE LOSS MEASUREMENT

FIGURE 1

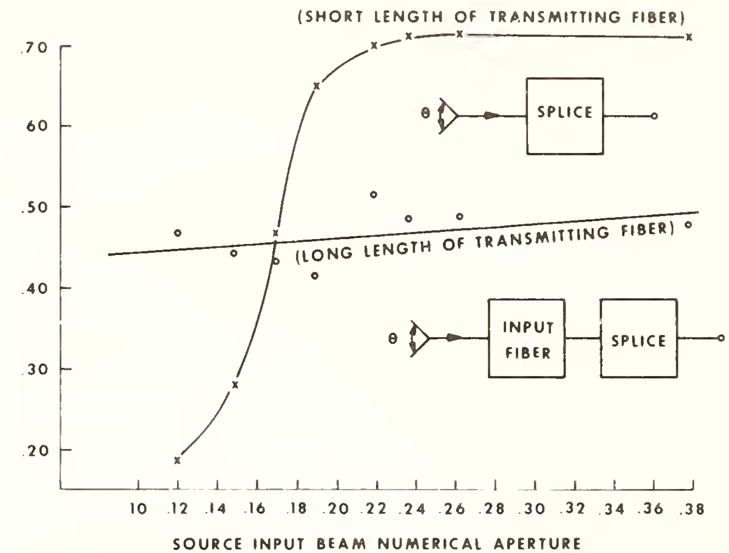


DEPENDENCE OF SPLICE LOSS ON SOURCE LOCATION AND NUMERICAL APERTURE

FIGURE 2

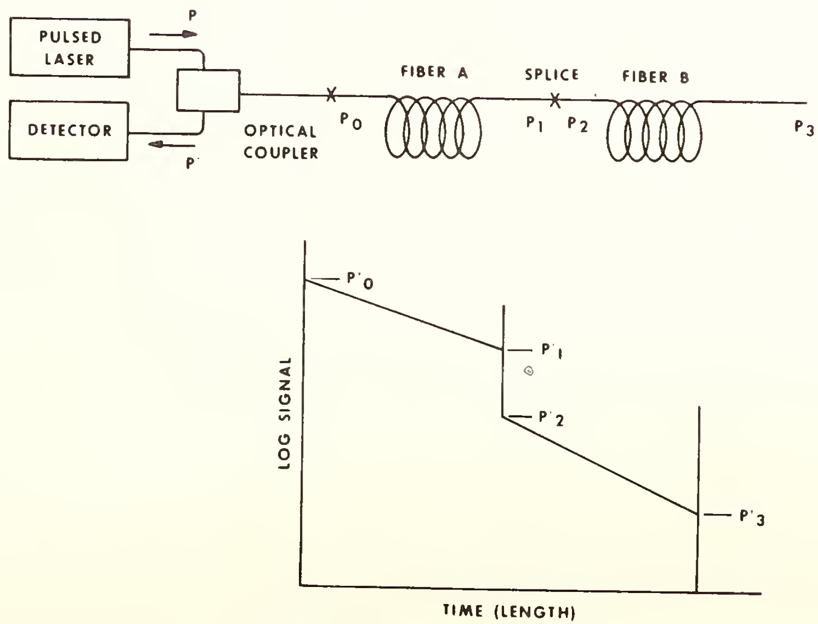


OTDR SPLICE LOSS MEASUREMENT

FIGURE 3

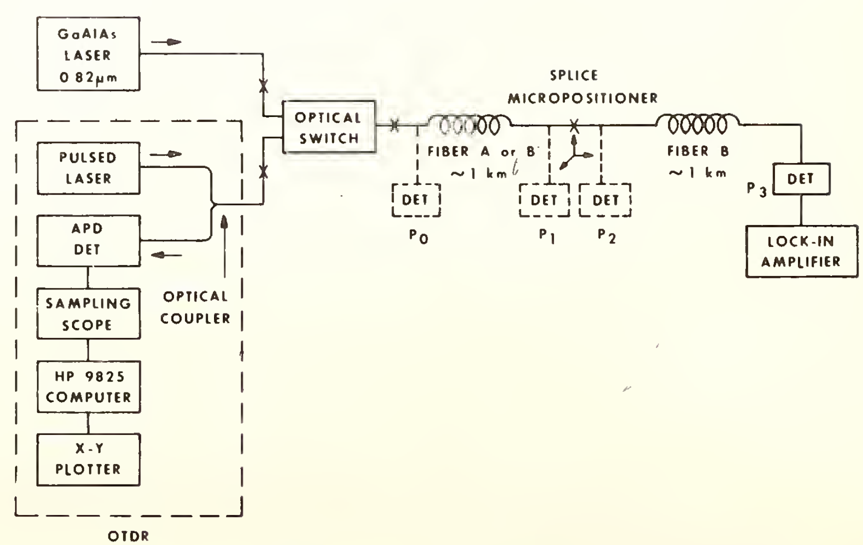


MEASUREMENT APPARATUS

FIGURE 4

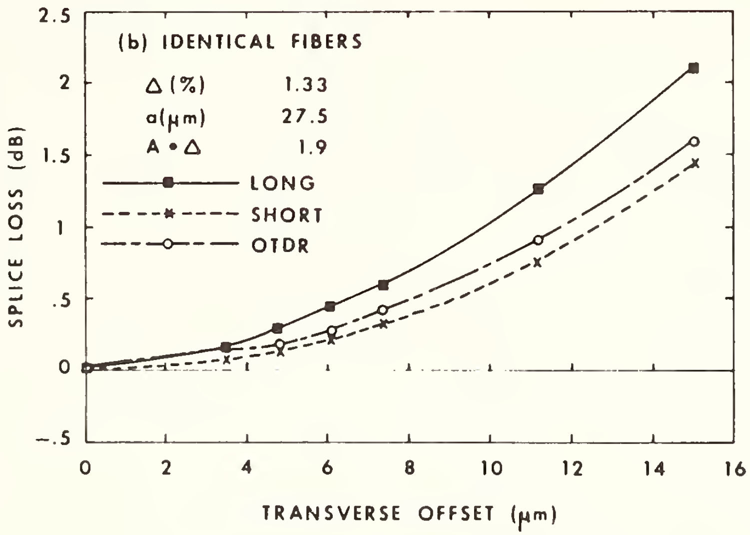


SPLICE LOSS vs. TRANSVERSE OFFSET
FOR IDENTICAL FIBERS

FIGURE 5

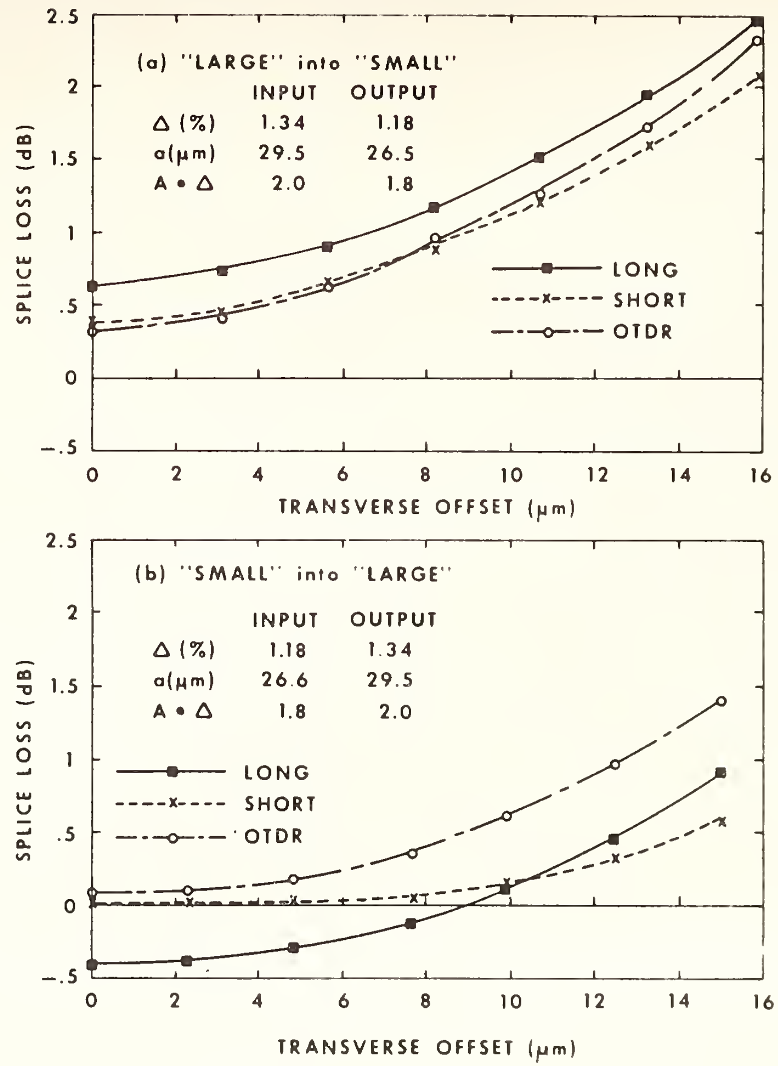


CORE RADIUS AND Δ MISMATCH

FIGURE 6

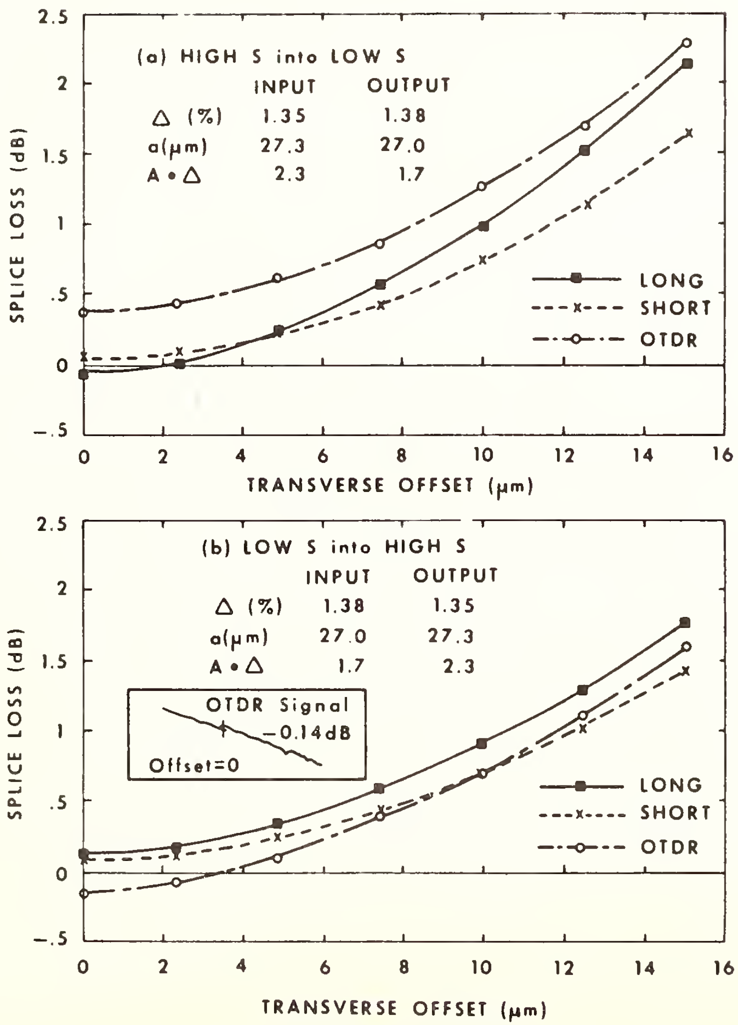


SCATTERING COEFFICIENT MISMATCH

FIGURE 7

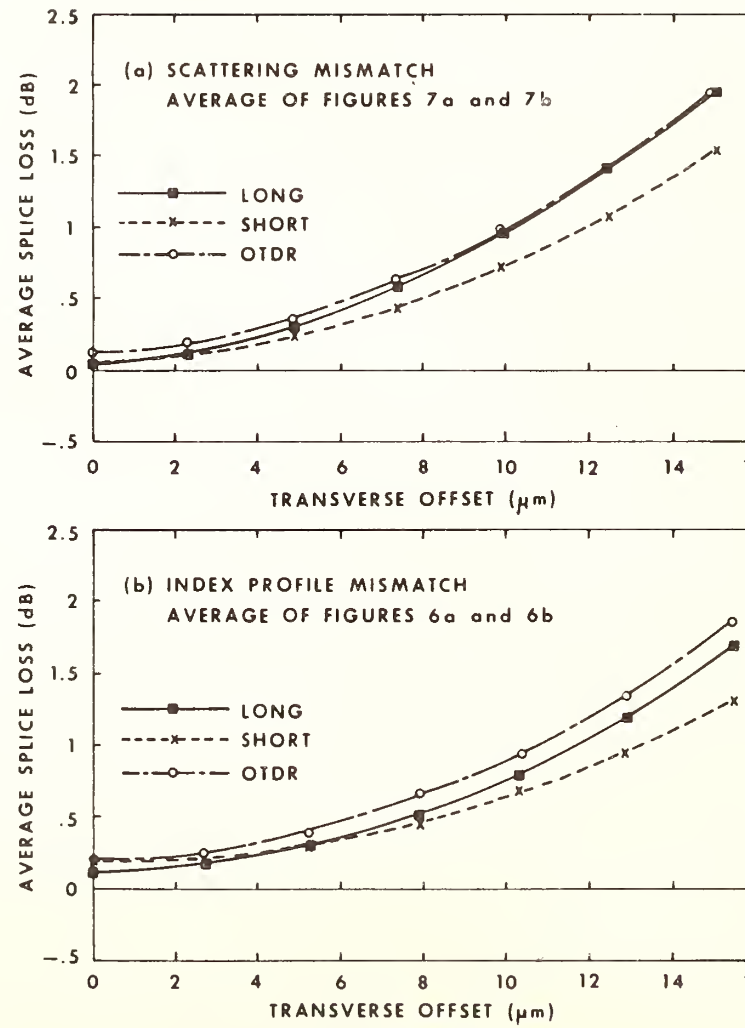


DIRECTIONAL AVERAGE SPLICE LOSS

FIGURE 8

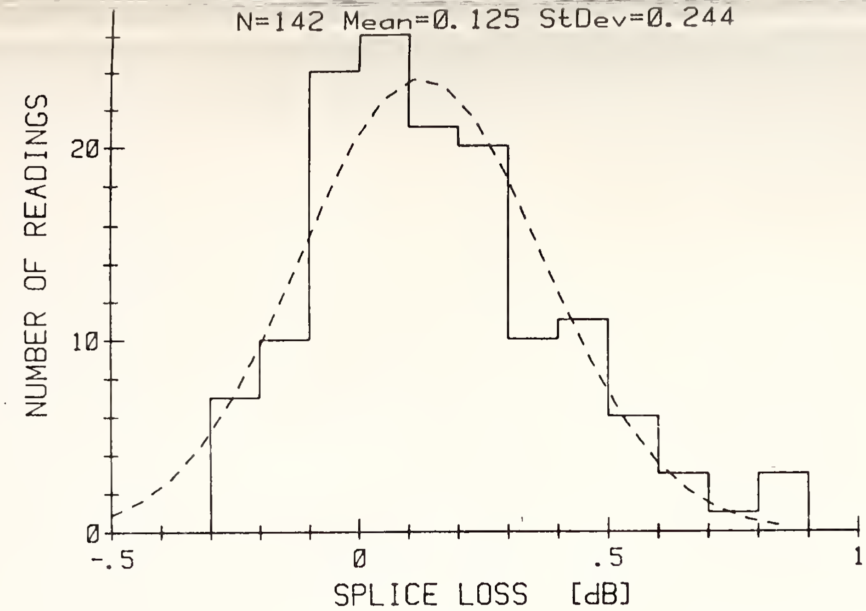


**FIGURE 9**

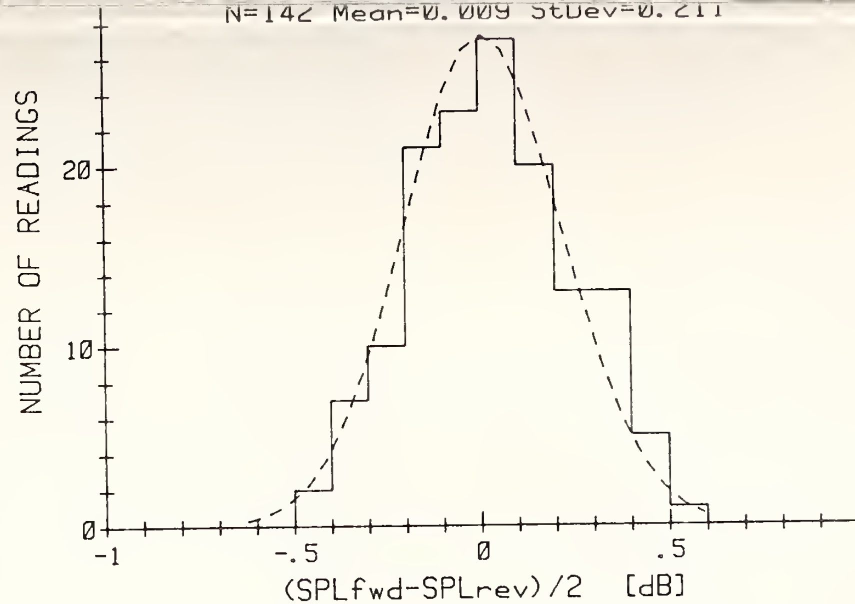


**FIGURE 10**

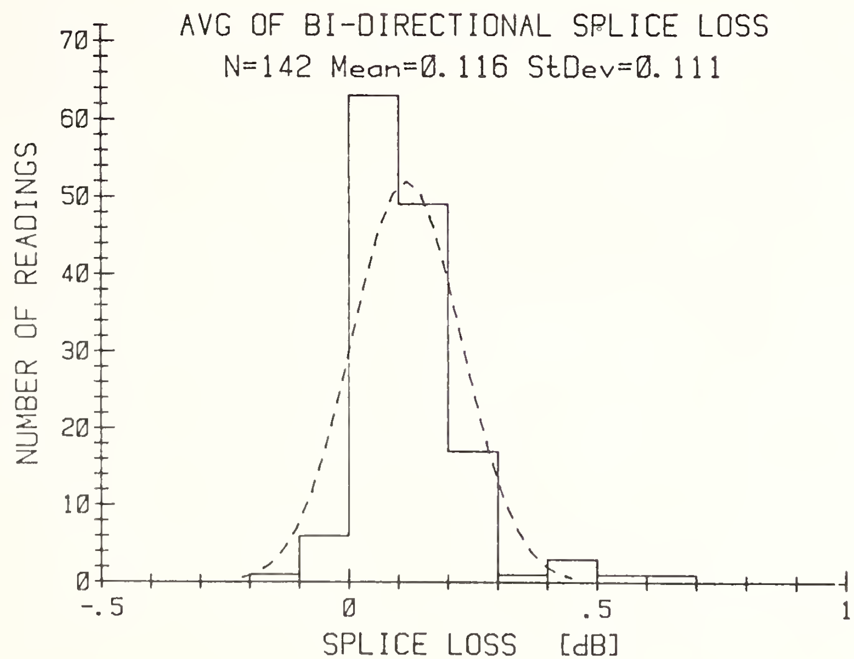


**FIGURE 11**

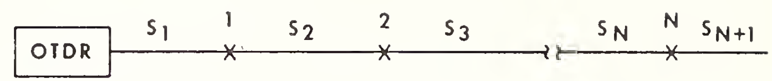


$$\epsilon_i = 5 \log \frac{S_{i+1}}{S_i}$$

$$\sum \epsilon_i = 5 \log \frac{S_2}{S_1} + 5 \log \frac{S_3}{S_2} + \cdots 5 \log \frac{S_{N+1}}{S_N}$$

$$= 5 \log \frac{S_{N+1}}{S_1}$$

ERROR REDUCTION WHEN MEASURING CONCATENATED SPLICES

FIGURE 12

OPTICAL CONNECTOR MEASUREMENT ASPECTS, INCLUDING SINGLE MODE CONNECTORS

P. Kaiser, W. C. Young, and L. Curtis
Bell Laboratories, Holmdel, N. J. 07733

SUMMARY

Optical and mechanical precision measurements required to achieve insertion losses below 0.4 dB with biconic multi and single-mode connectors are described. Connector losses depend on the measurement procedure, and in case of multimode connectors, may also depend on the direction of propagation and the modal power distribution existing at the connection point.

## I. INTRODUCTION

The most important performance parameter of an optical connector is its insertion loss. At first glance, a simple loss measurement should suffice to determine the connector loss to an accuracy which is only limited by the stability of the measuring apparatus used. To be meaningful, however, additional measurements are typically required in order to fully characterize a connector and to assure a certain performance level as we shall describe below.

Fiber connection and splice losses are affected by a mismatch of the intrinsic waveguide parameters such as core size and numerical aperture (NA), and extrinsic factors of influence such as transverse offset, angular misalignment, and end-separation. In a less obvious but very important way, multimode fiber connector losses are also affected by the modal power distribution existing at the connection point. This distribution is influenced by the launch conditions and the fiber transmission characteristics. Unique, steady-state connector losses are only obtained with a long reference fiber, or a properly designed mode filter.[1,2] For other conditions (such as for over-excitation with an LED), the connector loss has to be associated with the corresponding mode distribution as can be identified through effective NA, or radiation pattern measurements.[3,4] A complicating factor presently is still the lack of generally accepted definitions of some of above-mentioned fiber parameters such as the effective numerical aperture and equilibrium mode distribution in case of multimode fibers, and the effective core size and cut-off wavelength in case of single-mode fibers, but extensive efforts are underway to standardize the definition of these parameters.[5]

In addition to the intrinsic and extrinsic factors of influence, the connector loss may be affected by the cable design and the mounting technique (epoxies, crimps, etc.) used: Macro and micro-bends may inadvertently be incorporated into the connector body with ensuing excess losses which are unrelated to the fiber coupling mechanism itself.

In the following, we describe some of the measurements required in optical connector technology, using the transfer-molded connector developed for the Bell System FT3 (45 Mb/s) multimode lightwave system as an example.[6] In this design, the precise alignment of the two spring-loaded plugs is achieved in a biconic sleeve (Figure 1). Five of these connectors are used in a typical repeater span as illustrated in Figure 2. The laser package containing a premolded (Field Assembly-Type) connector plug is connected to the automatic plug-in connector at the back of the regenerator circuit board with a short jumper cable. A standard connector is used in the cable distribution frame. At the receiver end, the signal is routed analogously, with the detector package having a connectorized pigtail.

## II. MEASUREMENT OF PHYSICAL CONNECTOR PARAMETERS

A computer-controlled microscope test set with video scanning system has been developed which -- under observation of careful calibration procedures -- enables measurements of the core/plug eccentricity and the fiber deflection angle to an accuracy of 0.1 µm and <0.1 degree, respectively.[7] Eccentricities below 4 µm, and deflection angles below 1 degree have been obtained with high yield for multimode connector plugs in a manufacturing environment.[6] Using a modified plug fabrication process, eccentricities of ~0.4 µm, and deflection angles of ~0.26 degree (required for connection losses on the order of 0.5 dB, see Figure 3) have been obtained with single-mode plugs in laboratory experiments (Figures 4 and 5).[8]

By scanning both the near field of the core and its radiation pattern, the above-described test set simultaneously yields core diameter (beam profile) and NA data. More precise data are obtained from refractive index profile measurements. The degree with which these parameters can be controlled in the fiber fabrication process ultimately limits the lowest loss achievable even with a high-precision connector design. While fiber outer diameters can be measured with ±0.1 µm accuracy using mechanical or optical measurement techniques, diameter variations along real fibers amount to a multiple of this value even for distances on the order of a few centimeters. It appears, therefore, that fiber parameter matching is only assured if the fiber is broken and reconnected at exactly the same point ("identical fiber" case).

The concentricity of the two cones of the biconic alignment sleeve (Figure 1) can be determined with mechanical gauges, or preferably, through connector loss measurements using two precise reference plugs containing identical fibers.

The separation between the fiber end-faces is determined by the taper lengths of the plugs and sleeves. If the manufacturing tolerances are properly chosen, the end-faces can be brought into physical contact. This eliminates the ~0.31 dB Fresnel reflection losses and avoids instabilities caused by interference effects between the fiber end-faces.[6,9] A finite end-face seperation can be identified through optical time domain reflectometry (OTDR) techniques, and gap measurements with ~0.1 μm accuracy can be performed with an in - situ connector with a spectral scan since the gap causes resonance peaks in the transmitted and reflected power.[10]

In order to assure the integrity of the end-faces under repeated-contact conditions, they have to be polished flat within ~0.1 μm as can be determined with standard interferometric techniques.

## III. CONNECTOR LOSS MEASUREMENTS

In its simplest form, a connector loss measuring set-up consists of a source, a reference fiber terminated with a nominal reference plug and sleeve, and a large-area detector (Figure 6). The loss is determined from the reference power level and the output of the test cable after interconnection. Using this method, average connector losses of 0.28 dB have been measured for 5,700 multimode connectors produced in a manufacturing environment[6] (Figure 7). While the stability of the test set-up should permit measurements with ±0.01 dB precision, the accuracy with which the connector losses can be quoted is typically more than an order of magnitude worse because of a lack of precise reference plugs with ensuing loss variations for different rotational positioning of the connector plugs and sleeves. While this technique is suitable for the measurement of single-mode connectors where the loss is independent of the direction of propagation, in the case of multimode fibers with different core diameters and NA's, the loss may be negligibly small for transmission from a small-core/NA fiber to a large-core/NA fiber, and can be substantial in the opposite direction. Consequently, additional fiber parameter specifications have to be met to assure a desired system performance. Alternately, an average value for the high- and low-loss end of the test cable can be determined by inserting the cable with the test plugs between two nominal reference plugs (Figure 6b), whereby the previously determined loss of the reference fiber interconnection has to be added to the above combined loss value before averaging.[2]

The methods described thus far fail, however, to include the excess loss potentially originating in the reference plug body due to improper cable mounting techniques. To include this loss, the two-point cut-back method has to be used (Figure 6c).

If a rotational adjustment of the plugs and sleeves is possible, one may quote minimized, maximized, averaged, or random connection losses. Loss data which may be considered most meaningful for systems applications are obtained by determining the random loss measured during the concatenation of an ensemble of connectorized short cables containing different fibers satisfying specified tolerance conditions.[11] Data obtained in this fashion for a set of 51 multimode jumper cables are shown in Figure 8, with the average loss amounting to 0.33 dB ($\sigma$ = 0.18 dB).[6] Random connection losses of a set of 9 single-mode jumpers whose eccentricities and deflection angles were presented in Figures 4 and 5, are shown in Figure 9. Average losses amounted to 0.39 dB ($\sigma$ = 0.18 dB), using fiber from the same supply reel.

For long fiber sections, the loss of the fiber has to be taken into account, and the accuracy with which this loss is known directly affects the accuracy of the connector loss measurement. The loss of connectors and splices in long concatenated fiber sections can be determined in-situ and without knowing the fiber losses by employing OTDR techniques.[12] However, special procedures also have to be followed here (such as transmission in both directions) in order to obtain meaningful results.

## IV. CONCLUSIONS

A large variety of optical and mechanical precision measurements, including fiber characterization, are required to develop high-performance optical connectors as is described in this paper. In addition, optical connectors have to be evaluated in terms of their systems performance, since they may cause modal noise, and reflections back into the laser cavity, with an ensuing effect on the spectral characteristics and laser noise, all of which may result in system performance degradation. Finally, mechanical and environmental performance tests also have to be included in the evaluation program.

## REFERENCES


1. P. Kaiser, "Symp. on Opt. Fiber Measurements, Boulder (1980), NBS Publication 597, pp. 11
2. P. Kaiser, W. C. Young, N. K. Cheung, and L. Curtis, Ibid. pp. 73.
3. P. Kaiser, A. C. Hart, and L. L. Blyler, Jr., Appl. Opt. 14, 156 (1975).
4. Y. Daido, et al, Opt. Fiber Comm. Conf. Washington, D.C., ThE3 (1979).
5. A. H. Cherin and W. B. Gardner, SPIE Conf., Washington, D.C., (1980).
6. W. C. Young, et al, Int. Wire and Cable Symposium, Cherry Hill, 1981.
7. N. K. Cheung and N. M. Denkin, NBS Publication 597, pp. 45 (see Ref. 1)
8. W. C. Young and L. Curtis, to be published.
9. W. C. Young, et al, ECOC6, York (1980).
10. A. Tomita, submitted for publication in Appl. Optics.
11. P. Kaiser and D. L. Bisbee, Opt. Fiber Communication Conf., Washington, D.C., TuE3 (1979).
12. P. Matthijsse and C. M. Blok, ECOC5, Amsterdam, pp. 9.5 (1979).

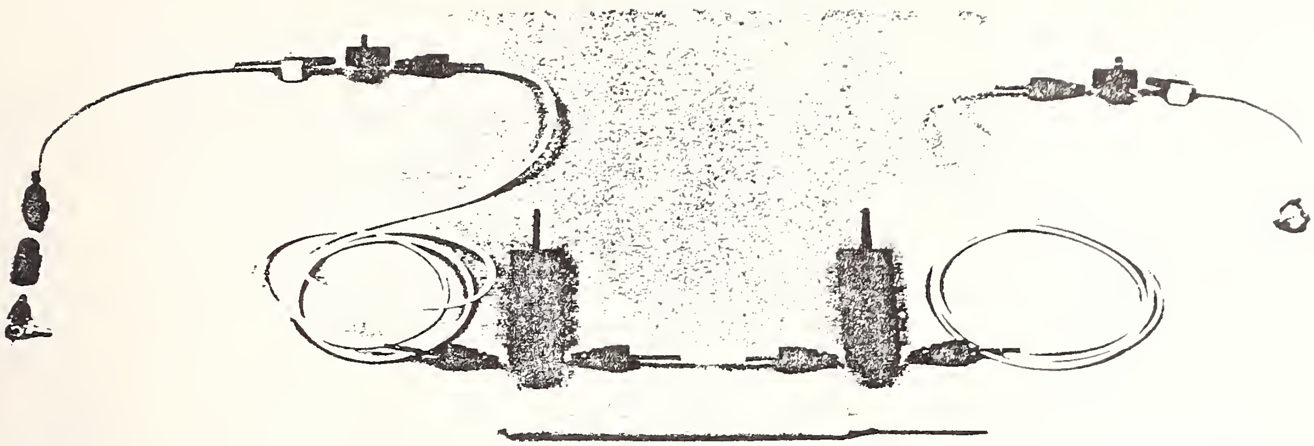

Fig. 2. Connector hardware used in a typical FT3 installation.

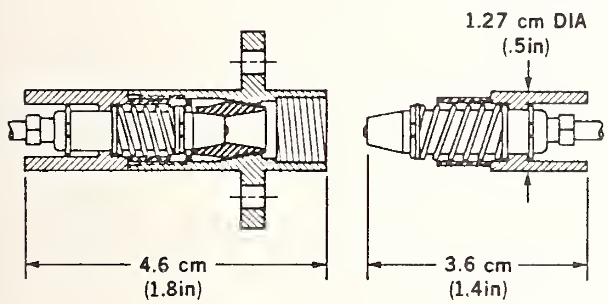


Fig. 1. Biconic connector design.

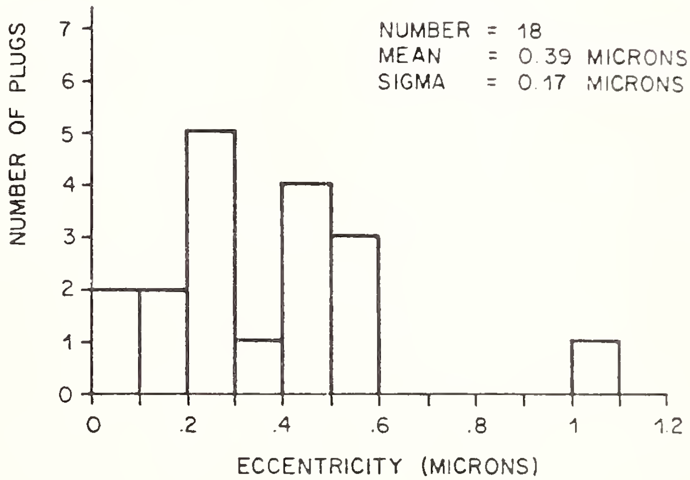


Fig. 4. Core/plug eccentricity data for 18 single-mode connector plugs.

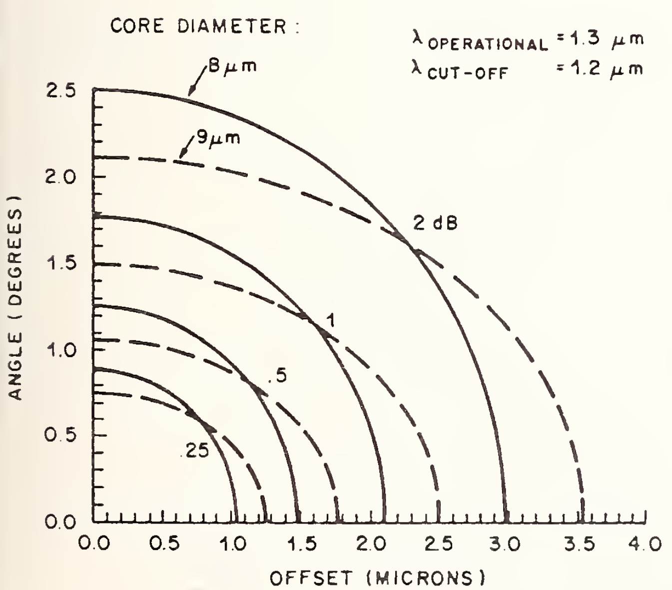


Fig. 3. Single-mode connector losses versus offset and deflection angle for 8 and 9 micron-core fibers operated at 1.3 μm (λcut-off:~1.2 μm).

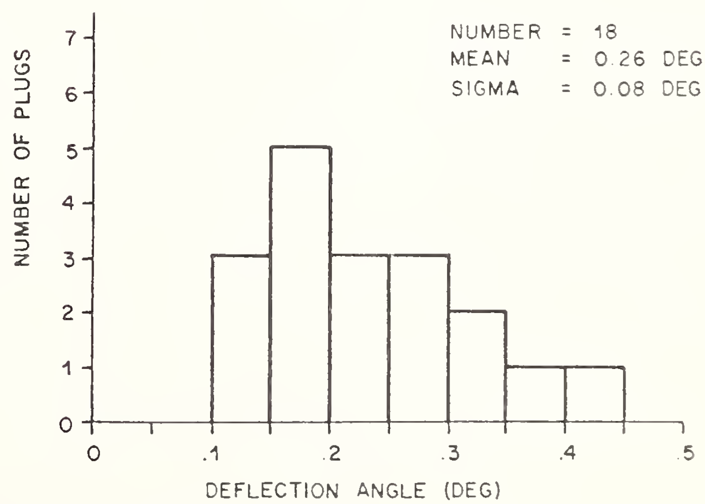


Fig. 5. Fiber deflection angles of the same set of plugs described in Figure 4.

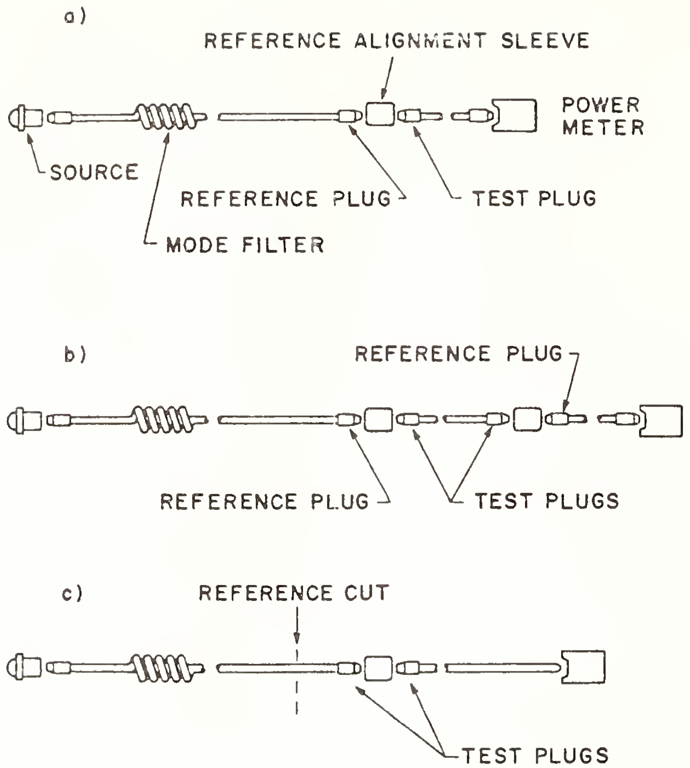


Fig. 6. Schematic of connector loss measuring test sets,
a) Single reference plug method
b) Insertion loss measurement with reference plugs at both ends of the test cable
c) Two-point cut-back technique

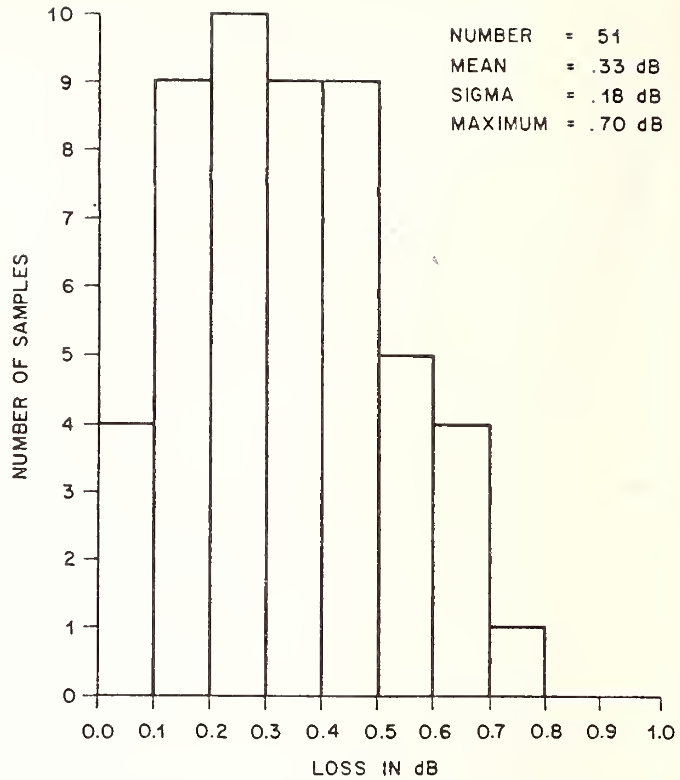


Fig. 8. Loss data of 51 biconic connectors at an FT3 installation measured during concatenation; corrected for fiber losses.

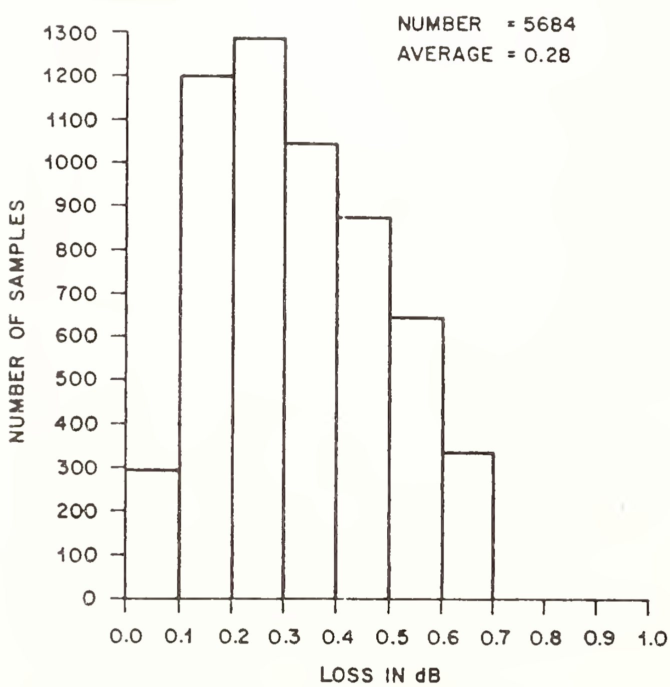


Fig. 7 Loss data of 5700 connector plugs produced in a manufacturing environment, and measured according to Figure 6a,
(Core diameter 50 µm, o.d.=125µm, NA=0.23)

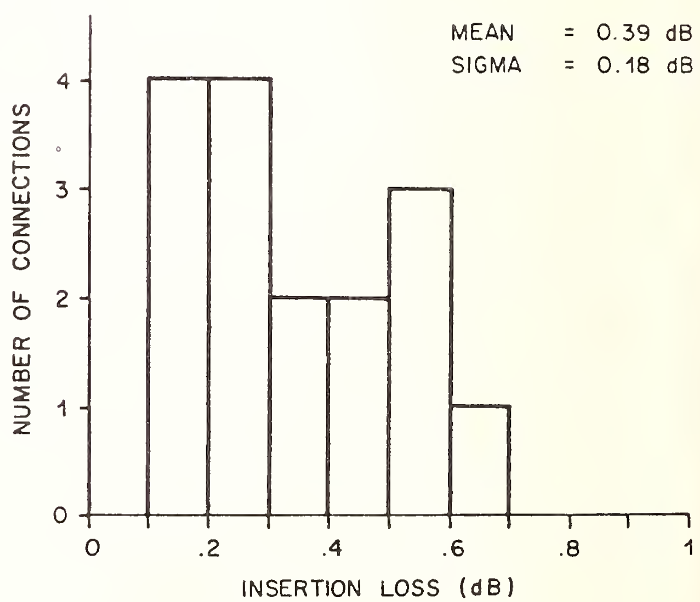


Fig. 9. Loss histogram of 16 random single-mode fiber connectors assembled with nine test cables (core diameter 9 µm, cut-off wavelength: 1.2 µm, measurement wavelength: 1.3 µm) (See also Figures 4 and 5).

EFFECTS OF MODE FILTER INSERTION ON CONNECTION LOSS

BETWEEN COMMERCIAL SINGLE-FIBRE CABLES

C. Marchesi - SIRTI S.p.A. - Via G.B. Pirelli 20 - 20124 Milano (I)

U. Rossi - CSELT - Via G.R. Romoli 274 - 10148 Torino (I)

Abstract

Measurements of mode power distribution on connectorized single-fibre cables stress the strong influence of launching and propagation conditions on connection loss. The large dispersion in coupling loss values (from 0.43 to 1.13 dB) produced in different conditions by the same connector can be explained on the basis of such measurements.

## 1. Introduction

Connectors for multimode optical fibres are widely employed in commercial transmission systems: their performances have a strong impact on the whole system design. On the other hand it is well known that the loss introduced by a joint in an optical link is not a uniquely defined variable: besides mismatches in fibre parameters and misalignments of the fibres, the mode power distribution (MPD) in the fibre section preceding the joint, the mode conversion introduced by the joint and the propagation conditions in the fibre following the joint can strongly influence the overall connection loss [1].

## 2. Measurement set-up

IEC [2] recommends to measure connector loss either in equilibrium or in uniform mode distribution excitation: the former situation simulates reception connectors, while the latter applies to transmission ones, if LED sources are employed. Unfortunately equilibrium MPD establishes only after propagation in a length of fibre which, if high quality low-loss fibres are employed, may amount to many kilometers. Several techniques have been proposed to simulate the equilibrium MPD in a short length of fibre: among the others, mandrel wrap mode filters (MW) [3] seem suitable for application to single-fibre cables, since they result effective without extracting the fibre from the cable.

A preliminary set of measurements, carried out in order to define test conditions on commercial connectors mounted on commercially available single-fibre cables, has been performed on the basis of both optical loss and MPD measurements; the latter were carried out following a technique whose effectiveness and relia bility has been previously demonstrated, provided that incoherent sources are em ployed [4]. The results reported in the following refer to a single set of measu rements: their purpose is not the connector characterization, but the definition of the test procedure.

The near-field intensity (NFI) measurements are performed by scanning a magnified image of the fibre with a large area Si photodetector, in front of which a pin-hole (~100 μm diameter) spatially limits the image. Removing the pin-hole allows to measure the whole power guided by the fibre: loss measurements refer to such "integral" data. A "lock-in" amplifier transfers NFI data to a desk-top computer, which processes them to obtain the MPD as a function of the collective mode para meter x (x=0: fundamental mode; x=1: cut-off modes [5]). The source is an LED (peak emission λ~850nm) which overfills the graded-index, 50/125 μm low-loss op tical fibre. From NFI measurements the MPD's can be calculated.

3. Results

Two jumpers, nominally equal, called here A and B, were connected, and the result ing measured NFI was assumed as the reference situation (case #1): this complies with what recommended by IEC in [2], method 5, and has the purpose of leaving launching and detection conditions fixed when inserting a further jumper. The in sertion on jumper A of a MW, obtained by wrapping 5 turns of the single-fibre ca ble around a smooth cylindrical mandrel 5 mm in diameter, produced a 6.1 dB loss and the MPD shown in Fig. 1 (full line, case #2). The filtering effect of the MW can be recognized from the drastic depletion of high order modes.

The insertion of a further MW, analogous to the previous one, on the cable B, produced only an additional loss of 0.66 dB, and a slight narrowing of the measured MPD (Fig. 1, case #3, dashed line).

The jumper under test, nominally equal to the previous ones, called X, was now inserted between A and B, keeping both MW's: the additional loss was 1 dB, and the relative MPD is reported in Fig. 1 (dotted line, case #4). The relatively high value of loss produced by the new connection can be explained by taking into account, besides joint loss, the additional loss introduced by the propagation in the jumper B of an MPD perturbed by the mode conversion at the connection. In fact, a comparison of the MPD's relative to cases # 3 and #4 (see Fig. 1), shows a further MPD depletion which justifies the 1 dB loss.

Removing the MW from the jumper B changed the situation completely: in this case the loss introduced by the connector was 0.43 dB with respect to the case # 2, and the relative MPD is shown in Fig. 2 (full line, case # 5). This allows to quantify the previous additional loss induced by the propagation in the jumper B with the MW to be 0.57 dB, a value higher than the connection loss itself. A comparison of MPD's of cases #2 and # 5 shows well the mode conversion introduced by the joint: a transfer of optical power from low to high order modes takes place. This mode conversion effect is shown, from a different point of view, by the MPD of case # 6 (Fig. 2, dashed line), obtained by removing also the first MW from jumper A. In this case, the connector produced a depletion of high order modes, which is shown by the departure of the relative MPD from the reference uniform one. The loss, with respect to the case # 1, was 1.13 dB, stressing its critical behaviour in nearly uniform MPD conditions [1].

Finally, the MW was inserted on the jumper B, keeping jumpers A and X undisturbed (case#7, Fig. 2, dotted line). The insertion of the MW behind both joints gave rise to a loss of 5.27 dB (with respect to case # 6); the power level detected at the end of the link was very close to the one of case #5, but the two MPD's (Fig. 2, full and dotted lines) show noticeable differences (depletion of low order modes and corresponding filling of high order ones passing from # 7 to # 5), due to the different position of the MW in the two cases.

## 4. Conclusions

The previous results confirm that the only measurement of detected power level is a poor characterization of connector performances; on the contrary, MPD measurements have proved to be a powerful and useful tool for the characterization of connectors and splices for multimode optical fibres, from which remarkable in formations can be deduced.

The present measurement set, carried out on unselected commercial single-fibre cables and connectors, has confirmed the strong dependence of joint loss on launching and propagation conditions: when figures concerning connector loss are provided, the measurement set-up should be carefully specified in order to perform meaningful comparisons. In this case, in fact, losses ranging from 0.43 to 1.13 dB were observed: the MPD measurement has supplied the key for understanding such apparent discrepancies.

## References


1. P. Di Vita, U. Rossi; Journal of Opt. Commun., Vol. 1, No. 1 (1980), pp. 26-32
2. IEC document No. 46E (Secretariat) 33
3. A.H. Cherin et al.; Fiber and Integr. Opt., Vol. 4, No. 1 (1982), pp. 49-65
4. M. Calzavara, P. Di Vita, U. Rossi; Electron. Lett., Vol. 17, No. 15 (1981), pp. 543-545
5. R. Olshansky; Appl. Opt., Vol. 14, No. 4 (1975), pp. 935-945


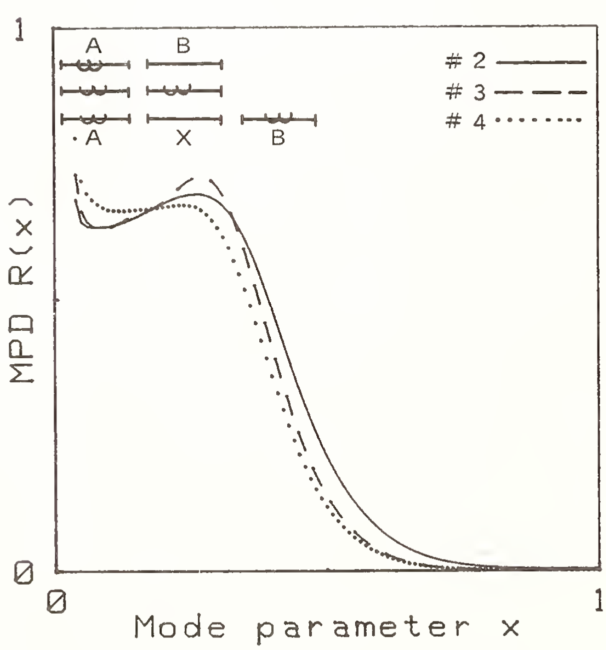


Fig. 1 - Measured MPD's of cases #2, #3 and #4

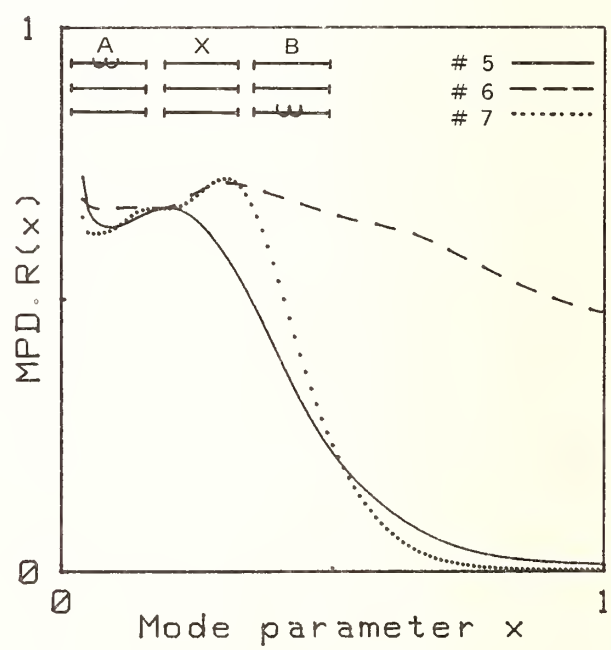


Fig. 2 - Measured MPD's of cases #5, #6 and #7

# A NEW APPROACH TO JOINT LOSS MEASUREMENT.

R. D. JEFFERY & J. L. HULLETT, University of Western Australia,
Department of Electrical & Electronic Engineering,
Nedlands, W.Aust. 6009.

We report here on a new display format for the accurate measurement of joint loss made possible by two-point processing of a backscatter signal. This display is clearly superior to the more usual log plot because it presents the results in a form that allows the direct interpretation of joint loss and a comparison of all joint losses within a regenerator span. Furthermore, a threshold level can be displayed as an aid to the acceptance or rejection of joints, a feature which simplifies the field testing of fiber splices.

The loss of fiber splices is an important consideration in the total loss budget of optical fiber links and therefore the accurate measurement of joint loss at distances commensurate with typical repeater spacings is necessary. For splices between identical fibers the backscatter method has been shown to give a good measure of joint insertion loss provided the results obtained from both ends of the fiber are averaged (1). Two-point processing of backscatter data not only provides a better format for joint loss estimation, but it is the technique which provides a controlled level of measurement accuracy throughout the entire fiber scan. Thus joint assessment at long range can be performed with the same accuracy as at the near end. The set accuracy is achieved at each point in the fiber scan by averaging that number of samples dictated by the primary (before averaging) signal to noise ratio. This ratio is estimated from the sample mean and variance (2,3).

With two-point processing two samples of the backscatter waveform separated by $\Delta\ell$ are taken for each pulse launched into the fiber, the attenuation being derived from the ratio of these samples. Thus for samples at $\ell_1$ and $\ell_2$ with $\Delta\ell = \ell_2 - \ell_1$, the spatial attenuation characteristic $\alpha(\frac{np}{m})$ is given by:

$$\alpha(\ell_1, \ell_2) = \frac{\ell n[i(\ell_1)/i(\ell_2)]}{2\Delta\ell} \qquad (1)$$

where $i(\ell)$ is the backscatter signal and $\ell$ the distance to the scattering point. The fiber is scanned by shifting the paired samples in adjoining steps along the fiber. The resultant alpha plot reveals the fine detail spatial loss characteristic of the fiber and its joints. Fig.1 is a typical alpha scan of a fiber regenerator link which highlights even small joint losses.

For direct joint loss measurement it is better to remove the spatial dependence $\Delta\ell$ from eq.(1) and plot the one way loss $\gamma(\ell_1, \ell_2)$ between the sample points $\ell_1$ and $\ell_2$, where

$$\gamma(\ell_1, \ell_2) = \alpha(\ell_1, \ell_2)\Delta\ell \qquad (2)$$

A plot of $\gamma(\ell_1, \ell_2)$ for the same link as used above is shown in Fig.2, with $\Delta\ell$ being 160m and the measurement accuracy set at ±0.016dB. Here the base line represents the relatively uniform loss of the fibers and the peaks above the base line the excess loss caused by the joints. With joint loss measurements the sample pair is scanned in interleaved steps 40m apart and it is this choice of sample step size that determines the spatial resolution for locating joints. Using the parameters stated the scan for Fig.2 over 6.6km was completed in two minutes. For comparison the more usual log plot of the back-scatter data is shown in Fig.3. This plot is formed by accumulating the loss $\gamma$ between samples spaced at 40m. Accuracy is maintained at ±0.02dB for the complete scan.

The significant advantage of the type of plot shown in Fig.2, and not applicable to the log plot of Fig.3, is that a threshold level indicating a poor quality joint can be marked on the display. If for example, the maximum acceptable splice loss is 0.3dB in a fiber link of nominal attenuation 2dB/km then the threshold level for a sample spacing of 160m is 0.62dB which accounts for 0.3dB joint loss and 0.32dB fiber loss. This threshold can be drawn on the results as shown in Fig.2. Clearly this feature lends itself to the field testing of fiber splices.

We have shown that two-point processing of backscatter waveforms is an accurate method for measuring the variation in loss as a function of length. The resulting graph of this data accurately indicates joint loss and further allows the display of a joint rejection level which simplifies the testing of fiber splices in the field. Although the results presented were made at 900nm this technique is applicable at 1300nm and results at this wavelength will be presented at a later date.

## REFERENCES


1. A. Leboutet, in NBS special publication 597.
2. J.L.Hullett & R.D.Jeffery, in technical digest, 3rd IOOC San Francisco, 1981.
3. J.L.Hullett & R.D.Jeffery, Opt.Quant.Electron. 14, No.1, 1982.

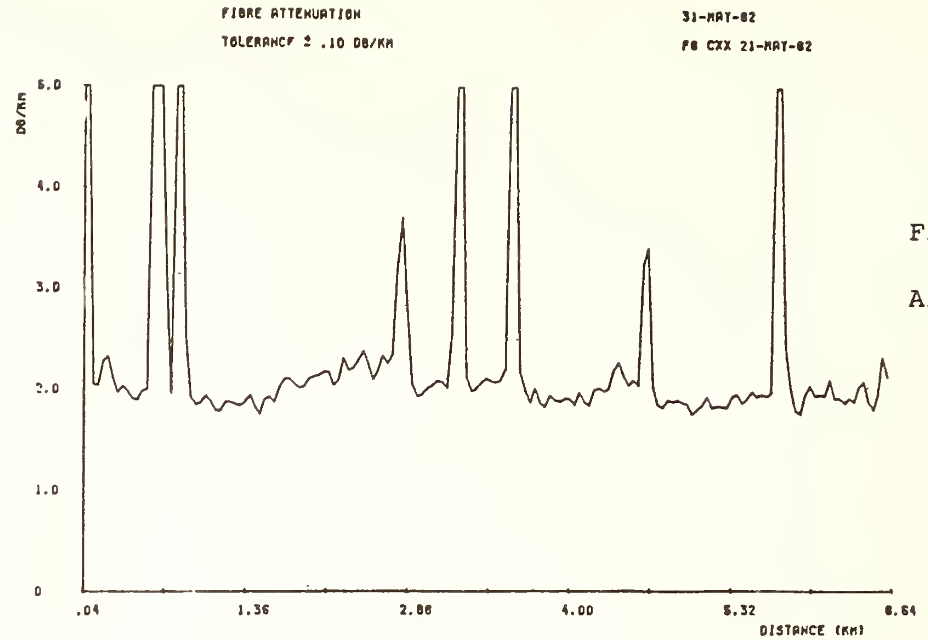


Fig.1.

Alpha Scan

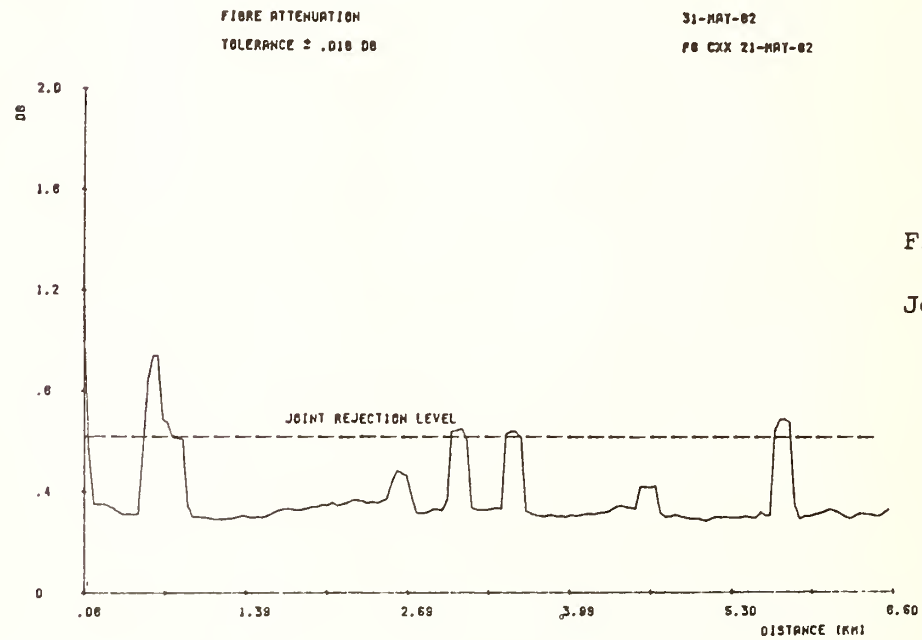


Fig.2.

Joint Loss Scan

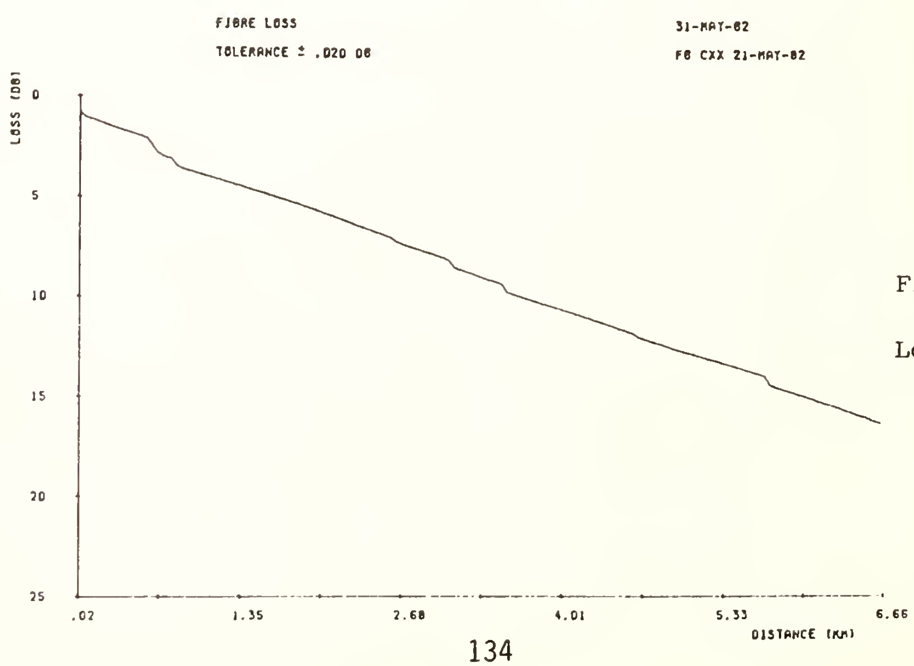


Fig.3.

Log Plot.

# INDEX PROFILE MEASUREMENTS

W.J. Stewart
Plessey Research (Caswell) Limited
Allen Clark Research Centre
Caswell, Towcester, Northants
England.

Index profiling is an essential measurement for optical fibres and preforms, since the index profile vitally affects system performance. Methods for determining diameter and NA that do not involve profile measurement are inevitably open to question, and similar difficulties arise with such parameters as eccentricity. With the increasing importance of monomode fibres in systems, the need for high resolution in fibre profiling is growing. Its significance and the growing technical needs of users are tending to keep up pressure for better and more convenient profiling methods.

Consider for the moment only those methods that actually measure refractive index. These are ideally required to have spatial accuracy of better than ½μm, and resolution preferably better than this. Index "resolution" (relative accuracy or linearity) is required to $\sim 10^{-5}$, with an absolute accuracy requirement a good deal looser than this. It might be supposed that all methods would share common ultimate limitations, since most methods essentially involve measuring differential phase delays through adjacent parts of the fibre. There is some truth in this. Define a 'figure-of-merit' F as

$$F \equiv \frac{dP/P}{dn} \cdot \frac{1}{(\text{resolution})^2}$$

Where dP/P is the fractional change in detected optical power for an index change of dn, and $1/(\text{res})^2$ is a measure of the smallest perceived area. Both the nearfield methods (Refracted and Bound) and axial interference (or phase contrast) now have F's that are independent of resolution. Values at 633nm are 39 and 24 respectively. The superiority of the nearfield methods probably reflects their greater use of the axial constancy of index, and might disappear for transverse interference. Reflection does not fit into this scheme, so F is not constant, but for comparison F $\sim$ 900 at 1μm resolution for plausible values, or $\sim 10^{-2}$ if signal variation as a fraction of input power is used.

The main significance of those numbers is to underline (for the first two) their relative similarity, and hence to make the point that choices of technique are in fact made on grounds other than ultimate performance. For example, very high resolution axial interference would require the preparation of very thin (micron) accurate cross-sectional slices of fibre, or again reflection measurement is optically very inefficient and this causes experimental problems.

It is not therefore the purpose of this paper, indeed it is probably not practicable, to define a 'best' profiling technique for all purposes, but to define the relative merits and demerits of the various techniques. Firstly to define the problem:- optical fibres and, generally, preforms have axially invariant index distributions over macroscopic distances (that is over a measurement length). The refractive indices do vary with wavelength but this does not normally affect profile to a measurable degree (c.f. the variation of optimum $\alpha$ with $\lambda$ which is different). The total index differences are generally less than $10^{-2}$. It may be possible to assume circular symmetry.

Techniques generally divide into axial and transverse, and beyond this they will be classified according to mechanism. This division is indicated in Figure 1. Table 1 indicates a rough 'batting order' for the various techniques according to various criteria, the most desirable being at the top.

In general axial methods are more useful for fibres and transverse methods for preforms.

The individual methods will be discussed at the meeting.

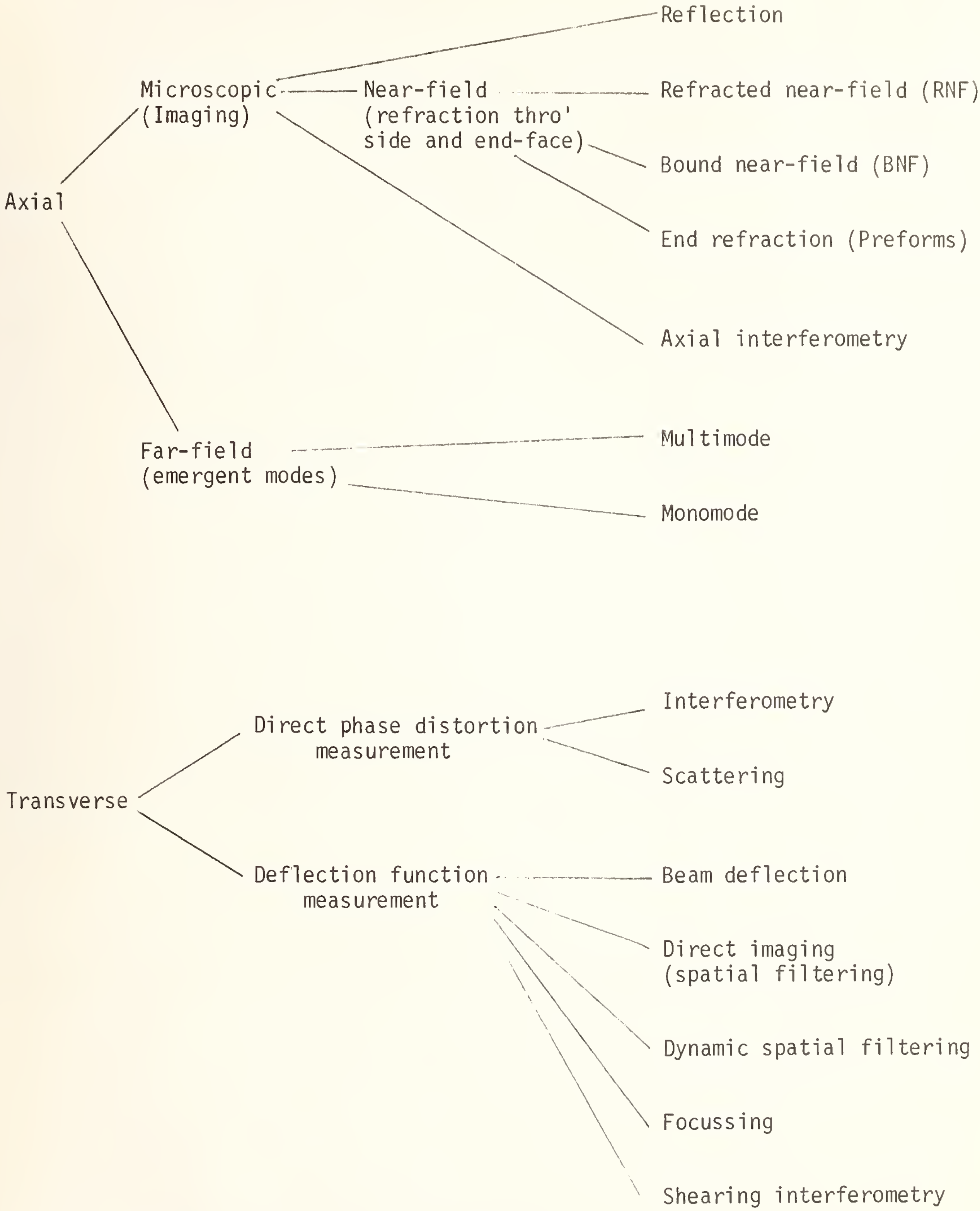
Axial
Microscopic (Imaging)
Near-field (refraction thro' side and end-face)
Reflection
Refracted near-field (RNF)
Bound near-field (BNF)
End refraction (Preforms)
Axial interferometry
Far-field (emergent modes)
Multimode
Monomode
Transverse
Direct phase distortion measurement
Interferometry
Scattering
Deflection function measurement
Beam deflection
Direct imaging (spatial filtering)
Dynamic spatial filtering
Focussing
Shearing interferometry

FIGURE 1

| Ease of Preparation | Practical Resolution |
|---|---|
| Transverse methods | Refracted near field |
| | Scattering |
| Near-field methods ) | Bound N.F. ) |
| ) | ) |
| ) | ) |
| Far-field methods ) | Transverse interference) |
| Reflection (if possible) | Axial interference<br>Focussing |
| Axial interference | Spatial Filtering |

Data Processing Required

R.N.F.

Reflection

B.N.F.

Axial Interference

Deflection Function Methods

Far-field

Scattering

TABLE 1

# A SIMPLE TECHNIQUE FOR HIGH ACCURACY CORE-CLADDING CONCENTRICITY MEASUREMENT OF SINGLE MODE FIBERS

D. N. Ridgway and L. J. Freeman
Bell Telephone Laboratories
2000 Northeast Expressway
Norcross, Georgia 30071

ABSTRACT Core-cladding concentricity has been measured, to an accuracy of approximately ± 0.1 μm using a simple technique that incorporates a vacuum chuck and a rotational stage. A butt-joint splice is assembled in the vacuum chuck and one fiber rotated 360°. Transmission loss from maximum to minimum is directly related to core-cladding concentricity for circularly symmetric fibers.

INTRODUCTION There are several contributors to splice loss in single mode fiber splices. These include transverse offset, end seperation, angular misalignment, unequal spot size, end face angle and smoothness. Core non-concentricity can cause a transverse offset in an otherwise identical fiber splice. Splicing techniques in which surface tension effects cause self alignment of the fiber OD are subject to this offset. In large scale manufacture, core concentricity may be difficult to maintain, therefore a simple, accurate measurement may be needed. This paper presents a technique for core non-concentricity measurement that meets these requirements. An earlier technique also based on fiber rotation was presented by Tynes and French.[1]

MEASUREMENT PROCEDURE AND APPARATUS The fiber under test is placed in the measurement system (Figure 1). This system consists of a 1.3 μm LED source, the measurement apparatus (Figure 2), an InGaAs Detector and a PAR 124 Lock-in Amplifier. The measurement procedure is simple and can be performed quickly. The test fiber is loose-tube spliced to the launch pigtail and the other end placed directly in the detector. This establishes a reference level for the unbroken fiber. The fiber under test, approximately four meters, is broken near the middle and the ends prepared. These fiber ends should be smooth and have an angle of less than 1°. The fibers are then spliced together through a rotational stage and held in a vacuum chuck. The fiber mounted in the rotational stage is then rotated 360° and the transmission levels recorded every 10°. The transmission level should return to the reference level to within ± .02 dB at some point during rotation. Maximum splice loss is calculated from the maximum and minimum transmission level. This maximum loss is related to transverse offset by the normalized lateral offset curve (Figure 3).[3,4] Core cladding concentricity is calculated from normalized offset, $d = x/s$, by the simple equation $e = \frac{d \cdot s}{2}$ ; where e is the eccentricity and s is the beam width of the fiber, and $x/s$ is the normalized offset from Figure 3. This calculation assumes a round core and round fiber OD.

The two most important parts of the measurement apparatus are the vacuum chuck and rotational stage. The chuck must be free from burrs and the groove straight. The chuck is made of stainless steel, eliminating oxidation that might cause problems during the measurement.

The rotational stage must be smooth and free from back lash and front to back movement. The elimination of any excess movement helps to provide a stable base for the rotational measurement.

RESULTS Several fibers have been measured using this apparatus and procedure. Fiber 104D showed little if any change in transmission level as can be seen in Figure 4. For this reason it is felt there is little eccentricity present and the variation in transmission level is within the measurement or noise level of the system. The second fiber, 104B, exhibits a small amount of change and the eccentricity is calculated to be .31 μm. The third fiber, 30B, in Figure 4 shows significant changes in transmission level and its eccentricity has been calculated to be .71 μm. Transmission level differences were repeatable to within ± 0.01 dB and combined with the accuracy of the lateral offset curve,[4] yields a resolution and accuracy of ≅ ± 0.1 μm.

CONCLUSION A simple, accurate technique has been presented to measure core eccentricity in single mode fibers. A butt-joint splice measurement provides transmission level information that is used to determine core eccentricity of the fiber. This technique could be useful for core eccentricity characterization in large scale fiber manufacturing.

REFERENCES

1. A. R. Tynes, W. G. French, "Measurement of Single-Mode Fiber Core-Cladding Concentricity," Electronics Letters, Vol. 14, No. 4, February 16, 1978, pp. 113-115.
2. C. M. Miller, "Loose Tube Splices for Optical Fibers," BSTJ, 54, No. 7, (September 1975), pp. 1215-1225.
3. D. Marcus, "Loss Analysis of Single-Mode Fiber Splices," Bell System Tech. J., (1972), 56, 703-718.
4. R. B. Kummer, S. R. Fleming, "Monomode Optical Fiber Splice Loss: Combined Effects of Misalignment and Spot Size Mis-Match," Optical Fiber Communication Tech. Digest, April 13-15, 1982, Phoenix, Arizona.

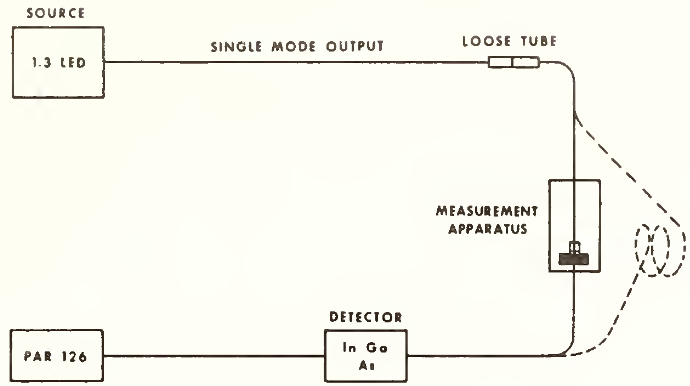


FIGURE 1

DIAGRAM OF MEASUREMENT SYSTEM

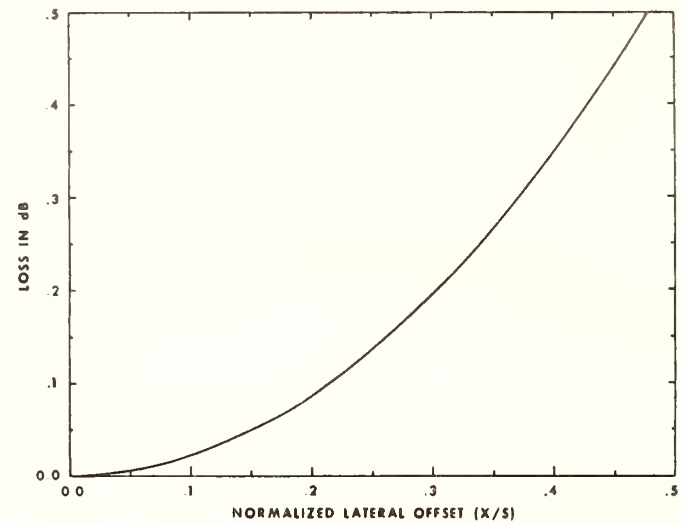


FIGURE 3

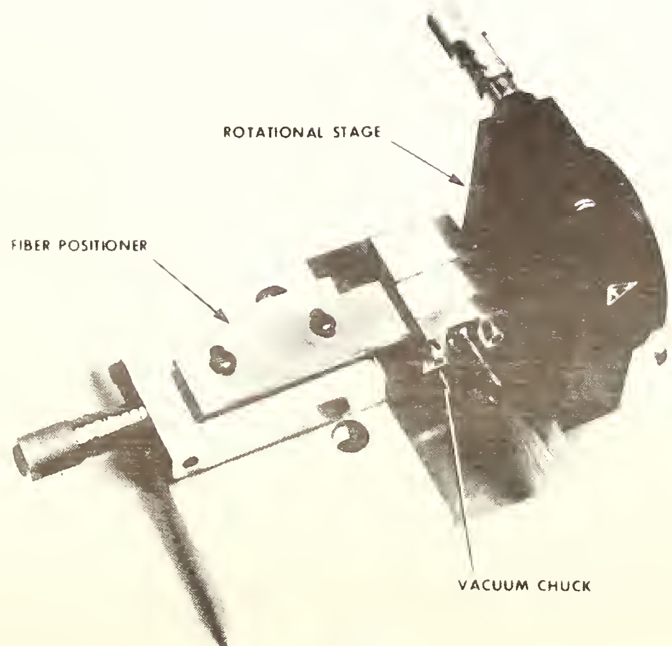


FIGURE 2

MEASUREMENT APPARATUS

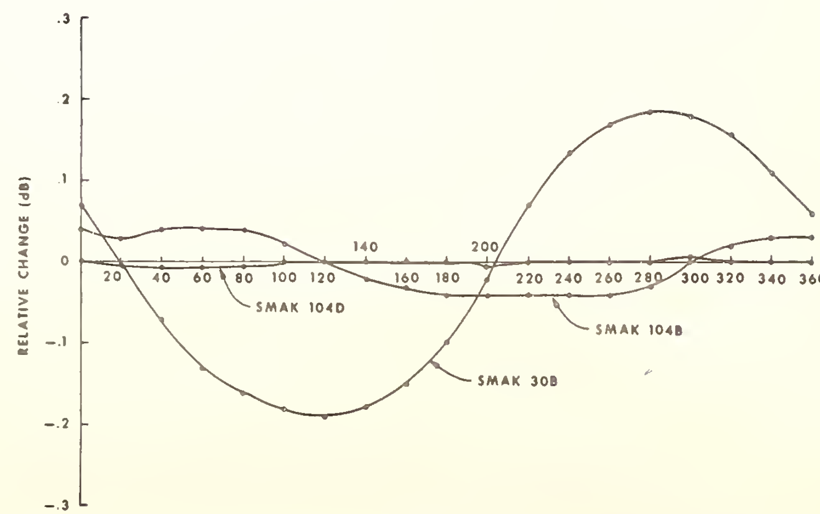


FIGURE 4

CHANGE IN LOSS vs. ROTATIONAL POSITION

An Interlaboratory Measurement Comparison of
Core Diameter on Graded-Index Optical Fibers

Ernest M. Kim
Douglas L. Franzen
U.S. National Bureau of Standards
Electromagnetic Technology Division
Optical Electronic Metrology Group
Boulder, Colorado 80303, USA

Core diameter is an important geometrical parameter used in fiber specification. Unnecessary splice loss can be reduced by joining fibers of similar dimension. A core diameter of 50 μm has been internationally accepted for multimode graded-index fibers.

Core diameter is usually defined by measuring a distance on the fiber refractive index profile at the points $n_3$, figure 1, where the value of $n_3$ is given by

$$n_3 = n_2 + k(n_1 - n_2) \tag{1}$$

with $n_1$ being the maximum index, $n_2$ the homogeneous cladding index, and k a constant generally chosen to be between 0 and 0.05 [1]. Different index profiling techniques reduced to common practice include transverse interferometry (TI), refracted near-field (RNF), and transmitted near-field (TNF). TI and RNF give a more direct measure of the index profile and are therefore believed to be more accurate. TNF is easy and inexpensive to implement; thus, it is often used by manufacturers for quality control measurements. Sladen has shown for uniform mode excitation on short lengths of graded-index fiber, the near-field intensity distribution across the output end face (TNF) closely resembles the index profile [2]. Principal deviations include the presence of tunneling leaky modes and loss of resolution near the core-cladding boundary due to the decrease in local numerical aperture [3].

While previous interlaboratory comparisons have assessed agreement on fiber attenuation, bandwidth, and numerical aperture; none have addressed core diameter. This paper describes a TNF comparison on core diameter; participants include the National Bureau of Standards and three manufacturing members of the Electronic Industries Association (EIA). The TNF procedures used in the comparisons and employed at a wavelength of 850 nm are currently pending before the EIA and require the following conditions: a test sample length of 2.0 ± 0.2 m; a launch having a uniform intensity distribution across the core with a launch numerical aperture exceeding 0.3; a cladding mode stripper; and a scan of the TNF image with a resolution at least consistent with theoretical limits. Core diameter was defined using Eq (1) with a k value of 0.05. Each reported value was the average of three measurements; one measurement included a new output end and another a fiber rotation of 90 degrees.

Since reported averages consist of a limited number of single scans across diameters, fibers chosen for the comparison were preselected for good core circularity. NBS measured the TNF core diameter of each fiber length supplied to participants. Seven lengths of each comparison fiber were measured with a random angular orientation; standard deviations ranged from 0.2 to 0.8 μm with an average of 0.4 μm for the six comparison fibers. Comparison fibers exhibited diverse behavior with respect to index profile. Fiber #1 has a step structure near the core-cladding boundary; fibers #2 and #6 have depressed index barrier layers at the core-cladding boundary; fiber #3 has a deep on-axis dip with deposition layer structure; fiber #4 has a non-circular symmetric index dip/peak; and fiber #5 is made by an outside vapor phase deposition process and has no central index dip.

Results of the 5 percent core diameter comparisons on the six fibers are given in table 1. Measurement standard deviations for fibers #1 to #6 are 0.3, 0.6, 0.6, 0.6, 0.6, and 0.4 μm, respectively. The average standard deviation, 0.5 μm, is slightly larger than the average precision, 0.4 μm one standard deviation, claimed by participants for their systems. Results are therefore about as good as one could expect.

Figure 2 gives the relative performance between the participants for each fiber compared to average measured values. Some participants are consistently high or low with respect to the average, indicating systematic offsets. The average of the absolute values of offsets between pairs of participants is 0.5 μm.

An NBS calibration reticle was also measured by participants to determine the degree of systematic offset caused by dimensional calibration error. Participants measured the distance between the centers of lines 1 and 3 on a photolithographically fabricated reticle using their usual TNF apparatus without a priori knowledge of the actual separation (figure 3). An absolute calibration of the reticle was made by referencing the line separation to multiple fringes from a Fabry-Perot interferometer using a 0.6328 μm HeNe laser. Table 2 gives participant results compared to the actual separation of 100.1 μm. In some cases, interlaboratory calibration differences between pairs of participants are greater than 3 percent or half of the proposed ±6 percent CCITT tolerance for core diameter. Such an offset could significantly affect the statistics of fibers accepted between two parties. Applying calibration corrections to the data in table 1 reduces the offsets between pairs of participants in most cases; however, for some the offsets increase indicating other sources of systematic error. Also, 5 percent core diameters for the comparison fibers were measured at Bell Laboratories by A. H. Cherin and M. J. Saunders using RNF and at Western Electric by C. Bice using RNF and TI; a comparison to the TNF results will be given.

## References


[1] This definition for core diameter is under consideration by the IEC, CCITT, and EIA.

[2] F. M. E. Sladen, D. N. Payne, and M. J. Adams, A.P.L. 28, 255 (1976).

[3] J. P. Hazan, Electron. Lett. 14, 158 (1978).


Table 1.

TNF 5% Core Diameters, μm

| Participant | Fiber # | | | | | |
|---|---|---|---|---|---|---|
| | 1 | 2 | 3 | 4 | 5 | 6 |
| 25 | 47.5 | 44.7 | 50.7 | 49.6 | 50.3 | 47.5 |
| 56 | 46.9 | 44.1 | 49.4 | 48.8 | 49.4 | 46.7 |
| 83 | 47.6 | 44.9 | 50.2 | 49.4 | 49.7 | 47.5 |
| 47 | 47.3 | 43.7 | 49.5 | 48.4 | 50.7 | 47.0 |
| Average | 47.3 | 44.4 | 50.0 | 49.1 | 50.0 | 47.2 |
| Standard Deviation | 0.3 | 0.6 | 0.6 | 0.6 | 0.6 | 0.4 |

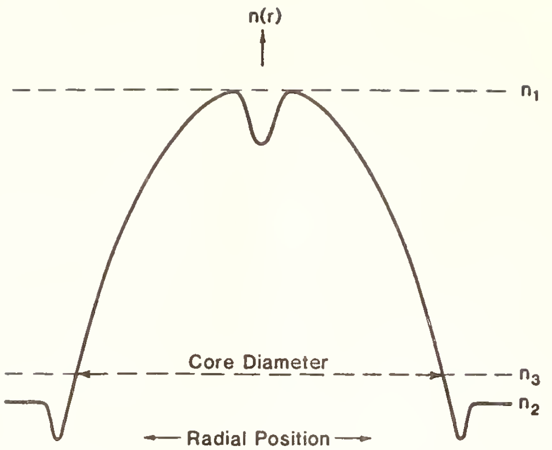


Figure 1. Points on a typical index profile used in determining core diameter. Absolute index values do not have to be known.

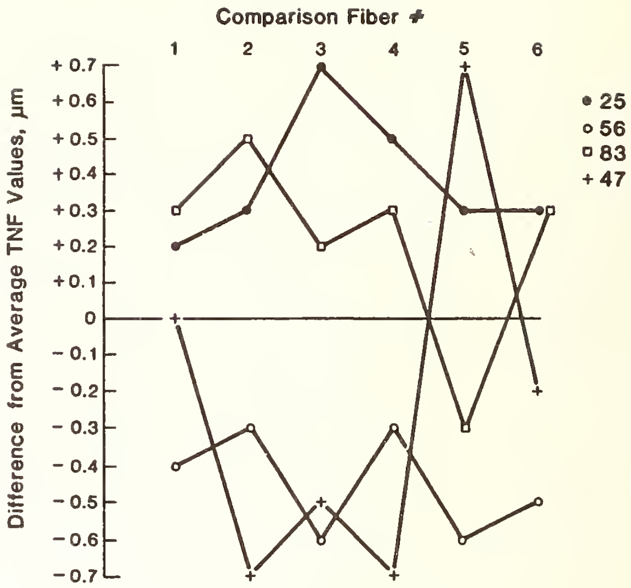


Figure 2. Relative performance of TNF participants compared to the average measured value for each fiber, uncorrected values.

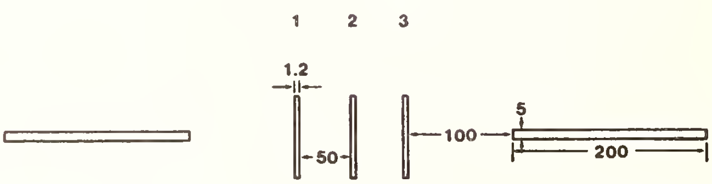


Figure 3. Calibration pattern on NBS reticle, all dimensions in micrometers.

Table 2. Measured 1 to 3 Distance on Test Reticle

| Participant, system | Measured value, µm | % Difference from actual |
|---|---|---|
| 25, TNF | 100.0 | -0.1 |
| 56, TNF | 98.9 | -1.2 |
| 83, TNF | 101.9 | +1.8 |
| 47, TNF | 98.7 | -1.4 |

## INDEX OF AUTHORS



* = Digest Supplement

☆ U.S. Government Printing Office 1982 - 580-048/360 Reg. 8

NBS-114A (REV. 2-80)

| U.S. DEPT. OF COMM. **BIBLIOGRAPHIC DATA SHEET** *(See instructions)* | 1. PUBLICATION OR REPORT NO. NBS SP-641 | 2. Performing Organ. Report No. | 3. Publication Date October 1982 |
|---|---|---|---|

4. TITLE AND SUBTITLE

Technical Digest - Symposium on Optical Fiber Measurements, 1982

5. AUTHOR(S)

D. L. Franzen, G. W. Day, and R. L. Gallawa

6. PERFORMING ORGANIZATION *(If joint or other than NBS, see instructions)*

**NATIONAL BUREAU OF STANDARDS**
**DEPARTMENT OF COMMERCE**
**WASHINGTON, D.C. 20234**

7. Contract/Grant No.

8. Type of Report & Period Covered

9. SPONSORING ORGANIZATION NAME AND COMPLETE ADDRESS *(Street, City, State, ZIP)*

Same as item 6

10. SUPPLEMENTARY NOTES

Library of Congress Catalog Card Number: 82-600594

☐ Document describes a computer program; SF-185, FIPS Software Summary, is attached.

11. ABSTRACT *(A 200-word or less factual summary of most significant information. If document includes a significant bibliography or literature survey, mention it here)*

This volume contains summaries of papers presented at the Symposium on Optical Fiber Measurements held October 13-14, 1982, at the National Bureau of Standards in Boulder, Colorado. Subjects include the measurement of attenuation, bandwidth, index profile/geometry, joint/defect, and single mode fibers. Also included are applied/field measurements and standards.

12. KEY WORDS *(Six to twelve entries; alphabetical order; capitalize only proper names; and separate key words by semicolons)*

Attenuation; bandwidth; fiber optics; fiber optic joints; fiber optics-single mode; index profile; measurements

13. AVAILABILITY

[X] Unlimited

☐ For Official Distribution. Do Not Release to NTIS

[X] Order From Superintendent of Documents, U.S. Government Printing Office, Washington, D.C. 20402.

☐ Order From National Technical Information Service (NTIS), Springfield, VA. 22161

14. NO. OF PRINTED PAGES

156

15. Price

$6.50

# NBS TECHNICAL PUBLICATIONS

## PERIODICALS

**JOURNAL OF RESEARCH**—The Journal of Research of the National Bureau of Standards reports NBS research and development in those disciplines of the physical and engineering sciences in which the Bureau is active. These include physics, chemistry, engineering, mathematics, and computer sciences. Papers cover a broad range of subjects, with major emphasis on measurement methodology and the basic technology underlying standardization. Also included from time to time are survey articles on topics closely related to the Bureau's technical and scientific programs. As a special service to subscribers each issue contains complete citations to all recent Bureau publications in both NBS and non-NBS media. Issued six times a year. Annual subscription: domestic $18; foreign $22.50. Single copy, $4.25 domestic; $5.35 foreign.

## NONPERIODICALS

**Monographs**—Major contributions to the technical literature on various subjects related to the Bureau's scientific and technical activities.

**Handbooks**—Recommended codes of engineering and industrial practice (including safety codes) developed in cooperation with interested industries, professional organizations, and regulatory bodies.

**Special Publications**—Include proceedings of conferences sponsored by NBS, NBS annual reports, and other special publications appropriate to this grouping such as wall charts, pocket cards, and bibliographies.

**Applied Mathematics Series**—Mathematical tables, manuals, and studies of special interest to physicists, engineers, chemists, biologists, mathematicians, computer programmers, and others engaged in scientific and technical work.

**National Standard Reference Data Series**—Provides quantitative data on the physical and chemical properties of materials, compiled from the world's literature and critically evaluated. Developed under a worldwide program coordinated by NBS under the authority of the National Standard Data Act (Public Law 90-396).

NOTE: The principal publication outlet for the foregoing data is the Journal of Physical and Chemical Reference Data (JPCRD) published quarterly for NBS by the American Chemical Society (ACS) and the American Institute of Physics (AIP). Subscriptions, reprints, and supplements available from ACS, 1155 Sixteenth St., NW, Washington, DC 20056.

**Building Science Series**—Disseminates technical information developed at the Bureau on building materials, components, systems, and whole structures. The series presents research results, test methods, and performance criteria related to the structural and environmental functions and the durability and safety characteristics of building elements and systems.

**Technical Notes**—Studies or reports which are complete in themselves but restrictive in their treatment of a subject. Analogous to monographs but not so comprehensive in scope or definitive in treatment of the subject area. Often serve as a vehicle for final reports of work performed at NBS under the sponsorship of other government agencies.

**Voluntary Product Standards**—Developed under procedures published by the Department of Commerce in Part 10, Title 15, of the Code of Federal Regulations. The standards establish nationally recognized requirements for products, and provide all concerned interests with a basis for common understanding of the characteristics of the products. NBS administers this program as a supplement to the activities of the private sector standardizing organizations.

**Consumer Information Series**—Practical information, based on NBS research and experience, covering areas of interest to the consumer. Easily understandable language and illustrations provide useful background knowledge for shopping in today's technological marketplace.

*Order the* **above** *NBS publications from: Superintendent of Documents, Government Printing Office, Washington, DC 20402.*

*Order the* **following** *NBS publications—FIPS and NBSIR's—from the National Technical Information Services, Springfield, VA 22161.*

**Federal Information Processing Standards Publications (FIPS PUB)**—Publications in this series collectively constitute the Federal Information Processing Standards Register. The Register serves as the official source of information in the Federal Government regarding standards issued by NBS pursuant to the Federal Property and Administrative Services Act of 1949 as amended, Public Law 89-306 (79 Stat. 1127), and as implemented by Executive Order 11717 (38 FR 12315, dated May 11, 1973) and Part 6 of Title 15 CFR (Code of Federal Regulations).

**NBS Interagency Reports (NBSIR)**—A special series of interim or final reports on work performed by NBS for outside sponsors (both government and non-government). In general, initial distribution is handled by the sponsor; public distribution is by the National Technical Information Services, Springfield, VA 22161, in paper copy or microfiche form.